

*IN VITRO AND IN VIVO* STUDIES OF CHEMOTHERAPEUTIC DOXORUBICIN  
ANALOGS

by  
Sangphil Moon

A thesis submitted in partial fulfillment  
of the requirements for the degree of  
Master of Science in Chemistry  
Boise State University

August 2017

© 2017

Sangphil Moon

ALL RIGHTS RESERVED

BOISE STATE UNIVERSITY GRADUATE COLLEGE

**DEFENSE COMMITTEE AND FINAL READING APPROVALS**

of the thesis submitted by

Sangphil Moon

Thesis Title: *In Vitro* and *In Vivo* Studies of Chemotherapeutic Doxorubicin Analogs

Date of Final Oral Examination: 9 June 2017

The following individuals read and discussed the thesis submitted by student Sangphil Moon, and they evaluated his presentation and response to questions during the final oral examination. They found that the student passed the final oral examination.

Kenneth A. Cornell, Ph.D.

Co-Chair, Supervisory Committee

Don Warner, Ph.D.

Co-Chair, Supervisory Committee

Kristen A. Mitchell, Ph.D.

Member, Supervisory Committee

The final reading approval of the thesis was granted by Kenneth A. Cornell, Ph.D., Co-Chair of the Supervisory Committee. The thesis was approved by the Graduate College.

## DEDICATION

The entire project is dedicated to the people who showed concern and care, and provoked me during my career at Boise State University. Particularly, I thank my family tremendously for pushing me outside of my comfort zone, and for being supportive from thousands of miles away. I also give my full gratitude to my friends who challenge, inspire me to grow and move forward, and remind me of what truly matters.

## ACKNOWLEDGEMENTS

I primarily acknowledge Dr. Ken Cornell for persuading me to pursue further education and providing me an opportunity to learn scientific research with countless feedback, both inside and outside of the lab. I also give massive credits to Dr. Don Warner for accepting me as a member of his lab family and sharing his insightful organic chemistry knowledge during my academic career. Additionally, I appreciate Dr. Cheryl Jorcyk and Dr. Kristen Mitchell for being on my committee, and supporting and discussing my work. Lastly, I want to thank Ryan Carfi for sharing his cell culture and *in vivo* experiences; LJ McKenzie and Sean Northington for their contribution to the *in vitro* project, and their patience in working with me.

The project described in this thesis was supported by an Institutional Development Award (IDeA) from the National Institute of General Medical Sciences of the National Institutes of Health (NIH/NIGMS) under Grants #R15CA113464, #P20GM103408 and #P20GM109095. Additional funding came from Gem Pharmaceuticals LLC. Furthermore, I sincerely appreciate the support from the Department of Chemistry and Biochemistry at Boise State University (BSU) for the teaching assistantships and summer research fellowship stipend, and the Biomolecular Research Center (BRC) at BSU with funding from the National Science Foundation (NSF), Grants #0619793 and #0923535; the MJ Murdock Charitable Trust; the Idaho State Board of Education; and Idaho Global Entrepreneurial Mission (IGEM).

## ABSTRACT

Anthracyclines remain widely prescribed and successful anticancer agents, despite serious side effects. Doxorubicin (DOX) is the most prominent anthracycline used to treat many cancers, including hematologic malignancies, soft-tissue sarcomas, cancers of the head and neck, and breast cancer. However, the clinical application of DOX is limited by the development of life-threatening cardiomyopathy and congestive heart failure. The main mechanisms of cardiotoxicity are thought to be mediated through the C-13 carbonyl and quinone ring structures in DOX. To improve the anticancer activity and reduce the cardiotoxic side effects of DOX, two synthetic analogs (GPX-150 and GPX-160) were developed and tested for *in vitro* and *in vivo* activity against a panel of soft tissue sarcoma cells. The analogs were further subjected to an array of tests to examine drug stability, transport properties, topoisomerase inhibitory activity and metabolism by cytochrome P450 enzymes.

The two analogs were effective anticancer agents against an array of cancer cells. In particular, GPX-160 exhibited *in vitro* cytotoxicity against human soft tissue sarcoma (STS) cells that was similar to DOX. Importantly, GPX-160 functioned equally well against both DOX-sensitive and DOX-resistant sarcoma cell lines, suggesting that its structural modifications allowed it to resist P-glycoprotein mediated drug efflux. Moreover, in a murine xenograft model of human STS, both GPX-150 and GPX-160 treatment resulted in significant decreases in both fibrosarcoma tumor volume and weight relative to the vehicle-treated controls.

The stability of the DOX analogs in tissue culture media suggest that in the absence of drug metabolizing enzymes, GPX-150 ( $t_{1/2} = 55.9$  hr) will persist approximately 8-fold longer than DOX ( $t_{1/2} = 6.8$  hr) and 3-fold longer than GPX-160 ( $t_{1/2} = 20.7$  hr). *In vitro* drug absorption studies across Caco-2 cell monolayers indicate that GPX-150 and GPX-160 have higher permeability coefficients than DOX in both apical-to-basolateral and basolateral-to-apical directions. However, the transport of the analogs is not as heavily polarized in the basolateral-to-apical direction, as is seen with DOX. Both analogs also inhibited human topoisomerase II $\alpha$  at low micromolar concentrations, supporting the possibility that they share a similar primary mechanism of action with DOX. Finally, human liver microsome metabolism of the two analogs showed that they were insensitive to aldo-keto reductase activity, which was expected based on the loss of the C-13 carbonyl and quinone structures. However, GPX-150 and GPX-160 remained sensitive to CYP2C8 and CYP3A4 activity.

Overall, these studies serve as an initial characterization of two DOX analogs that appear to hold great promise as a next generation of anthracyclines that overcome problems of drug resistance, while mitigating the cardiotoxicity that has limited the use of DOX.

## TABLE OF CONTENTS

DEDICATION .....	iv
ACKNOWLEDGEMENTS .....	v
ABSTRACT.....	vi
TABLE OF CONTENTS.....	viii
LIST OF TABLES .....	xii
LIST OF FIGURES .....	xiii
LIST OF ABBREVIATIONS.....	xv
CHAPTER ONE: INTRODUCTION.....	1
1.    Cancer .....	1
2.    Soft Tissue Sarcomas.....	2
3.    History of Doxorubicin.....	3
4.    Structures of Doxorubicin and Early Analogs .....	3
5 Mechanisms of Action of Doxorubicin.....	4
5.1 DNA Intercalation and Topoisomerase II Poisons .....	5
5.2 Production of Free Radicals and Reactive Oxygen Species (ROS).....	9
5.3 DNA Adducts and Cross-linking.....	10
6.    Mechanisms of Cardiotoxicity.....	12
6.1 DOX-induced RONS Mediated Cardiotoxicity .....	14
6.2 DOX-induced Doxorubicinol Mediated Cardiotoxicity .....	16

7.	Prevention of Cardiotoxicity.....	17
8.	Anthracycline Analogs.....	17
	8.1 Epirubicin.....	18
	8.2 Idarubicin .....	19
	8.3 Dissaccharide Anthracyclines .....	20
	8.4 C-13 Deoxy Anthracyclines.....	22
	8.5 Cancer-Targeted Formulations .....	23
	8.6 Cardioprotective Agents .....	23
9.	Conclusion .....	25
	REFERENCES .....	27
	CHAPTER TWO: <i>IN VITRO</i> AND <i>IN VIVO</i> ACTIVITY OF NOVEL DOXORUBICIN ANALOGS AGAINST SOFT TISSUE SARCOMA.....	42
	Abstract.....	42
1.	Introduction.....	42
2.	Results/Discussion .....	45
	2.1 Inhibition of Topoisomerase II $\alpha$ .....	45
	2.2 Cytotoxicity studies.....	46
	2.3 Inhibition of human sarcoma xenografts.....	49
3.	Conclusion .....	52
4.	Materials and Methods.....	53
	4.1 Materials and Reagents .....	53
	4.2 Topoisomerase II $\alpha$ Assay.....	53
	4.3 Cell Lines and Cell Culture.....	54
	4.4 Antiproliferative Assays.....	55

4.5 <i>In vivo</i> Fibrosarcoma Xenograft Model .....	55
5. Acknowledgment .....	57
REFERENCES .....	58
CHAPTER THREE: ANALYSIS OF NOVEL IMINOQUINONE ANALOGS REVEALS DISTINCT <i>IN VITRO</i> PHARMACOKINETIC PROFILES .....	
Abstract .....	61
1. Introduction .....	62
2. Materials and methods .....	64
2.1 Drug stability studies .....	64
2.2 Drug transport studies .....	64
2.3 Microsomal metabolism of DOX and DOX analogs .....	66
2.4 Identification of DOX and DOX analog metabolic products by mass spectrometry .....	67
3. Results .....	68
3.1 Drug stability of DOX, GPX-150, and GPX-160 .....	68
3.2 Transport studies of DOX analogs across intestinal epithelia .....	68
3.3 Microsomal metabolism of DOX and DOX analogs .....	70
3.4 Identification of DOX and DOX analog metabolic products .....	72
4. Discussion .....	76
5. Conclusion .....	81
REFERENCES .....	82
CHAPTER FOUR: CONCLUSION .....	
APPENDIX A .....	88
Fluorescence Profiles and Calibration Curves for DOX, GPX-150 and GPX- 160 .....	89

APPENDIX B .....	91
B1. Doxorubicin.....	92
B2. GPX-150.....	92
B3. Schematic of DOX Metabolism .....	94
B4. Schematic of GPX-150 Metabolism .....	94

## LIST OF TABLES

Table 2.1. Summary of drug activity against human sarcoma and carcinoma cell lines..	48
Table 2.2 Summary of drug activity against normal human cell lines. ....	48
Table 3.1. Summary of apparent permeability rates (P <sub>app</sub> ) of bidirectional drug transport. ....	70
Table 3.2. Identities of the m/z peaks in the mass spectra of HLM metabolized (A) DOX, (B) GPX-150, and (C) GPX-160.....	75

## LIST OF FIGURES

Figure 1.1	The structures of early analogs .....	4
Figure 1.2	Stereoscopic skeletal sketch of the DOX-DNA intercalation.....	6
Figure 1.3	Topoisomerase II poisoning by DOX.....	8
Figure 1.4	RONS and free radical production of DOX.....	9
Figure 1.5	DOX-DNA adduct .....	11
Figure 1.6	DOX-induced cardiotoxicity mechanisms.....	14
Figure 1.7	The structures of epirubicin .....	18
Figure 1.8	The structures of idarubicin .....	19
Figure 1.9	The structures of disaccharide anthracyclines .....	20
Figure 1.10	The structures of C-13 deoxy anthracyclines, GPX-150 .....	22
Figure 1.11	The structures of dexrazoxane and ADR-925.....	23
Figure 2.1	The structures of doxorubicin, GPX-150, and GPX-160.....	44
Figure 2.2	Topoisomerase II $\alpha$ inhibitory activity.....	45
Figure 2.3	<i>In vitro</i> drug sensitivity profiles for human uterine sarcoma cell lines ....	47
Figure 2.4	<i>In vivo</i> results of DOX analogs.....	51
Figure 3.1	The structures of doxorubicin, GPX-150, and GPX-160.....	63
Figure 3.2	Drug degradation of DOX, GPX-150, and GPX-160.....	68
Figure 3.3	Apparent permeability rate .....	69
Figure 3.4	Metabolic turnover rates with selective CYP450 inhibitors.....	71

Figure 3.5	HPLC separation of GPX-160 and its metabolites .....	72
Figure 3.6	MS spectra of GPX-160 and its metabolites.....	73
Figure 3.7	Proposed schematic of metabolites of GPX-160 via CYP450.....	76
Figure A.1	Spectrofluorometric profiles of DOX, GPX-150, and GPX-160.....	89
Figure A.2	Calivration curves of DOX, GPX-150, and GPX-160.....	90
Figure B.1	Identification of DOX metabolites by MS.....	92
Figure B.2	Identification of GPX-150 metabolites by MS .....	93
Figure B.3	Schematic of DOX metabolism .....	94
Figure B.4	Schematic of GPX-150 metabolism.....	94

## LIST OF ABBREVIATIONS

ADME	Absorption, distribution, metabolism, and excretion
AKR	Aldo-keto reductase
ALL	Acute lymphocytic leukemia
AML	Acute myeloid leukemia
AP	Apical
ATP	Adenosine triphosphate
ATPase	Adenylpyrophosphatase
BL	Basolateral
BLI	Bioluminescent imaging
CBR	Carbonyl reductase
CHF	Congestive heart failure
CYP450	Cytochrome P450
DAD	Diode array detector
DMEM	Dulbecco's Modified Eagle Medium
DMSO	Dimethyl sulfoxide
DNA	Deoxyribonucleic acid
DNR	Daunorubicin
DOX	Doxorubicin
DOXi1	Pegylated-liposomal doxorubicin
DOXol	Doxorubicinol

DOX <sup>R</sup>	Doxorubicin-resistant
DOX <sup>S</sup>	Doxorubicin-sensitive
DSBs	Double-strand breaks
DZR	Dexrazoxane
EDTA	Ethylenediaminetetraacetic acid
EKG	Electrocardiogram
EPI	Epirubicin
EPIol	Epirubicinol
ER	Efflux ratio
ESI	Electrospray ionization
FAC	Cyclophosphamide
FBS	Fetal bovine serum
GI tract	Gastrointestinal tract
HADF	Human adult dermal fibroblast
HBSS	Hank's balanced salt solution
HCl	Hydrogen chloride
HFS	Hand-foot syndrome
HLMs	Human liver microsomes
HPLC	High-performance liquid chromatography
HUVEC	Human umbilical vein endothelial cord
IC <sub>50</sub>	Inhibitory concentration at 50% of cell viability
IDA	Idarubicin
iNOS	isoform of nitrogen oxide synthase

IRP	Iron-responsive element-binding protein
IV	Intravenous
kDNA	Kinetoplast DNA
LVEF	Left ventricular ejection fraction
LY	Lucifer yellow
MEM	Minimum Essential Medium
MMDX	Nemorubicin
MS	Mass spectrometry
NADPH	Nicotinamide adenine dinucleotide phosphate-reduced form
NMR	Nuclear magnetic resonance
NO	Nitric oxide
$P_{app}$	Apparent permeability coefficient
PBS	Phosphate buffered saline
PEG	Polyethylene glycol
Pen/strep	Penicillin and streptomycin
P-gp	P-glycoprotein
PTFE	Polytetrafluoroethylene
PXR	Pregnane X receptor
RNA	Ribonucleic acid
RONS	Reactive oxygen and nitrogen species
SEM	Standard error of the mean
SER	Smooth endoplasmic reticulum
STS	Soft tissue sarcoma

TEER	Transepithelial electrical resistance
Top2 $\alpha$	Topoisomerase II $\alpha$
UDP	Uridine diphosphate
UV-VIS	Ultraviolet-visible spectrophotometry
WHO	World Health Organization

## CHAPTER ONE: INTRODUCTION

### 1. Cancer

Cancer is marked by the uncontrolled proliferation of genetically damaged cells that do not respond to the normal regulatory mechanisms employed in multicellular organisms. The uncontrolled proliferation of cancer cells interferes with the nutrient uptake of adjacent normal cells. With time, growing masses of cancer cells can crowd and outcompete healthy cells for resources and compromise vital tissue functions.

Abnormal cells can become either benign or malignant tumors. Benign tumors are not cancerous as they grow slowly, are limited to a specific location, and rarely cause death. On the other hand, malignant tumors are eventually lethal as they undergo metastasis and often spread through lymph vessels or the bloodstream to distant parts of the body. Malignant tumors disrupt biological activities of normal cells, and if left untreated, can lead to death.

Cancer is the second most common cause of death in the U.S, preceded only by heart disease. An estimated 1.7 million new cancer cases are presumed to be diagnosed in 2017 and about 600,000 patients are expected to die of cancer<sup>1</sup>. Breast carcinomas and prostate cancers are the most common cancers for females and males, respectively. Lung cancers are the leading cause of death for both women and men.

Cancers are classified by the tissues affected. The majority of cancerous tumors are carcinomas, in which tumors originated from epithelial tissue, such as skin, glands, and the lining of most internal organs. Leukemias are cancers of the bone marrow where leukocytes

are produced. Similarly, lymphomas are cancers in which lymphocytes uncontrollably proliferate in the lymph nodes. Tumors originating in connective tissue are called sarcomas. Compared to the other cancer types, sarcomas are understudied due to their low rate of occurrence.

## **2. Soft Tissue Sarcomas**

Soft tissue sarcomas (STS) are a rare type of cancer derived from transformed cells of mesenchymal origin. STS represent 1% of all adult cancers and can originate in many types of tissue including adipose tissue (liposarcoma), skeletal muscle (rhabdomyosarcoma), smooth muscle (leiomyosarcoma), and blood and lymph nodes (angiosarcoma)<sup>2</sup>. The identification of STS relies on clinical examination, imaging, and histologic analysis<sup>3</sup>. There are more than 50 subtypes of STS<sup>4</sup>. Most sarcomas occur in the extremities account for 60-70% (about 40% lower and 20% upper) of STS<sup>3</sup>.

Surgery is the typical treatment for local control of extremity STS followed by radiation and chemotherapy. The 5-year local control rates in patients with adjuvant radiotherapy improved by 18% compared with those treated with surgery alone<sup>5</sup>. Adjuvant doxorubicin-based chemotherapy also improves overall survival for metastatic STS as it reduces the risk of local recurrence by 27% with an absolute benefit of 6% at 10 years. Even though systematic control by chemotherapy can be useful, the overall outcome of STS treatment is unsatisfactory and survival rates have remained stagnant for more than 50 years<sup>6</sup>. In addition, the use of adjuvant chemotherapy is limited and controversial. Doxorubicin, the single most active chemotherapeutic agent for STS, shows a 30% overall response rate but causes cardiotoxicity as a side effect, which limits its use<sup>6</sup>. Therefore, new chemotherapeutic regimens are required for treatment of STS.

### 3. History of Doxorubicin

Doxorubicin (DOX, Adriamycin<sup>®</sup>, 14-hydroxydaunorubicin, NSC-123,127) is one of the anthracycline-based antitumor agents considered as a mainstay chemotherapeutic since its approval for use in 1974<sup>7</sup>. The parent compound of DOX is daunorubicin (DNR). DNR was first isolated in the early 1960's from pigment-releasing *Streptomyces peucetius var. caesioides* strains, followed by the discovery of DOX<sup>8</sup>. Early on, DNR was found to be potent in treating leukemias and lymphomas<sup>9</sup>. Later, DOX was found to be a better anticancer agent than DNR for treating a variety of cancers, including leukemias, Hodgkin's and non-Hodgkin's lymphomas, and solid tumors of the breast, lung, ovaries, bladder, thyroid, and stomach<sup>10</sup>. DOX was also found to be effective in the treatment of multiple myeloma and STS, including Kaposi's sarcoma<sup>11</sup>.

Since the 1960s, hundreds of DOX analogs have been synthesized and investigated for anticancer activity<sup>12</sup>, although few have progressed to common clinical use. Despite the potential for significant adverse effects, DOX remains one of the most prescribed chemotherapeutic agents. It is considered by the World Health Organization to be so important that it is on their "List of Essential Medicines" that should be available in a health care system<sup>13</sup>.

### 4. Structures of Doxorubicin and Early Analogs

Structurally, anthracyclines consist of a daunosamine sugar moiety linked to a tetracycline with neighboring quinone and hydroquinone groups in the center, a methoxy group at C-4, and a short side chain with a carbonyl group at C-13 (see Figure 1). The daunosamine sugar is composed of a 3-amino-2, 3, 6-trideoxy-L-fucosyl substituent, and is attached at C-7 of the tetracyclic ring. The differences between DNR and DOX exist at

the short side chain next to the C-13 carbonyl group attached to the A ring. DNR contains a methyl group that is hydroxylated in DOX. Idarubicin (IDA, 4-demethoxydaunorubicin) and epirubicin (EPI, 4'-epidoxorubicin) are first generation anthracycline derivatives of DNR and DOX, respectively. IDA represents DNR without a C-4 methoxy group on ring D. EPI resembles DOX, but has an axial-to-equatorial epimerization of hydroxyl group in the sugar moiety, thus forming an acosamine instead of daunosamine sugar. Due to the very similar structures, these compounds share similar mechanisms of action for their antitumor effects.

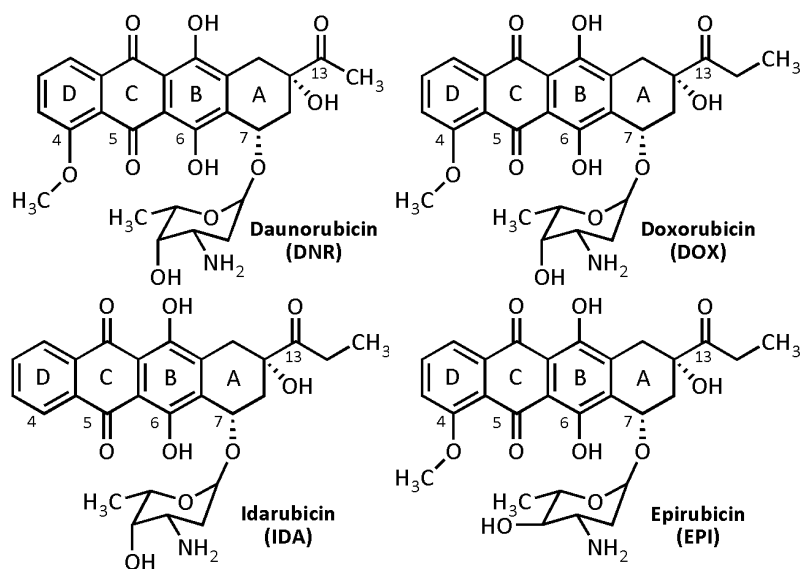


**Figure 1.1 Structures of early anthracyclines**

### 5 Mechanisms of Action of Doxorubicin

The antitumor activity of DOX has been investigated for several decades since its discovery. The three most widely accepted mechanisms of action are as follows: (1) DNA intercalation and inhibition of topoisomerase activity<sup>14</sup>, (2) production of reactive oxygen and nitrogen species (RONS) yielding DNA damage and/or lipid peroxidation<sup>15</sup>, (3) and

formation of DNA adducts and/or crosslinking to proteins to interrupt replication and transcription<sup>16</sup>.

### 5.1 DNA Intercalation and Topoisomerase II Poisons

DOX initially intercalates between DNA base pairs to form a stable DOX-DNA-topoisomerase II, ternary complex. As a result, both DNA strands are cut but not resealed, ultimately leading to extensive DNA damage. The structure of DOX explains how it intercalates DNA and forms this stable complex. For instance, the planar ring system of DOX drives DNA intercalation through numerous hydrophobic interactions as the B and C ring overlaps adjacent base pairs, and the D ring passes through the intercalation site (see Figure 2). The non-intercalating groups such as the sugar moiety and ring A, stabilize the cleavable complex<sup>17</sup>. The sugar moiety associates with the minor groove of DNA and topoisomerase complex to deform the DNA structure<sup>18,19</sup>. It has been demonstrated that the removal or modification of amino- substituents at the C-3' position in the sugar and/or methoxy group at C-4 in the D ring increases the topoisomerase II (Top2) poisoning, thereby increasing the overall anticancer activity<sup>20-22</sup>.

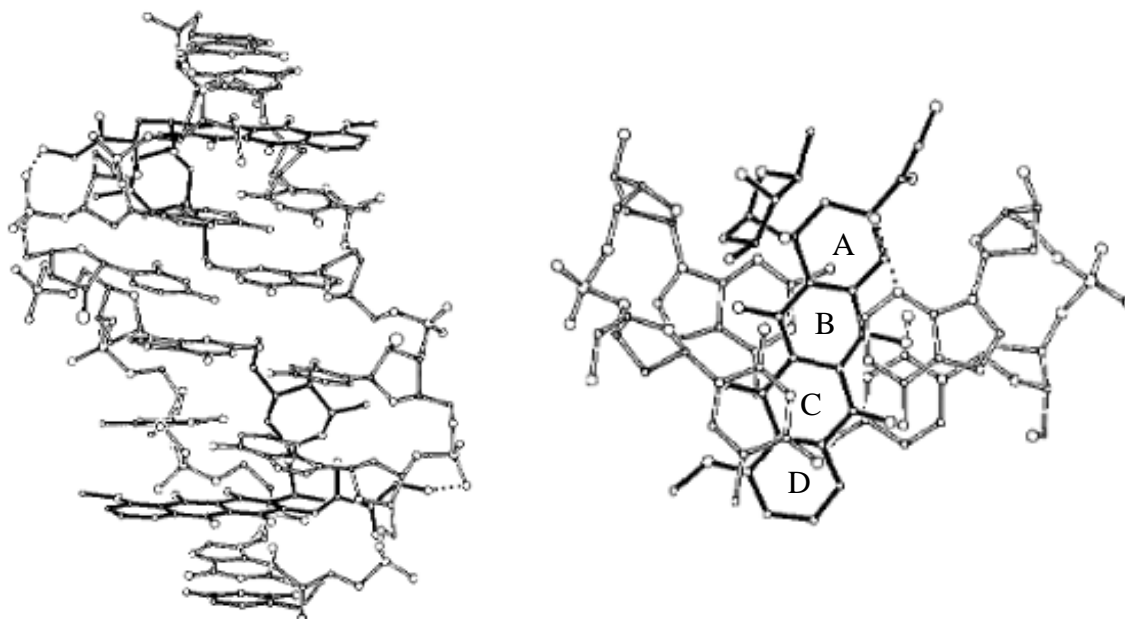


**Figure 1.2.** Stereoscopic skeletal sketch of the DOX-DNA complexes (left) and stacking interaction between DOX and the adjacent base pairs in a perpendicular view (right). DOX (dark bonds) intercalates between the terminal two base pairs of DNA as the sugar moiety penetrates through the helix. The sugar residue and ring A reside outside of the intercalation site and stabilize the ternary complex. The N-3 amino group of the sugar lies in the minor groove, and can also form a covalent bond with the guanine base of DNA (modified from Zhang et al., 1993).

Several studies have classified DOX as a Top2 poison<sup>23,24</sup>. DNA topoisomerases are ubiquitous enzymes that play a crucial role in regulating genomic integrity. These enzymes supervise the topology of cellular DNA by catalyzing the unwinding of DNA supercoiling through DNA strand passage and re-ligation without altering its sequence and structure. Topoisomerases regulate DNA replication, recombination, repair, transcription, and apoptotic DNA degradation<sup>25</sup>. Topoisomerases are divided into two subfamilies based on their chemical structure: topoisomerase I (type 1) and II (type 2). Topoisomerase I is a monomer, which transiently cleaves a single-strand of DNA duplex to unwind the supercoiled-DNA. In contrast, topoisomerase II is an oligomer that transiently cleaves both

strands of the DNA duplex, relaxing the supercoiled-DNA<sup>26</sup>. Six different topoisomerases exist in human cells: 1A (Top3 $\alpha$  and  $\beta$ ), 1B (Top1 and Top1mt), and 2a (Top2 $\alpha$  and  $\beta$ )<sup>27</sup>.

Top2 $\alpha$  is a nuclear isozyme composed of a dimer of two identical subunits that requires ATP hydrolysis (Figure 3)<sup>28</sup>. The enzyme appears in fast-growing cancer cells, and is a primary molecular target for DOX<sup>29</sup>. DOX interaction with Top2-DNA covalent complexes induces DNA damage, including double-strand breaks (DSBs). DSBs in chromosomal DNA induced by DOX are stabilized by the proteosome<sup>31,32</sup>. In response to DSBs, the histone H2A variant  $\gamma$ -H2AX is phosphorylated and initiates a signaling cascade that alerts the cell to DNA damage, leading to growth arrest in G<sub>1</sub> and G<sub>2</sub> phases, and apoptosis<sup>33,34</sup>.

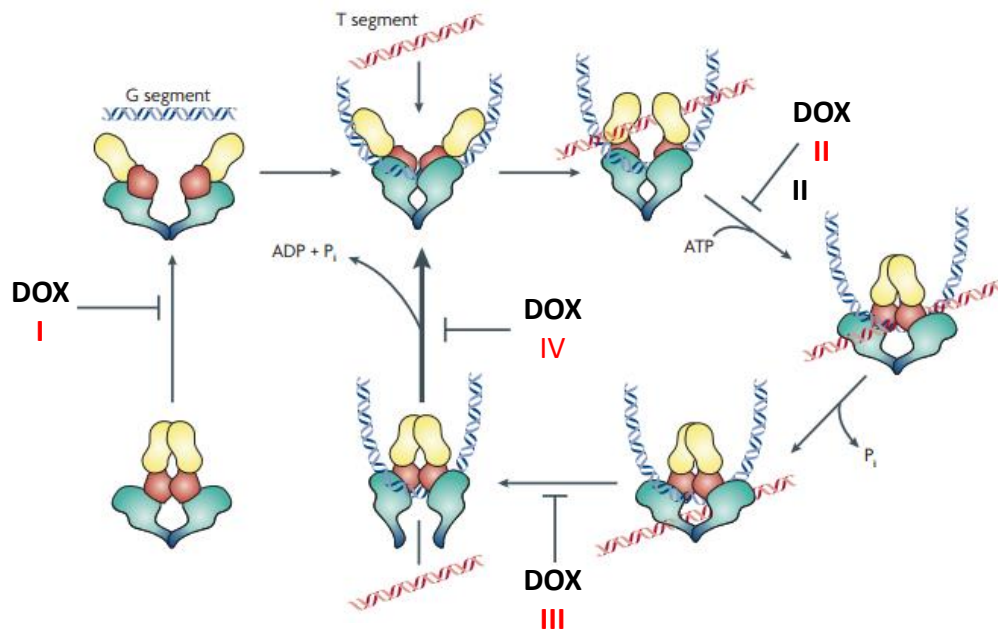


**Figure 1.3.** DOX inhibits topoisomerase II (Top2) at several sites in the reaction cycle: I. DOX can block Top2 binding to the G segment of DNA (blue). II. DOX can also inhibit the advancement of the DNA T segment (red) into the central hole before ATP binds to the ATPase domain (yellow). III. DOX interferes with release of the T segment from the A and A' domains (green) at the bottom of the dimer. IV. DOX interrupts ATP hydrolysis and regeneration of the starting state (modified from Nitiss, 2009).

## 5.2 Production of Free Radicals and Reactive Oxygen Species (ROS)

The quinone moiety in ring C of DOX can undergo a one-electron reduction catalyzed by flavin oxido reductases<sup>35</sup>, forming a semiquinone that decomposes to the parent quinone and reduces oxygen to reactive species such as hydrogen peroxide ( $\text{H}_2\text{O}_2$ ), superoxide anion ( $\text{O}_2^{\cdot-}$ )<sup>36</sup>, and ultimately hydroxyl radical ( $\cdot\text{OH}$ ) (Figure 4). In a biological environment,  $\cdot\text{OH}$  can interact with cellular constituents, creating adducts of cellular DNA, peroxidizing lipids, or oxidizing tryptophan-, tyrosine-, and thiol-

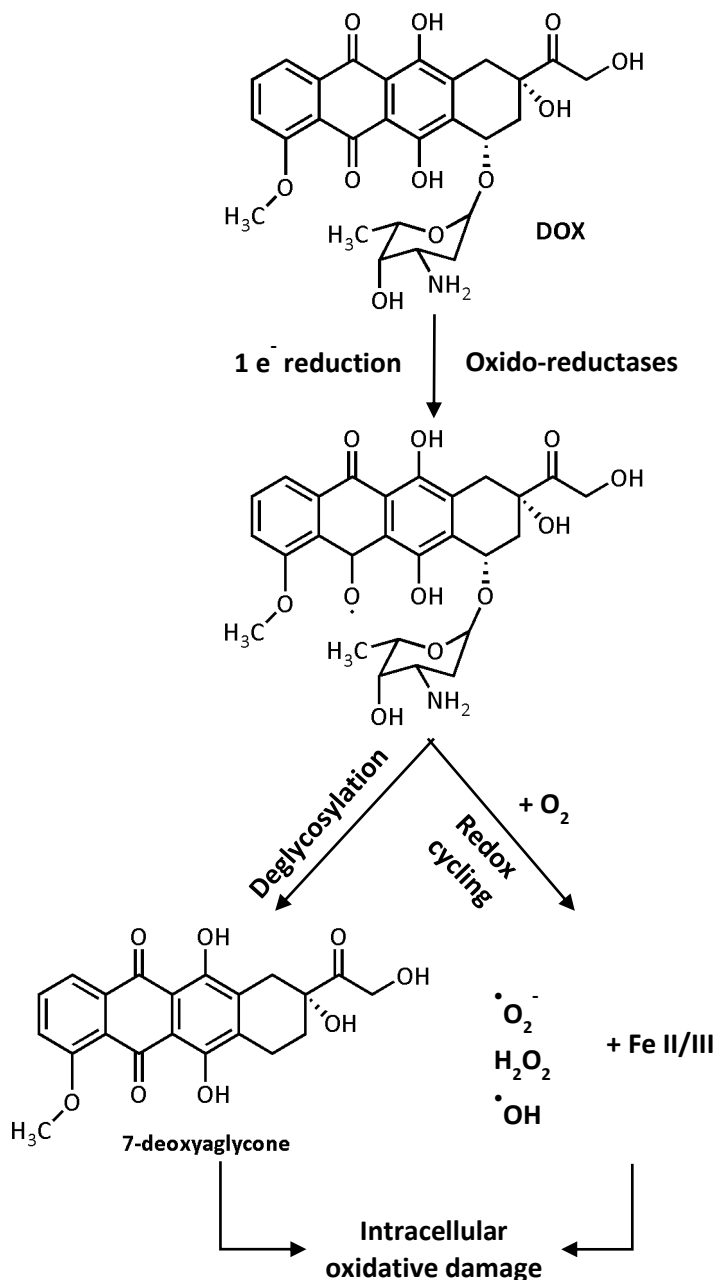


**Figure 1.4.** The production of reactive oxygen species (ROS) and free radicals from doxorubicin by one-electron reduction catalyzed by oxido-

**containing functional groups in proteins and enzymes. Ultimately, these events disrupt function and lead to cell death<sup>37</sup>.**

DOX decomposition can create RONS through other routes as well. Reductive deglycosylation of DOX to a 7-deoxyaglycone is generated during the one-electron reduction cycle as the semiquinone may also oxidize the bond between the A ring and sugar moiety<sup>38</sup>. These aglycone products can readily permeate cells and organelles because of their increased lipid solubility to produce intracellular RONS<sup>39</sup>. RONS can also oxidize signaling molecules that modulate the activity of kinases or transcription factors, disrupting the cell cycle and stimulating apoptosis<sup>40-43</sup>.

Free radical generation can also be mediated by metals, particularly iron. DOX forms an iron coordination complex with dinucleotides<sup>44,45</sup>. Several studies have shown that the presence of the C-11 hydroxyl group is fundamental for iron binding and thiol-dependent oxygen consumption. DOX can complex with iron to directly reduce Fe (III) to Fe (II), which then reacts with molecular oxygen or hydrogen peroxide to sponsor DNA adduct formation<sup>46</sup>. This iron-DOX complex mediates oxidative damage and is considered one of the primary mechanisms of DOX anticancer action.

### 5.3 DNA Adducts and Cross-linking

In addition to creating DOX-DNA-Top2 complexes that disrupt DNA replication through stabilized double strand breaks, DOX can also directly form covalent DNA adducts that lead to cytostatic effects<sup>47,48</sup>. These direct DNA-adducts were first described by Sinha and Chignell in 1979<sup>49</sup>. Formaldehyde in the cell creates a methylene group at the 3' amino moiety on the sugar of DOX and binds to the N-2 residue of guanine in the DNA (Figure 5). This reactive intermediate attacks the 2-amino group of deoxyguanosine residues in the DNA via Schiff base chemistry to create the DOX-DNA adduct<sup>16,50,51</sup>. Reaction rates can

be increased through catalysis by xanthine oxidase and NADPH<sup>52</sup>. Cullinane and Philips discovered that DOX can create adducts with both single and double stranded DNA and hypothesized that this occurred through a quinone methide intermediate<sup>12</sup>. Taatjes and Koch et al. suggested that DOX iron-catalyzed free radical reactions induce formaldehyde production from cellular carbon sources such as lipids and spermine in an oxidative stress environment, thus stimulating DOX-DNA adduct formation<sup>53,54</sup>.

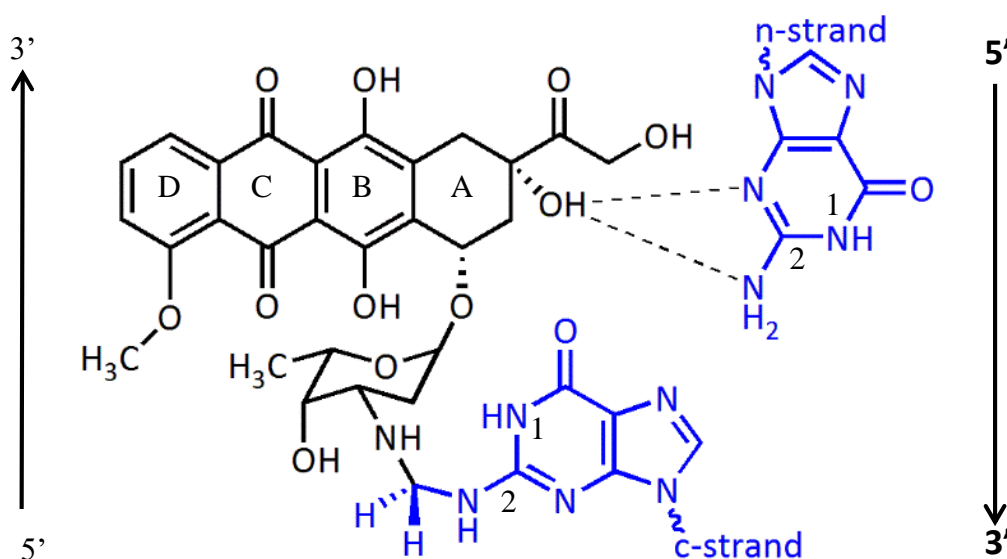


**Figure 1.5.** Structure of doxorubicin showing its covalent and non-covalent bonding position to the c- and n-strands of DNA. Rings B, C, and D can intercalate in the minor groove of DNA. DNA-adducts are mediated through N-2 guanine nucleoside (blue) of DNA in either strand. The non-covalent strand form hydrogen bonds with the hydroxyl group at ring A of DOX. The covalent linkage between the amino group of DOX and c-strand guanine N-2 derives from direct reaction with formaldehyde. The aminor (N-C-N) bond between N-3 amino group of guanine and daunosamine sugar forms DNA covalent cross linkages at 5'-GC-3' sites.

DNA cross-linkage is proposed to occur in a series of steps. Step 1 involves the interaction of DOX with the binding site of DNA, which yields the drug-DNA complex. In step 2, formaldehyde released from carbon sources via iron-catalyzed free radical reactions interacts to generate a covalent complex between the amine group on the DOX

sugar and the N-2 amine group on the guanine base of the c-strand. Meanwhile, the N-3 amine group in the guanine base of the DNA n-strand hydrogen bonds with the hydroxy group on ring A of DOX. Lastly, in step 3, formaldehyde produces the cross-linked ternary complex<sup>55</sup>. This primarily occurs between the daunosamine sugar and the N-2 amino group of guanine via an aminal (N-C-N) bond<sup>49,55,56</sup>, predominantly cross-linking at 5'-GC-3' sites in DNA<sup>12</sup>.

The concentration of formaldehyde is often higher in cancer cells than in normal cells<sup>57</sup>, thus DOX-DNA cross-linkage occurs more readily in cancer cells. As well, novel DOX analogs that more readily conjugate to formaldehyde should produce significantly enhanced rates of DNA adducts. A number of these analogs have been developed such as doxazolidine, doxoform, and doxaliform. DNA-drug adducts formed by these compounds and formaldehyde exhibited increased cytotoxicity in comparison to DOX, and they were less susceptible to drug-efflux based drug resistance<sup>58,59</sup>. The structure of DNA adducts is well supported by mass spectrometry<sup>16,50</sup>, 2D NMR<sup>51</sup>, and X-ray crystallography<sup>60</sup>.

## 6. Mechanisms of Cardiotoxicity

Although DOX is one of the most successful chemotherapeutic compounds, its clinical use is restricted by selective myocardial dysfunction, and dose-dependent reversible and irreversible cardiotoxicity<sup>60,61,62,63,64</sup>. This can result in pericarditis, arrhythmias, and left ventricular dysfunction<sup>65,66</sup>. The decreased left ventricular ejection fraction (LVEF) eventually leads to congestive heart failure (CHF)<sup>67</sup>. A decrease in LVEF and asymptomatic abnormalities may occur in patients at cumulative doses of DOX as low as 300 mg/m<sup>2</sup>. The characterization of dose-induced cardiomyopathy is seen as a flattening of the T-wave, increased Q-T interval, reduced R-wave amplitude, atrial flutter, and

premature atrial and ventricular beats<sup>68,69</sup>. LVEF dysfunction results in a decrease in both systolic and diastolic function, with a substantial increase in left ventricular end-diastolic pressure<sup>70</sup>. At cumulative doses of 240 mg/m<sup>2</sup> of DOX, significant histopathologic changes can also be seen in endomyocardial biopsy specimens, including loss of myofibrils, alteration to the sarcoplasmic reticulum, and increased vacuoles in the cytoplasm<sup>18,34,40,54,55,58,59</sup>.

Cardiotoxicity can be categorized into three distinctive types: acute/subacute, early, and late-onset chronic progressive cardiotoxicity. Acute/subacute cardiotoxicity occurs within a week of DOX treatment, and explains observed transient arrhythmias<sup>72,73,74,75</sup>. In contrast, both early- and late-onset cardiotoxicity are categorized by a dose-induced, progressive reduction in LVEF with either symptomatic or asymptomatic cardiac abnormalities<sup>76,77</sup>. Early-onset cardiotoxicity occurs within a year of treatment, while late-onset chronic cardiotoxicity may develop between 4 and 15 years after treatment has ended.<sup>78</sup>

A number of investigations have studied the pathophysiology of DOX-induced cardiomyopathy. However, the molecular mechanisms still remain debatable and are incompletely understood. The main proposed mechanisms of cardiotoxicity are RONS overproduction by single electron reduction reactions<sup>39,79-82</sup>, and the reduction of the DOX C-13 carbonyl group to an alcohol to generate a toxic metabolite, doxorubicinol (DOXol) (Figure 6)<sup>81-86</sup>.

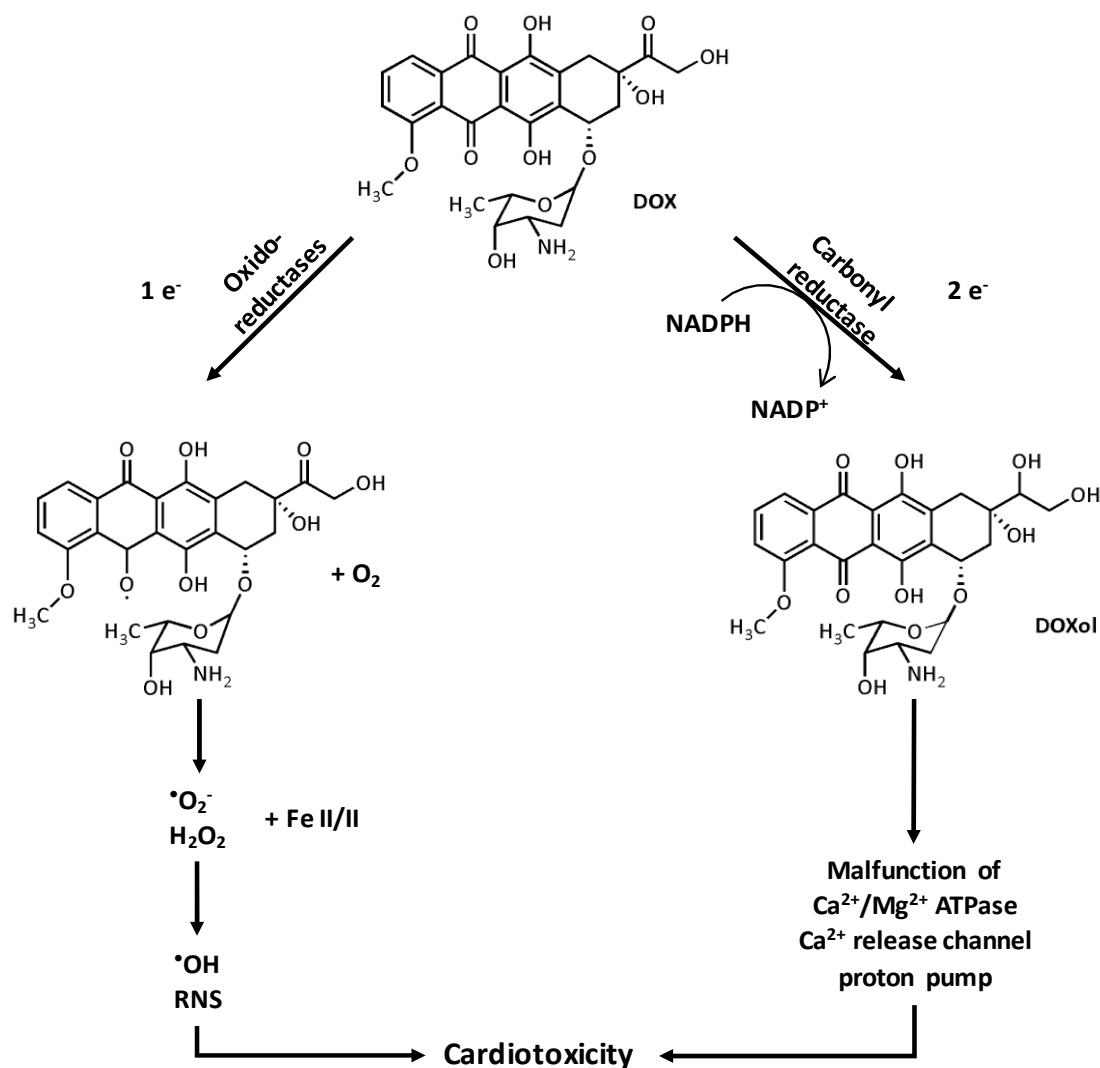


**Figure 1.6. Doxorubicin-induced mechanisms of cardiotoxicity via 1 electron and 2 electron pathways. The 1 electron reduction pathway explains the production of reactive oxygen and nitrogen species (RONS). The two electrons reduction pathway leads to production of the secondary alcohol**

### 6.1 DOX-induced RONS Mediated Cardiotoxicity

ROS can be generated via two significant molecular mechanisms: an enzymatic pathway triggered by several oxidoreductases via one-electron reduction, and an enzyme-free pathway induced by anthracycline-iron complexes. In the first pathway, oxidoreductases catalyze reduction of the quinone moiety of the central anthracycline ring into a radical semiquinone. The semiquinone reduces oxygen to create superoxide anion

and hydrogen peroxide, and regenerate the parent quinone. This pathway occurs in mitochondria by NADPH dependent ubiquinone oxidoreductase<sup>39,79,87-92</sup>, in microsomes via NADPH-cytochrome P450 or NADPH-cytochrome b<sub>5</sub> reductases<sup>88,93,94</sup>, and in the cytosol by xanthine dehydrogenase and nitric oxide synthases<sup>36,52,95-97</sup>.

On the other hand, increased RONS formation can also be induced by anthracycline-iron complexes. In the presence of oxygen, anthracycline binds to free Fe (III), becoming a drug-metal coordination complex. The complex generates superoxide anion and H<sub>2</sub>O<sub>2</sub> as it alternates redox interaction between Fe (II) and Fe (III). DOX also associates with both hemoglobin<sup>98</sup> and myoglobin, those can interact with iron<sup>98-103</sup> or copper<sup>104-106</sup>, to generate metal complexes that can form free radical species by spontaneous oxidation in solution. The presence and amount of the respective oxidoreductases in specific cell types determine the source and amount of free radical formation, and where it occurs within the cell<sup>69</sup>.

DOX-stimulated RONS production in cardiomyocytes causes mitochondrial damage that leads to apoptotic cell death through activation of caspase pathways<sup>107-109</sup>. The aglyconic form of DOX can also intercalate into mitochondrial membranes due to its high lipophilicity, and create even more RONS as it directs more electrons towards oxygen in single electron transfer reactions. In addition, DOX can generate peroxynitrite (ONOO<sup>-</sup>) as a result of excess production of superoxide anion and nitric oxide (NO) from overexpression of the inducible isoform of NO synthase (iNOS)<sup>110-113</sup>. Eventually, ONOO<sup>-</sup> can cause lipid peroxidation, protein nitrosylation, DNA strand breaks, and damage to a variety of cellular macromolecules. Overall, this futile oxidative and nitrosative stress lead cardiac dysfunction, mitochondrial damage<sup>69,114-118</sup>, energy imbalance<sup>116,119</sup>, and apoptosis<sup>17,108,120</sup>.

Cardiomyocytes are acutely susceptible to RONS, since they lack sufficient levels of detoxifying enzymes such as superoxide dismutase, catalase, and glutathione peroxidase, to respond to the added oxidative stress elicited by DOX treatment<sup>121–123</sup>. The high metabolic activity in heart tissue also causes cardiac failure<sup>124</sup>. Additionally, DOX inactivates RONS detoxifying enzymes, thus increasing the likelihood of anthracycline-induced cardiomyopathy.<sup>122,125</sup>

### 6.2 DOX-induced Doxorubicinol Mediated Cardiotoxicity

Doxorubicinol (DOXol) is a major metabolite of DOX that accumulates in cardiomyocytes, where it is produced by mitochondrial aldo-keto reductases (AKR) that reduce the C-13 carbonyl group to a secondary C-13 alcohol<sup>83</sup>. DOXol contributes to the delocalization and swelling of mitochondrial matrix of cardiomyocytes<sup>126,127,128</sup>. DOXol causes significant disruption to mitochondrial metabolism leading to declines in myocardial ATP, lactate, and phosphocreatine concentrations. Ultimately, this disrupts both oxidative and glycolytic metabolic pathways, causing severe cardiomyopathy<sup>129,130</sup>.

DOXol seems more effective than DOX at blocking the  $\text{Ca}^{2+}$ - $\text{Mg}^{2+}$  ATPase of sarcoplasmic reticulum, the  $\text{F}_0$ - $\text{F}_1$  proton pump of mitochondria, and the  $\text{Na}^+$ - $\text{K}^+$  ATPase and  $\text{Na}^+$ - $\text{Ca}^{2+}$  exchangers of the sarcolemma<sup>131</sup>. DOXol is also better than DOX at inhibiting spontaneous or caffeine-triggered  $\text{Ca}^{2+}$ -release from the sarcoplasmic reticulum<sup>132</sup>. *In vivo* studies in rabbits suggest DOXol induces LVEF dysfunction and interruption of the ryanodine receptor associated with the  $\text{Ca}^{2+}$  release channel of the sarcoplasmic reticulum, whereas less LVEF shortening was found with treatment using C-13 deoxy-DOX<sup>133</sup>. DOXol also modifies the aconitase/IRP-1 complex to a “null protein” that is devoid of aconitase and RNA binding activity by causing oxidative damage to

cysteine residues required to reconfigure an essential Fe-S cluster<sup>134-136</sup>. The inactivated aconitase/IRP-1 complex is incapable of sensing iron and fails to trigger iron uptake or sequestration, which consequence inactivates regulatory and metabolic pathways in the cardiomyocyte<sup>15</sup>. Ultimately this imbalance in iron homeostasis negatively impacts the heart systolic/diastolic cycle<sup>86</sup>.

## **7. Prevention of Cardiotoxicity**

The effective use of DOX as an antineoplastic agent relies on the tissue concentration of drug and/or the total systemic exposure over time, rather than the peak plasma concentration<sup>146</sup>. Thus some of the problems encountered with acute or early DOX-induced cardiotoxicity can be avoided by altering the schedule of administration. Instead of a single bolus of drug by intravenous (IV) injection every 3 weeks, IV delivery of DOX over a period of 48-96 hours and lower weekly doses have been shown to reduce CHF rates<sup>46,147-150</sup>. Regular monitoring for any clinical signs of cardiotoxicity by physical examination, x-rays, echocardiogram, electrocardiogram (EKG), endomyocardial biopsy, and radionuclide angiography before, during, and after DOX chemotherapy is necessary to avoid severe CHF and morbidity. Physical examination by itself can detect more than 50% of early and reversible DOX-dependent CHF.<sup>152-154</sup>

## **8. Anthracycline Analogs**

The cardiotoxicity encountered with DOX is inherent to its chemical structure. For decades, DOX analogs have been explored to reduce the required drug dose to achieve a therapeutic response, and to reduce cardiotoxic side effects and drug resistance. Some of these DOX analogs are discussed below.

### 8.1 Epirubicin

Epirubicin (4'-epidoxorubicin, EPI) is synthesized from DOX by epimerization of a hydroxyl group in the daunosamine sugar (Figure 7). This minor positional change discriminates the physicochemical and pharmacokinetic properties of EPI from DOX.

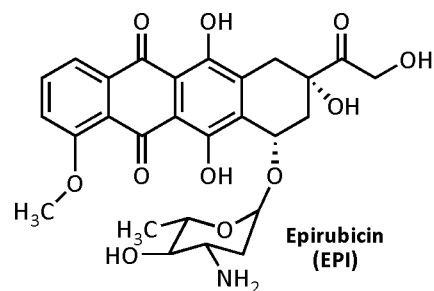


**Figure 1.7. The structure of epirubicin.**

EPI is more lipophilic, has weaker base characteristics, and a shorter half-life than DOX<sup>137,138</sup>. The rapid overall body clearance of EPI is due to  $\beta$ -glucuronidation by liver UDP-glucuronosyl transferase 2B7<sup>139</sup>, which diminishes its overall dose-induced cardiotoxicity<sup>140</sup>. EPI also undergoes limited one-electron reduction that predominantly occurs in cytoplasmic acid organelles, rather than the mitochondria<sup>141</sup>. Like DOX, AKR converts EPI to epirubicinol (EPIol) by limited two-electron reduction<sup>67,142,143</sup>. Several clinical studies have shown that EPI treatment does not produce as much of the toxic secondary alcohol in cardiac tissue<sup>149,150</sup>. CHF is not encountered with EPI at a single-dose level of 900-1000 mg/m<sup>2</sup>, which is 1.5 times higher than the dose limit for DOX<sup>141,144</sup>. In a study of breast cancer patients co-treated with 5-fluorouracil, cyclophosphamide, and EPI (90 mg/m<sup>2</sup>), followed by radiation therapy, patients did not show sign of symptomatic CHF in the first year of treatment<sup>145</sup>. Moreover, EPI-taxane combination therapy allowed a cumulative dose of EPI that was almost twice as high as that recommended for DOX<sup>146</sup>. However, minor LVEF was identified following cumulative EPI doses of 360-450 mg/m<sup>2</sup>. EPI is still reduced to EPIol and the minor formation of RONS can harm cardiomyocytes and decrease cardiac function<sup>147</sup>.

## 8.2 Idarubicin

Idarubicin (4-demethoxydaunorubicin, IDA) is a DNR derivative that lacks a methoxy group at position 4 (Figure 8). Like DOX and other anthracyclines, IDA is a DNA intercalating agent that interrupts topoisomerase II function and DNA

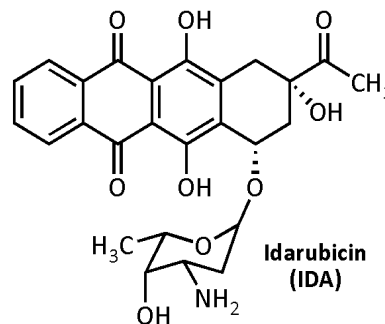


**Figure 1.8.** The structure of idarubicin.

replication<sup>14</sup>. IDA has a higher lipophilicity than DNR, which results in an improved rate of cellular uptake<sup>21</sup>, a longer half-life, and increased ability to cross the blood-brain barrier<sup>148</sup>. IDA is another key component of chemotherapy regimens, and is potentially superior to DNR in treatment of acute myeloid leukemia (AML)<sup>149,150</sup> and acute lymphocytic leukemia (ALL)<sup>151</sup>. Whereas DNR and DOX must be administered IV, IDA shows good oral bioavailability, although no benefit between oral and IV administration was observed for acute leukemia patients<sup>22</sup>. In randomized treatment trials, IDA showed less cardiotoxicity than DNR<sup>152</sup>. The increased drug effectiveness and prolonged survival in AML treatment makes IDA a better therapeutic than the parent DNR compound. However, in AML patients receiving a cumulative dose of 290 mg/m<sup>2</sup>, decreased LVEF and cardiomyopathy was observed<sup>21</sup>. Lastly, although IDA shows great potency in leukemia treatment, it appears to be less effective than DOX in treatment of metastatic breast cancer, and it still induces dose-dependent cardiotoxicity to those patients.<sup>153,154</sup>

### 8.3 Dissaccharide Anthracyclines

A third generation of anthracycline analogs, Sabarubicin (MEN-10755) and morpholinyl-derivatives such as nemorubicin (PNU-152243A), are now being investigated to satisfy the need to have both anticancer effectiveness and reduced dose-induced cardiotoxicity (Figure 9). Both of these compounds are designed to investigate the role of the C-3 amino group of the daunosamine sugar to disrupt type-II topoisomerase activity through DNA cleavage and stabilization of the drug-DNA-topoisomerase complex.<sup>155-157</sup>

Sabarubicin is known to be a leading disaccharide analog that is reported to have a better antitumor efficacy than DOX. Structurally, sabarubicin contains a 2,6-dideoxy-L-fucose between the aglycone and sugar moieties with an elimination of the methoxy substituent at C-4 in the aglycone. Sabarubicin exhibits an increased spectrum of antiproliferative activity in human tumor xenografts<sup>158</sup>, improved anti-topoisomerase II action<sup>159</sup>, and reduced cardiomyopathy when compared to DOX<sup>160</sup>. The drug half-life of sabarubicin is 50% shorter than DOX and its cellular uptake and tissue accumulation are slower<sup>161</sup>. Several *in vivo* studies report reduced conversion of sabarubicin to its toxic secondary alcohol metabolite (sabarubicinol, MEN-10755ol), hence lowering its cardiotoxic potential<sup>135,160</sup>. In addition, the alcohol metabolite of sabarubicin is less reactive than DOXol toward the [Fe-S] cluster of cytoplasmic aconitase/IRP-1,

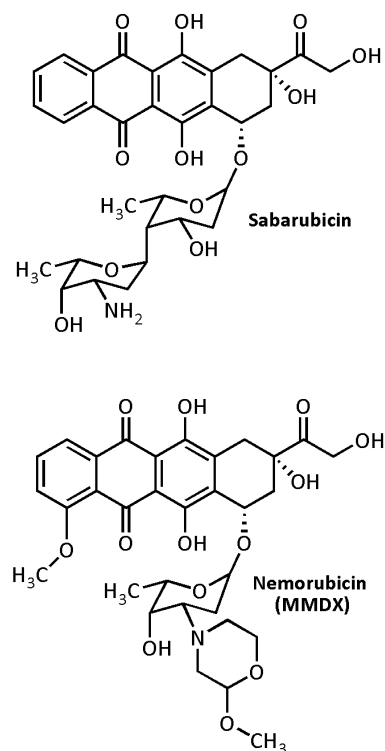


**Figure 1.9. The structures of sabarubicin and nemorubicin.**

which is involved in mediating anthracycline-induced cardiotoxicity<sup>162</sup>. In a phase I clinical trial, sabarubicin still caused myelosuppression, but the overall cumulative cardiotoxicity was mild, and only two patients showed decreased LVEF<sup>163</sup>. Furthermore, a phase II study of sabarubicin showed no CHF, although cardiotoxicity was observed in clinical trials in patients with regionally advanced or metastatic platinum/taxane resistant ovarian cancer<sup>164</sup>.

Another disaccharide derivative that is being explored for clinical use is nemorubicin (3'-deamino-3' [2''-(S)-methoxy-4-morpholinyl] doxorubicin; MMDX), which is a DOX derivative that retains a methoxymorpholinyl group at C-3 of the daunosamine sugar. Phase I and II clinical trials show promising results for the intrahepatic artery delivery of MMDX to treat hepatocellular carcinoma<sup>165-167</sup>. MMDX also shows encouraging efficacy against multidrug-resistant tumor cells *in vitro* and *in vivo*<sup>168,169</sup>. While minor damage to cardiac tissue was found by histological examination, *in vivo* studies of MMDX treatment at optimal therapeutic doses did not result in abnormal EKG<sup>170</sup>. In both animal and human clinical studies, MMDX appears to be 50-130 times more effective than DOX<sup>168,171</sup>. However, MMDX is only 2-10 fold more potent than DOX against adenocarcinomas (i.e ovarian and lung tumors) and hemocytoblasts in *in vitro* studies<sup>170,172</sup>. The increased anti-tumor activity may be due to the biotransformation of MMDX that leads to more cytotoxic metabolites (MMDX N-oxide, PNU-159696, and PNU-159682)<sup>165,167</sup>.

#### 8.4 C-13 Deoxy Anthracyclines

Since the carbonyl group at C-13 and/or in the quinone moiety has the notorious impact of causing anthracycline-induced cardiomyopathy, novel compounds lacking these structures have been developed. GPX-150 (5-imino 13-deoxydoxorubicin; DIDOX) is one such compound.

In GPX-150 the C-13 carbonyl has been removed, and the quinone carbonyl has been replaced with nitrogen to generate an iminoquinone. This structure is less capable of generating ROS and cardiotoxic alcohols (Figure 10). Experimentally, GPX-150 is a poor substrate for carbonyl reductase<sup>173</sup>, likely due to the absence of C-13 carbonyl group and quinone moiety. Holstein et al. demonstrated in a phase I dose escalation study (as high as 265 mg/m<sup>2</sup>) that GPX-150 did not elicit acute cardiomyopathy among patients with advanced solid tumors<sup>174</sup>. In fact, GPX-150 treatment produced no clinically significant harm to cardiac function, even in patients with prior anthracycline history and minor LVEF shortening<sup>174</sup>. Unlike other anthracyclines, GPX-150 treatment does not cause common patient side effects such as mucositis, stomatitis, or hand-foot syndrome. Further, a recent phase II study of GPX-150 for treatment of advanced and/or metastatic malignant STS patients revealed that this novel analog was well tolerated by patients with different sarcoma subtypes<sup>175</sup>. Furthermore, no irreversible cardiotoxicity was found and the toxicity profile that did result from the drug treatment appears to be manageable<sup>175</sup>.

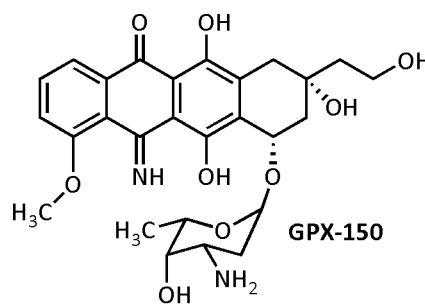


**Figure 1.10. The structure of C-13 deoxy anthracycline, GPX-150.**

### 8.5 Cancer-Targeted Formulations

In an attempt to overcome the therapy-limiting toxicity of conventional anthracyclines and to restrict anthracycline uptake into heart tissue, new pharmacological approaches have been developed. One innovative approach is a liposomal formulation that shows promising drug carrier technology to increase the therapeutic profile of DOX<sup>176,177</sup>. Liposomal systems allow easy drug-delivery from the circulation into tumor tissue, in which cells are not as tightly joined as cells in normal tissues<sup>202</sup>. However, the application of liposome-encapsulated DOX is limited due to its short half-life in plasma and the formation of cardiotoxic metabolites<sup>179</sup>.

A number of liposomal DOX formulations that incorporate polymers such as polyethylene glycol (PEG), ganglioside, and cerebroside sulfate have been shown to actively target tumors and prolong serum half-life<sup>180</sup>. Pegylated-liposomal DOX (DOXil) is an FDA-approved formulation that resists drug uptake by the reticuloendothelial system (RES), improving its plasma half-life up to 4 days<sup>181</sup>. Also, DOXil remains encapsulated until it has reached the tumor cells<sup>182,183</sup>. Despite the promising effects of DOXil, it can still cause hand-foot syndrome (HFS or palmar-plantar erythrodyesthesia), which is characterized by skin eruptions on the palms of the hands and soles of the feet<sup>184</sup>.

### 8.6 Cardioprotective Agents

Dexrazoxane (DZR, ICRF-187, Cardioxane<sup>®</sup>) is the only drug that has been approved in the U.S, Canada, and Europe to protect against anthracycline-mediated

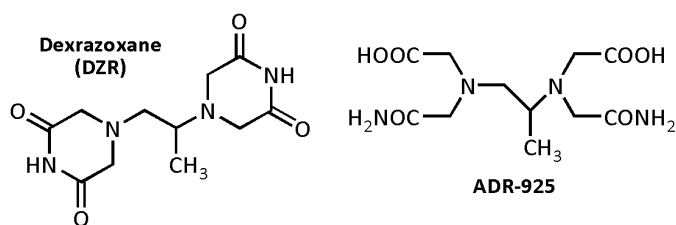


**Figure 1.11. The structures of dexrazoxane and its metal ion chelating hydrolysis product, ADR-925.**

cardiotoxicity<sup>185,186</sup>. DZR is a bisdioxopiperazine and an enantiomer of razoxane, which was initially discovered as a chemotherapeutic agent. DZR quickly penetrates the cell membrane and is enzymatically hydrolyzed to produce ADR-925, an active metal chelator (Figure 11). ADR-925 ligates free iron and inhibits the generation of ROS by anthracycline-Fe complexes. ADR-925 also readily dissociates Fe (III) from the anthracycline-iron complexes. The cardioprotective mechanism of DZR is not fully understood, but it is proposed to be a better chelator of Fe (III) than DOX, and thus blocks iron-driven RONS production<sup>187</sup>. DZR also disrupts Top2 activity like DOX, although through a distinct mechanism. DZR stabilizes the ATP-bound closed-clamp configuration of Top2 through antagonist interaction with the Top2-DNA complexes<sup>188,189,190</sup>.

In the U.S, DZR is labeled as an orphan drug for treatment of metastatic breast cancer in patients who have already received 300 mg/m<sup>2</sup> DOX. The results of two Phase III clinical studies reported that concomitant DZR treatment with fluorouracil, doxorubicin, and cyclophosphamide (collectively referred to as “FAC”) in advanced breast cancer produced significant cardioprotection<sup>191</sup>. Also, Swain et al. reported that DZR decreased cardiac risk during DOX treatment 2.5-fold<sup>192</sup>. DZR is highly active in both adults and children, and prevents DOX-induced oxidative damage to cardiomyocytes without interruption of DOX anticancer activity<sup>193,194</sup>. Despite this, DZR use is limited due to severe exacerbation of DOX mediated myelosuppression<sup>195</sup>.

## 9. Conclusion

Studies to improve the clinical potency, efficacy, and safety of DOX and its analogs are ongoing. DOX is the primary anticancer anthracycline in clinical use. It is hypothesized that the mechanisms of DOX action as an anticancer agent include the fast diffusion into the nucleus, where it intercalates between nucleotide base pairs of the DNA based on the planar ring structure of the aglycone. Following intercalation, covalent adducts to the DNA strand and DNA intrastrand cross-linkage are possible, as well as inhibition of topoisomerase II activity that leads to DSBs and interruption of DNA replication.

Although DOX may be a useful chemotherapeutic due to its versatility in treating many tumor types, it causes adverse effects in cancer patients. The main adverse effect of DOX treatment is acute and chronic cardiotoxicity. This remains major problems to be resolved in DOX therapy. The mechanisms by which DOX induces cardiotoxicity include accumulation of reactive iron species ( $\text{Fe}^{2+}$  and  $\text{Fe}^{3+}$ ), formation of a toxic secondary alcohol metabolite by carbonyl reductases, overproduction of hazardous RONS, interference with calcium ion homeostasis, and mitochondrial dysfunction. Due to these therapeutic problems with DOX, the design of second and third generation DOX analogs to prevent cardiotoxicity and drug resistance, without losing the anticancer activity, has progressed. The development of DOX disaccharides, C-13 deoxy anthracyclines, liposomal formulations, and cardioprotective agents are new approaches to improve the therapeutic profile of anticancer anthracyclines.

The goal of this study was to evaluate the ability of DOX derivatives to exert *in vitro* cytotoxic effects against various human STS and normal cells, and reduce tumor growth in an *in vivo* human STS xenograft model in nude mice. In addition, the ability of DOX

analogs to overcome drug efflux mediated drug resistance, inhibit topoisomerase II, and pharmacokinetics was characterized. The results indicate that the newest generation of analogs are promising anticancer agents that should not stimulate cardiotoxicity and should overcome drug resistance issues commonly encountered with DOX.

## REFERENCES

- (1) American Cancer Society. *Cancer Facts and Figures 2017*. Retrieved from <https://www.cancer.org/content/dam/cancer-org/research/cancer-facts-and-statistics/annual-cancer-facts-and-figures/2017/cancer-facts-and-figures-2017.pdf>
- (2) Byerly S, Chopra, S, Nassif, NA, Chen, P, Sener SF, Eisenberg BL, Tseng WW. *J. Surg. Oncol.* 2016 Mar 11;113(3):333-8 [PubMed: 26662660].
- (3) Clark MA, Fisher C, Judson I, Thomas JM. *N. Engl. J. Med.* 2005 Aug 18;353(7):701-11 [PubMed: 16107623].
- (4) Fletcher CDM, Unni KK, Mertens Fredrik. *Cancer* 2002, 177 (3), 1365.
- (5) Kanas GP, Taylor A, Primrose JN, Langeberg WJ, Kelsh MA, Mowat, FS, Alexander DD, Choti MA, Poston G. *Clin. Epidemiol.* 2012;4:283-301 [PubMed: 23152705].
- (6) Wang S, Ren W, Liu J, Lahat , Torres K, Lopez G, Lazar AJ, Hayes-Jordan A, Liu K, Bankson J, Hazle JD, Lev D. *Clin. Cancer Res.* 2010 May1;16(9);2591-604[PubMed: 20406839].
- (7) Blum RH, Carter SK. *Ann. Intern. Med.* 1974 Feb;80(2):249-59 [PubMed:4590654].
- (8) Mross K. *Eur. J. Cancer.* 1991;27(12):1542-4.
- (9) Hortobagyi GN. *Drugs* 1997;54 Suppl 4:1-7 [PubMed: 9361955].
- (10) Arcamone F, Cassinel G, Fantini G, Grein A, Orezzi P, Pol C, Spalla C. *Biotechnol. Bioeng.* 1969 Nov;11(6):1101-10 [PubMed: 5365804].
- (11) Cortés-Funes H, Coronado C. *Cardiovasc. Toxicol.* 2007;7(2):56-60 [PubMed: 17652804].
- (12) Cullinane C, Phillips DR. *Biochemistry.* 1990 Jun 12;29(23):5638-46 [PubMed: 2386792].

- (13) World Health Organization. "19th WHO Model List of Essential Medicines (April 2015)." *Geneva, Switzerland* (2015).
- (14) Gewirtz, DA. *Biochem. Pharmacol.* 1999 Apr 1;57(7):727-41 [PubMed: 10075079].
- (15) Cairo G, Pietrangelo A. *Biochem. J.* 2000 Dec 1;352 Pt 2:241-50 [PubMed: 11085915].
- (16) Taatjes DJ, Gaudiano G, Resing K, Koch TH. *J. Med. Chem.* 1996 Oct 11;39(21):4135-8 [PubMed: 8863788].
- (17) Minotti G, Menna P, Salvatorelli E, Cairo G, Gianni L. *Pharmacol. Rev.* 2004 Jun;56(2): 185-229 [PubMed: 15169927].
- (18) Guano F, Pourquier P, Tinelli S, Binaschi M, Bigioni M, Animati F, Manzini S, Zunino F, Kohlhagen G, Pommier Y, Capranico G. *Mol. Pharmacol.* 1999 Jul;56(1):77-84 [PubMed: 10385686].
- (19) Cipollone A, Berettoni M, Bigioni M, Binaschi M, Cermele C, Monteagudo E, Olivieri L, Palomba D, Animati F, Goso C, Maggi CA. *Bioorg. Med. Chem.* 2002 May;10(5):1459-70 [PubMed: 11886808].
- (20) Nagy A, Armatis P, Schally AV. *Proc. Natl. Acad. Sci. U. S. A.* 1996 Mar 19;93(6):2464-9 [PubMed: 8637897].
- (21) Anderlini P, Benjamin RS, Wong FC, Kantarjian HM, Andreeff M, Kornblau SM, O'Brien S, Mackay B, Ewer MS, Pierce SA. *J. Clin. Oncol.* 1995 Nov;13(11):2827-34 [PubMed: 7595745].
- (22) Weiss RB. *Semin. Oncol.* 1992 Dec;19(6):670-86 [PubMed: 1462166].
- (23) Kellner U, Sehested M, Jensen PB, Gieseler F, Rudolph P. *Lancet Oncol.* 2002 Apr;3(4):235-43 [PubMed: 12067686].
- (24) Zunino F, Capranico G. *Anticancer. Drug. Des.* 1990 Nov;5(4):307—317 [PubMed: 1963303].
- (25) Nitiss JL. *Biochim. Biophys. Acta.* 1998 Oct 1;1400(1-3):63-81 [PubMed: 9748506].

- (26) Soret J, Gabut M, Dupon C, Kohlhagen G, Stévenin J, Pommier Y, Tazi J. *Cancer Res.* 2003 Dec 1;63(23):8203-11 [PubMed: 14678976].
- (27) Wang JC. *Q. Rev. Biophys.* 1998 May;31(2):107-44 [PubMed: 9794033].
- (28) Nitiss JL. *Nat. Rev. Cancer* 2009 May;9(5):338-50 [PubMed: 19377506].
- (29) Sandri MI, Hochhauser D, Ayton P, Camplejohn RC, Whitehouse R, Turley H, Gatter K, Hickson ID, Harris AL. *Br. J. Cancer* 1996 Jun;73(12):1518-24 [PubMed: 8664122].
- (30) Iorio MV, Visone R, Di Leva G, Donati V, Petrocca F, Casalini P, Taccioli C, Volinia S, Liu CG, Alder H, Calin GA, Ménard S, Croce CM. *Cancer Res.* 2007 Sep 15;67(18):8699-707 [PubMed: 17875710].
- (31) Zhang A, Lyu YL, Lin CP, Zhou N, Azarova AM, Wood LM, Liu LF. *J. Biol. Chem.* 2006 Nov 24;281(47):359976003 [PubMed: 16973621].
- (32) Xiao H, Mao Y, Desai S, Zhou N, Ting C, Hwang J, Liu LF. *Proc. Natl. Acad. Sci. U. S. A.* 2003 Mar 18;100(6):3239-44 [PubMed: 12629207].
- (33) Kuriyama M, Tsutsui K, Tsutsui K, Ono Y, Tamiya T, Matsumoto K, Furuta T, Ohmoto T. *Neurol. Med. Chir. (Tokyo).* 1997 Sep;37(9):655-62 [PubMed: 9330528].
- (34) Tewey KM, Rowe TC, Yang L, Halligan BD, Liu LF. *Science.* 1984 Oct 26;226(4673): 466-8 [PubMed: 6093249].
- (35) Kalyanaraman B, Perez-Reyes E, Mason RP. *Biochim. Biophys. Acta.* 1980 Jun 5;630(1):119-30 [PubMed: 6248123].
- (36) Vasquez-Vivar J, Martasek P, Masters BS, Pritchard KA, Kalyanaraman B. *Biochemistry* 1997 Sep 23;36(38):11293-7 [PubMed: 9333325].
- (37) Sinha BK. *Chem. Bio. Interact.* 1989;69(4):293-317 [PubMed: 2659197].
- (38) Ramji S, Lee C, Inaba T, Patterson AV, Riddick DS. *Cancer Res.* 2003 Oct 15;63(20):6914-9 [PubMed: 14583491].
- (39) Gille L, Nohl H. *Free Radic. Biol. Med.* 1997;23(5):775-82 [PubMed: 9296455].

- (40) Laurent G, Jaffrézou JP. *Blood*. 2001 Aug 15;98(4):913-24 [PubMed: 11493433].
- (41) Martín D, Salinas M, Fujita N, Tsuruo T, Cuadrado A. *J. Biol. Chem.* 2002 Nov 8;277(45):42943-52 [PubMed: 12213802].
- (42) Bezombes C, de Thonel A, Apostolou A, Louat T, Jaffrézou, JP, Laurent G, Quillet-Mary A. *Mol. Pharmacol.* 2002 Dec;62(6):1446-55 [PubMed: 12435813].
- (43) Kim R, Tanabe K, Uchida Y, Emi M, Inoue H, Toge T. *Cancer Chemother. Pharmacol.* 2002 Nov;50(5):343-52 [PubMed: 12439591].
- (44) Sugioka K, Nakano H, Noguchi T, Tsuchiya J, Nakano M. *Biochem. Biophys. Res. Commun.* 1981 Jun 16;100(3):1251-8 [PubMed: 6791644].
- (45) Katsuaki S, Minoru N. *Biochim. Biophys. Acta.* 1982 Nov 12;713(2):333-43.
- (46) Muindi J, Sinha BK, Gianni L, Myers C. *Mol. Pharmacol.* 1985 Mar;27(3):356-65 [PubMed: 2983184].
- (47) Cutts SM, Nudelman A, Rephaeli A, Phillips DR, *IUBMB Life*. 2005 Feb;57(2):73-81 [PubMed: 16036566].
- (48) Cutts SM, Rephaeli A, Nudelman A, Hmelnitsky I, Phillips DR. *Cancer Res.* 2001 Nov 15;61(22):8194-202 [PubMed: 11719450].
- (49) Sinha BK, Chignell CF. *Chem. Biol. Interact.* 1979 Dec;28(2-3):301-8 [PubMed: 549745].
- (50) Taatjes DJ, Gaudiano G, Resing K, Koch TH. *J. Med. Chem.* 1997 Apr 11;40(8):1276-86 [PubMed: 9111302].
- (51) Zeman SM, Phillips DR, Crothers DM. *Proc. Natl. Acad. Sci. U. S. A.* 1998 Sep 29;95(20):11561-5 [PubMed: 9751705].
- (52) Pan SS, Bachur NR. *Mol. Pharmacol.* 1980 Jan;17(1):95-9 [PubMed: 6892948].
- (53) Stepankova J, Studenovský M, Malina J, Kasparkova J, Liskova B, Novakova O, Ulbrich K, Brabec V. *Biochem. Pharmacol.* 2011 Aug 1;82(3):227-35 [PubMed: 21570955].

- (54) Taatjes DJ, Koch TH. *Curr. Med. Chem.* 2001 Jan;8(1):15-29 [PubMed: 11172689].
- (55) Leng F, Savkur R, Fokt I, Przewloka T, Priebe W, Chaires JB. *J. Am. Chem. Soc.* 1996 May 22;118(20):4731-4738.
- (56) Wang AHJ, Gao YG, Liaw YC, Li YK. *Biochemistry* 1991 Apr;30(16):3812-15 [PubMed: 2018756].
- (57) Kato S, Burke P, Koch T, Bierbaum V. *Anal. Chem.* 2001 Jul 1;(73):2991.
- (58) Cutts SM, Nudelman A, Pillay V, Spencer DM, Levovich I, Rephaeli A, Phillips DR. *Oncol. Res.* 2005;15(4):199-213 [PubMed: 17822280].
- (59) Taatjes DJ, Fenick DJ, Koch TH. *Chem. Res. Toxicol.* 1999 Jul;12(7):588-96 [PubMed: 10409398].
- (60) DD V, MW L, Basa P, Davis HL, Von Hoff AL. *Ann. Intern. Med.* 1979, 91 (5), 710 [PubMed: 496103].
- (61) Steinherz LJ, Steinhezs PG, Tan CT, Heller G, Murphy ML. *JAMA* 1991 Sep 25;266(12):1672-7 [PubMed: 1886191].
- (62) Bristow MR, Billingham ME, Mason JW, Daniels JR. *Cancer Treat. Rep.* 1978 Jun;62(6):873-9 [PubMed: 667861].
- (63) Billingham ME, Bristow MR, Glatstein E, Mason JW, Masek MA, Daniels JR. *Am. J. Surg. Pathol.* 1977, 1 (1) [PubMed: 602969].
- (64) Giantris A, Abdurrahman L, Hinkle A, Asselin B, Lipshultz SE. *Crit. Rev. Oncol. Hematol.* 1998 Jan;27(1):53-68 [PubMed: 9548017].
- (65) Bristow MR, Thompson, PD, Martin RP, Mason JW, Billingham ME, Harrison DC. *Am. J. Med.* 1978 Nov;65(5):823-32 [PubMed: 707541].
- (66) Steinberg JS, Cohen AJ, Wasserman AG, Cohen P, Ross AM. *Cancer* 1987 Sep 15;60(6):1213-8 [PubMed: 3621107].
- (67) Salvatorelli E, Menna P, Gianni L, Minotti G. *J. Pharmacol. Exp. Ther.* 2007 Feb;320(2):790-800 [PubMed: 17135345].

- (68) Bristow MR, Mason JW, Billingham ME, JR, D. *Ann. Intern. Med.* 1978, 88 (2), 168 [PubMed: 626445].
- (69) Wallace, KB, *Pharmacol. Toxicol.* 2003 Sep;93(3):105-15 [PubMed: 12969434].
- (70) Boucek R, Olson RD, Brenner DE, Ogunbunmi EM, Inui M, Fleischer, S. *J. Biol. Chem.* 1987 nov 25;262(33):15851-6 [PubMed: 2890636].
- (71) Buzdar AU, Gutterman JU, Blumenschein GR, Hortobagyi GN, Tashima CK, Smith TL, Hersh EM, Freireich EJ, Gehan EA. *Cancer.* 1978 Mar;41(3):1064-75 [PubMed: 638948].
- (72) Lipshultz SE, Colan SD, Gelber RD, Perez-Atayde AR, Sallan SE, Sanders SE, N. *Engl. J. Med.* 1991 Mar 21;324(12):808-15 [PubMed: 1997853].
- (73) Lipshultz SE, Lipsitz SR, Sallan SE, Dalton VM, Mone SM, Gelber RD, Colan SD. *J. Clin. Oncol.* 2005 Apr 20;23(12):2629-36 [PubMed: 15837978].
- (74) Jones, RL, Swanton C, Ewer MS. *Expert Opin. Drug Saf.* 2006, Nov;5(6):791-809 [PubMed: 17044806].
- (75) Scully RE, Lipshultz SE. *Cardiovasc. Toxicol.* 2007;7(2):122-8 [PubMed: 17652816].
- (76) van Dalen EC, van der Pal HJ, Kok WE, Caron HN, Kremer LC. *Eur. J. Cancer* 2006 Dec;42(18):3191-8 [PubMed: 16987655].
- (77) Pinder MC, Duan Z, Goodwin JS, Hortobagyi GN, Giordano SH, *J. Clin. Oncol.* 2007 Sep 1;25(25):3808-15 [PubMed: 17664460].
- (78) Zambetti M, Moliterni A, Materazzo C, Stefanelli M, Cipriani S, Valagussa P, Bonadonna G, Gianni L. *J. Clin. Oncol.* 2001 Jan1;19(1):37-43 [PubMed: 11134193].
- (79) Doroshov JH, Davies KJ. *J. Biol. Chem.* 1986 Mar 5;261(7):3068-74 [PubMed: 3005279].
- (80) Gianni L, Herman EH, Lipshultz SE, Minotti G, Sarvazyan N, Sawyer DB. *J. Clin. Oncol.* 2008 Aug1;26(22):3777-84 [PubMed: 18669466].

- (81) Singal PK, Iliskovic N, Li T, Kumar D. *FASEB J.* 1997 Oct;11(12):931-6 [PubMed: 9337145].
- (82) Kalyanaraman B. *Cardiovasc. Toxicol.* 2007;7(2):92-4 [PubMed: 17652811].
- (83) Licata S, Saponiero A, Mordente A, Minotti G. *Chem. Res. Toxicol.* 2000 May;13(5):414-20 [PubMed: 10813659].
- (84) Bozcali E, Dedeoglu DB, Karpuz V, Suzer O, Karpuz H. *Acta Cardiol.* 2012 Feb;67(1):87-96 [PubMed: 22455094].
- (85) Menna P, Salvatorelli E, Minotti G. *Chem. Res. Toxicol.* 2008 May;21(5):978-89 [PubMed: 18376852].
- (86) Minotti G, Cairo G, Monti E. *FASEB J.* 1999 Feb;13(2):199-212 [PubMed: 9973309].
- (87) Singal Pk, Iliskovic N. *N. Engl. J. Med.* 1998 Sep 24;339(13):900-5 [PubMed: 9744975].
- (88) Powis G. *Free Radic. Biol. Med.* 1989;6(1):63-101 [PubMed: 2492250].
- (89) Doroshow JH. *Cancer Res.* 1983 Oct;43(10):4543-51 [PubMed: 6309369].
- (90) Davies KJ, Doroshow JH. *J. Biol. Chem.* 1986 Mar 5;261(7):3060-7 [PubMed: 3456345].
- (91) Myers C. *Semin. Oncol.* 1998 Aug;25(4 Suppl 10):10-14 [PubMed: 9768818].
- (92) Doroshow JH. *Cancer Res.* 1983 Feb;43(2):460-72 [PubMed: 6293697].
- (93) Cummings J, Allan L, Willmott N, Riley R, Workman P, Smyth JF. *Biochem. Pharmacol.* 1992 Dec 1;44(11):2175-83 [PubMed: 1472082].
- (94) Pawłowska J, Tarasiuk J, Borowski E, Wąsowska M, Oszczapowicz I, Wolf CR. *Acta. Biochim Pol.* 2000;47(1):141-7 [PubMed: 10961687].
- (95) Yee SB, Pritsos C. *Arch. Biochem. Biophys.* 1997 Nov 15;347(2):235-41 [PubMed: 9367530].

- (96) Garner AP, Paine MJ, Rodriguez-crespo I, Chinje EC, Montellano PO De, Stratford IJ, Tew DG, Wolf CR. *Cancer Res.* 1999 Apr 15;59(8):1929-34 [PubMed: 10213502].
- (97) Neilan TG, Blake SI, Ichinose F, Raheer MJ, Buys ES, Jassal DS, Furutani E, Perez-Sanz TM, Graveline A, Janssens SP, Picard MH, Scherrer-Crosbie M, Bloch KD. *Circulation* 2007 Jul 31;116(5):506-14 [PubMed: 17638931].
- (98) Bates DA, Winterbourn CC. 1982 Apr 1;203(1):155-60 [PubMed: 6285890].
- (99) Zweier JL. *J. Biol. Chem.* 1984 May 25;259(10):6056-8 [PubMed: 6327662].
- (100) Beraldo H, Garnier-Suillerot A, Tosi L, Lavelle F. *Biochemistry* 1985 Jan 15;24(2):284-9 [PubMed: 2983753].
- (101) Zweier JL. *Biochim. Biophys. Acta.* 1985 Apr 17;839(2):209-13 [PubMed: 2985121].
- (102) Hasinoff BB. *Biochem. J.* 1990 Feb 1;265(3):865-70 [PubMed: 2306220].
- (103) Hasinoff BB. *Biochem. Cell Biol.* 1990 Dec;68(12):1331-16 [PubMed: 1964792].
- (104) Wallace KB. *Toxicol. Appl. Pharmacol.* 1986 Oct;86(1):69-79 [PubMed: 3094197].
- (105) Dutta PK, Hutt JA. *Biochemistry* 1986 Feb;25(3):691-5 [PubMed: 3955025].
- (106) Malatesta V, Morazzoni F, Gervasini A, Arcamone F. *Anticancer. Drug Des.* 1985 Oct;1(1):53-57 [PubMed: 2835962].
- (107) Kotamraju S, Konorev EA, Joseph J, Kalyanaraman B. *J. Biol. Chem.* 2000 Oct 27;275(43):33585-92 [PubMed: 10899161].
- (108) Kotamraju S, Kalivendi SV, Konorev E, Chitambar CR, Joseph J, Kalyanaraman B. *Methods Enzymol.* 2004;378:362-82 [PubMed: 15038980].
- (109) Dowd NP, Scully M, Adderley SR, Cunningham AJ, Fitzgerald DJ. *J. Clin. Invest.* 2001 Aug;108(4):585-90 [PubMed: 11518732].
- (110) Fogli S, Nieri P, Breschi MC. *FASEB J.* 2004 Apr;18(6):664-75 [PubMed: 15054088].

- (111) Mihm MJ, Yu F, Weinstein DM, Reiser PJ, Bauer JA, *Br. J. Pharmacol.* 2002 Feb;135(3):581-8 [PubMed: 11834605].
- (112) Weinstein DM, Mihm MJ, Bauer JA. *J. Pharmacol. Exp. Ther.* 2000 Jul;294(1):396-401 [PubMed: 10871338].
- (113) Aldieri E, Bergandi L, Riganti C, Costamagna C, Bosia, Ghigo D. *Toxicol. Appl. Pharmacol.* 2002 Dec 1;185(2):85-90 [PubMed: 12490132].
- (114) Wallace KB. *Cardiovasc. Toxicol.* 2007;7(2):101-7 [PubMed: 17652813].
- (115) Berthiaume JM, Wallace KB. *Cell Biol. Toxicol.* 2007 Jan;23(1):15-25 [PubMed: 17009097].
- (116) D'Amico G, Lam F, Hagen T, Moncada S. *J. Cell Sci.* 2006 Jun 1;119(Pt 11):2291-8 [PubMed: 16723735].
- (117) Xiong Y, Liu X, Lee CP, Chua BH, Ho YS. *Free Radic. Biol. Med.* 2006 Jul 1;41(1):46-55 [PubMed: 16781452].
- (118) Oliveira PJ, Santos MS, Wallace KB. *Biochemistry. (Mosc).* 2006 Feb;7(2):194-9 [PubMed: 16489925].
- (119) Tokarska-Schlattner M, Zaugg M, Zuppinger C, Wallimann T, Schlattner U. *J. Mol. Cell. Cardiol.* 2006 Sep;41(3):389-405 [PubMed: 16879835].
- (120) Kalyanaraman B, Joseph J, Kalivendi S, Wang S, Konorev E, Kotamraju S. *Biochem. J.* 2002 Nov 1;367(Pt3):729-40 [PubMed: 12139490].
- (121) Li G, Chen Y, Saari JT, Kang YJ. *Am. J. Physiol.* 1997 Sep;273(3 Pt 2):1090-5 [PubMed: 9321793].
- (122) Doroshov JH, Locker GY, Myers CE. *J. Clin. Invest.* 1980 Jan;65(1):128-35 [PubMed: 7350193].
- (123) Chen Y, Saari JT, Kang YJ. *Free Radic. Biol. Med.* 1994 Dec;17(6):529-36 [PubMed: 7867969].
- (124) Goffart S, Von Kleist-Retzow JC, Wiesner RJ, *Cardiovasc. Res.* 2004 Nov 1;64(2):198- 207 [PubMed: 15485678].

- (125) Siveski-Iliskovic N, Hill M, Chow DA, Singal PK. *Circulation* 1995 Jan 1;91(1):10-15 [PubMed: 7805190].
- (126) Aversano RC, Boor PJ. *J. Mol. Cell. Cardiol.* 1983 Aug;15(8):543-53 [PubMed: 6672210].
- (127) Friedman MA, Bozdech MJ, Billingham ME, Rider AK. *JAMA.* 1978 Oct 6;240(15):1603-6 [PubMed: 691145].
- (128) Rosenoff SH, Olson HM, Young DM, Bostick F, Young RC. *J. Natl. Cancer Inst.* 1975 Jul;55(1):191-4 [PubMed: 1159813].
- (129) Dekker T, van Echteld CJ, Kirkels JH, Ruigrok TJ, van Hoesel QG, de Jong WH, Schornagel JH. *NMR Biomed.* 1991 Feb;4(1):16-24 [PubMed: 2029456].
- (130) Ferrero ME, Ferrero E, Gaja G, Bernelli-Zazzera A. *Biochem. Pharmacol.* 1976 Jan 15;25(2):125-30 [PubMed: 177021].
- (131) Olson RD, Mushlin PS. *FASEB J.* 1990 Oct;4(13):3076-86 [PubMed: 2210154].
- (132) Zucchi R, Yu G, Ghelardoni S, Ronca F, Ronca-Testoni S. *Br. J. Pharmacol.* 2000 Sep;13(2):342-8 [PubMed: 10991929].
- (133) Gambliel HA, Burke BE, Cusack BJ, Walsh GM, Zhang YL, Mushlin PS, Olson RD. *Biochem. Biophys. Res. Commun.* 2002 Mar 1;291(3):433-8 [PubMed: 1855807].
- (134) Brazzolotto X, Andriollo M, Guiraud P, Favier A, Moulis JM. *Biochim. Biophys. Acta.* 2003 Feb 17;1593(2-3):209-18 [PubMed: 12581865].
- (135) Minotti G, Ronchi R, Salvatorelli E, Menna P, Cairo G. *Cancer Res.* 2001 Dec 1;61(23):8422-8 [PubMed: 11731422].
- (136) Minotti G, Recalcati S, Mordente A, Liberi G, Calafiore AM, Mancuso C, Preziosi P, Cairo G. *FASEB J.* 1998 May;12(7):541-52 [PubMed: 9576481].
- (137) Danesi R, Fogli S, Gennari A, Conte P, Del Tacca M. *Clin. Pharmacokinet.* 2002;41(6):431-44 [PubMed: 12074691].
- (138) Robert J, Gianni L. *Cancer Surv.* 1993;17:219-52 [PubMed: 8137342].

- (139) Innocenti F, Iyer L, Ramirez J, Green, MD, Ratain MJ. *Drug Metab. Dispos.* 2001 May;29 (5):686-92 [PubMed: 11302935].
- (140) Bonadonna G, Gianni L, Santoro A, Bonfante V, Bidoli P, Casali P, Demicheli R, Valagussa P. *Ann. Oncol.* 1993 May;4(5):359-69 [PubMed: 8353070].
- (141) Salvatorelli E, Guarnieri S, Menna P, Liberi G, Calafiore AM, Mariggio MA, Mordente A, Gianni L, Minotti G. *J. Biol. Chem.* 2006 Apr 21;281(16):10990-1001 [PubMed: 16423826].
- (142) Salvatorelli E, Menna P, Cascegnà S, Liberi G, Calafiore AM, Gianni L, Minotti GJ. *Pharmacol. Exp. Ther.* 2006 Jul;318(1):424-33 [PubMed: 16614166].
- (143) Sacco G, Giampietro R, Salvatorelli E, Menna P, Bertani N, Graiani G, Animati F, Goso C, Maggi CA, Manzini S, Minotti G. *Br. J. Pharmacol.* 2003 Jun;139(3):641-51 [PubMed: 12788824].
- (144) Vicente-Hernández B, Sarre-Álvarez, D, Rodríguez-Weber FL, Díaz-Greene EJ. *Med. Interna Mex.* 2015, 31 (5), 567.
- (145) Meinardi MT, van Veldhuisen DJ, Gietema JA, Dolsma WV, Boomsma F, van den Berg MP, Volkers C, Haaksma J, de Vries EG, Sleijfer DT, van der Graaf WT. *J Clin Oncol* 2001 May 15;19(10):2746-53 [PubMed: 11352968].
- (146) Pagani O, Sessa C, Nole F, Crivellari D, Lombardi D, Thurlimann B, Hess D, Borner M, Bauer J, Martinelli G, Graffeo R, Zucchetti M, D'Incalci M, Goldhirsch A. *Ann. Oncol.* 2000 Aug;11(8):985-91 [PubMed: 11038035].
- (147) Salvatorelli E, Menna P, Lusini M, Covino E, Minotti G. *J. Pharmacol. Exp. Ther.* 2009 Apr;329(1):175-84 [PubMed: 19144686].
- (148) Bassan R, Lerede T, Rambaldi A, Di Bona E, Rossi G, Pogliani E, Lambertenghi-Deliliers G, Porcellini A, Fabris P, Barbui T. *Leukemia* 1996 Jun;10 Suppl 2:s58-61 [PubMed: 8649053].
- (149) Berman E, Heller G, Santorsa J, McKenzie S, Gee T, Kempin S, Gulati S, Andreeff M, Kolitz J, Gabrilove J. *Blood.* 1991 Apr15;77(8):1666-74 [PubMed: 2015395].

- (150) Vogler WR, Velez-Garcia E, Weiner RS, Flaum MA, Bartolucci AA, Omura GA, Gerber MC, Banks PL. *J. Clin. Oncol.* 1992 Jul;10(7):1103-11 [PubMed: 1607916].
- (151) Weiss, RB. *Contemp. Oncol.* 1992, 2, 30-9.
- (152) Casazza AM, Bertazzoli C, Pratesi G, Marco AD. *Astr.* 1979. 16.
- (153) Lopez M, Contegiacomo A, Vici P, Dello Loio C, Di Lauro L, Pagliarulo C, Carpano S, Giannarelli D, De Placido S, Fazio S. *Cancer.* 1989 Dec 15;64(12):2431-6 [PubMed: 2684383].
- (154) Crivellari D, Lombardi D, Corona G, Massacesi C, Talamini R, Sorio R, Magri MD, Lestuzzi C, Lucenti A, Veronesi A, Toffoli G. *Ann. Oncol.* 2006 May;17(5):807-12 [PubMed: 16497825].
- (155) Mordente A, Meucci E, Silvestrini A, Martorana GE, Giardina B. *Curr. Med. Chem.* 2009;16(13):1656-72 [PubMed: 19442138].
- (156) Capranico G, Supino R, Binaschi M, Capolongo L, Grandi M, Suarato A, Zunino F. *Mol Pharmacol.* 1994 May;45(5):908-15 [PubMed: 8190107].
- (157) Binaschi M, Bigioni M, Cipollone A, Rossi C, Goso C, Maggi CA, Capranico G, Animati F. *Curr. Med. Chem. Anticancer. Agents* 2001 Aug;1(2):113-30 [PubMed: 12678762].
- (158) Bigioni M, Salvatore C, Bullo A, Bellarosa D, Iafrate E, Animati F, Capranico G, Goso C, Maggi CA, Pratesi G, Zunino F, Manzini S. *Biochem. Pharmacol.* 2001 Jul 1;62(1):63-70 [PubMed: 11377397].
- (159) Pratesi G, De Cesare M, Caserini C, Perego P, Dal Bo L, Polizzi D, Supino R, Bigioni M, Manzini S, Iafrate E, Salvatore C, Casazza A, Arcamone F, Zunino F. *Clin. Cancer Res.* 1998 Nov;4(11):2833-9 [PubMed: 9829750].
- (160) Cirillo R, Sacco G, Venturella S, Brightwell J, Giachetti A, Manzini S. *J. Cardiovasc. Pharmacol.* 2000. Jan;35(1):100-8 [PubMed: 10630739].
- (161) Gonzalez-Paz O, Polizzi D, De Cesare M, Zunino F, Bigioni M, Maggi CA, Manzini S, Pratesi G. *Eur J Cancer* 2001 Feb;37(3):431-7 [PubMed: 11239767].

- (162) Minotti G, Licata S, Saponiero A, Menna P, Calafiore AM, Di Giamniarco G, Liberi G, Animati F, Cipollone A, Manzini S, Maggi CA. *Chem. Res. Toxicol.* 2000 Dec;13(12):1336-41 [PubMed: 11123976].
- (163) Schrijvers D, Bos AM, Dyck J, de Vries EG, Wanders J, Roelvink M, Fumoleau P, Bortini S, Vermorken JB. 2002 Mar;13(3):385-91 [PubMed: 11996468].
- (164) Caponigro F, Willemse P, Sorio R, Floquet A, Van Belle S, Demol J, Tambaro R, Comandini A, Capriati A, Adank S, Wanders J. *Invest. New Drugs* 2005 Jan;23(1):85-9 [PubMed: 15528985].
- (165) Quintieri L, Fantin M, Palatini P, De Martin S, Rosato A, Caruso M, Geroni C, Floreani M. *Biochem. Pharmacol.* 2008 Sep 15;76(6):784-95 [PubMed: 18671948].
- (166) Sessa C, Valota O, Geroni C. *Cardiovasc. Toxicol.* 2007;7(2):75-9 [PubMed: 17652808].
- (167) Quintieri L, Geroni C, Fantin M, Battaglia R, Rosato A, Speed W, Zanovello P, Floreani M. *Clin. Cancer. Res.* 2005 Feb 15;11(4):1608-17 [PubMed: 15746066].
- (168) Ripamonti M, Pezzoni G, Pesenti E, Pastori A, Farao M, Bargiotti A, Suarato A, Spreafico F, Grandi M. *Br. J. Cancer* 1992 May;65(5):703-7 [PubMed: 1586598].
- (169) Bakker M, Renes J, Groenhuijzen A, Visser P, Timmer-Bosscha H, Müller M, Groen HJ, Smit EF, de Vries EG. *Int. J. Cancer* 1997 Nov 4;73(3):362-6 [PubMed: 9359483].
- (170) Danesi R, Agen C, Grandi M, Nardini V, Bevilacqua G, Del Tacca M. *Eur. J. Cancer* 1993;29A(11):1560-5 [PubMed: 8217363].
- (171) Vasey PA, Bissett D, Strolin-Benedetti M, Poggesi I, Breda M, Adams L, Wilson P, Pacciarini MA, Kaye SB, Cassidy J. *Cancer Res.* 1995 May 15;55(10):2090-6 [PubMed: 7743508].
- (172) Quintieri L, Rosato A, Amboldi N, Vizler C, Ballinari D, Zanovello P, Collavo D. *Br. J. Cancer.* 1999 Mar;79(7-8):1067-73 [PubMed: 10098738].

- (173) Slupe A, Williams B, Larson C, Lee LM, Primbs T, Bruesch AJ, Bjorklund C, Warner DL, Peloquin J, Shadle SE, Gambliel HA, Cusack BJ, Olson RD, Charlier HA Jr. *Cardiovasc. Toxicol.* 2005 Fall;5(4):365-76 [PubMed: 16382174].
- (174) Holstein SA, Bigelow JC, Olson RD, Vestal RE, Walsh GM, Hohl RJ. *Invest. New Drugs* 2015. Jun;33(3):594-602 [PubMed: 25698442].
- (175) Van Tine BA, Agulnik M, Olson RD, Walsh GM, Klausner A, Milhem MM. *J. Clin. Oncol.* 2016, 34 (suppl).
- (176) Abraham SA, Waterhouse DN, Mayer LD, Cullis PR, Madden TD, Bally MB, *Methods Enzymol.* 2005. Feb;391:71-97 [PubMed: 15721375].
- (177) Drummond DC, Meyer O, Hong K, Kirpotin DB, Papahadjopoulos D. *Pharmacol. Rev.* 1999 Dec;51(4):691-743 [PubMed: 10581328].
- (178) Batist BG, Ramakrishnan G, Rao CS, Chandrasekharan A, Gutheil J, Guthrie T, Shah P, Khojasteh A, Nair MK, Hoelzer K, Tkaczuk K, Park YC, Lee LW. *J. Clin. Oncol.* 2001 Mar 1;19(5):1444-54 [PubMed: 11230490].
- (179) Rivankar S. *J. Cancer Res. Ther.* 2014 Oct-Dec;10(4):853-8 [PubMed: 25579518].
- (180) Hong R, Huang CJ, Tseng YL, Pang VF, Chen ST, Liu JJ, Chang FH. *Clin Cancer Res* 1999 Nov;5(11):3645-52 [PubMed: 10589782].
- (181) Hilger RA, Richly H, Grubert M, Oberhoff C, Strumberg D, Scheulen ME, Seeber S. *Int. J. Clin. Pharmacol. Ther.* 2005 Dec;43(12):588-9 [PubMed: 16372528].
- (182) Gabizon A, Martin F. *Drugs* 1997;54 Suppl 4:15-21 [PubMed: 9361957].
- (183) Martin, F.; Huang, A.; Uziely, B.; Kaufman, B.; Safra, T. *Cancer Res.* 1994, 54 (4), 987 [PubMed: 9361957].
- (184) Park, JW. *Breast Cancer Res.* 2002;4(3):95-9 [PubMed: 12052251].
- (185) Hasinoff BB, Herman EH. *Cardiovasc. Toxicol.* 2007;7(2):140-4 [PubMed: 17652819].

- (186) Schuchter LM, Hensley ML, Meropol NJ, Winer EP. *J. Clin. Oncol.* 2002 Jun 15;20(12):2895-903 [PubMed: 12065567].
- (187) Hasinoff BB, Hellmann K, Herman EH, Ferrans VJ. *Curr. Med. Chem.* 1998 Feb;5(1):1-28 [PubMed: 9481032].
- (188) Hasinoff BB, Kuschak TI, Yalowich JC, Creighton AM. *Biochem. Pharmacol.* 1995 Sep 28;50(7):953-8 [PubMed: 7575679].
- (189) Overholtzer M, Rao PH, Gorlick R, Levine AJ, Linkiewicz AM, Dubcovsky J, Hummel D, Lazo GR, Chao S, Anderson OD, David J, Qi L, Echaliier B, Gill BS, Gustafson JP, Rota ML, Wennerlind EJ, Nduati V, Anderson JA, Qualset CO, Dvorak J. *Proc. Natl. Acad. Sci. U. S. A.* 2003, Sep;100(20):11547.
- (190) Buzdar AU. *J. Clin. Oncol.* 2006 Jun 1;24(16):2409-11 [PubMed: 16682721]
- (191) Gianni L, Baselga J, Eiermann W, Guillem Porta V, Semiglazov V, Lluch A, Zambetti M, Sabadell D, Raab G, Llombart Cussac A, Bozhok A, Martinez-Agulló A, Greco M, Byakhov M, Lopez Lopez JJ, Mansutti M, Valagussa P, Bonadonna G. *Clin. Cancer Res.* 2005 Dec 15;11(24):8715-21 [PubMed: 16361558].
- (192) Swain SM, Whaley FS, Gerber MC, Weisberg S, York M, Spicer D, Jones SE, Wadler S, Desai A, Vogel C, Speyer J, Mittelman A, Reddy S, Pendergrass K, Velez-Garcia E, Ewer MS, Bianchine JR, Gams RA. *J. Clin. Oncol.* 1997 Apr;15(4):1318-32 [PubMed: 9193323].
- (193) Herman EH, Ferrans VJ. *Cancer Treat. Rev.* 1990 Sep;17(2-3):60-155 [PubMed: 125530].
- (194) Pouillart P. *Cancer Treat. Rev.* 2004 Nov;30(7):643-50 [PubMed: 15531396].
- (195) Speyer JL, Green MD, Zeleniuch-Jacquotte A, Wernz JC, Rey M, Sanger J, Kramer E, Ferrans V, Hochster H, Meyers M. *J. Clin. Oncol.* 1992 Jan 1;10(1):117-127 [PubMed: 1727913].

CHAPTER TWO: *IN VITRO* AND *IN VIVO* ACTIVITY OF NOVEL DOXORUBICIN  
ANALOGS AGAINST SOFT TISSUE SARCOMA

**Abstract**

Two novel synthetic analogs (GPX-150, GPX-160) of the anticancer agent doxorubicin (DOX) were assessed for topoisomerase inhibitory activity and cytotoxicity against a panel of human soft tissue sarcoma, breast carcinoma, and normal cell lines. *In vitro* cytotoxicity experiments showed that GPX-160 generally exhibited sub-micromolar activity, with IC<sub>50</sub> values against cancer cells that were similar to DOX. In contrast, GPX-150 was uniformly less potent than either DOX or GPX-160. GPX-160 also retained equivalent sub-micromolar potency against both DOX-sensitive (MES-SA) and DOX-resistant (MES-SA/MX2) cell lines, suggesting reduced susceptibility to efflux pump mediated drug resistance found in the MES-SA/MX2 cell line. Finally, in an *in vivo* human xenograft model of fibrosarcoma, mice treated with GPX-150 and GPX-160 showed significant decreases in both tumor volume and tumor weight relative to control animals.

**1. Introduction**

Soft tissue sarcomas (STS) are a rare heterogeneous type of cancer that originate from mesenchymal cells<sup>1</sup>. STS accounts for approximately 1% of all adult malignancies and 8% of pediatric cancers<sup>2</sup>. While they can arise in any part of the body, STS more frequently occur in the extremities (50% of patients) or in the trunk/retroperitoneal areas (40% of

patients)<sup>1</sup>. More than 50 different histological types of STS are recognized by World Health Organization (WHO)<sup>3</sup>. Disease severity and prognosis relies on several factors including patient age and gender, tumor size, tumor spread, histological phenotype, and anatomical location<sup>4,5</sup>.

STS treatment usually involves surgical resection of the primary tumor, followed by radiation, and/or chemotherapy<sup>1</sup>. The primary chemotherapeutic used to treat STS is doxorubicin (Adriamycin<sup>®</sup>), a water-soluble anthracycline first discovered in cultures of *Streptomyces peuceitus var. caesius* in the 1960s after the discovery of daunorubicin (DNR), its parent compound<sup>6,7</sup>. Doxorubicin (DOX) is a versatile chemotherapeutic that is also used to treat a wide array of other cancers, including leukemias, lymphomas, and solid tumors of the breast, ovaries, lungs and thyroid<sup>8,9</sup>. The primary mechanisms of anticancer activity are mediated by intercalation into DNA and subsequent inhibition of topoisomerase activity that ultimately interrupts DNA replication<sup>10</sup>.

Although DOX is one of the major prescribed anticancer drugs, its use is clinically constrained due to well-known cardiotoxic side effects<sup>11</sup>. DOX treatment can cause both acute and chronic dose-dependent cardiotoxicity, which eventually leads to congestive heart failure. Acute cardiotoxicity can present itself within a week of a single dose of DOX treatment<sup>12,13</sup>, while chronic cardiotoxicity may occur 4-15 years after the completion of treatment<sup>14</sup>. The recommended cumulative dose of DOX is generally limited to less than 500 mg/m<sup>2</sup> to reduce the increasing risk of heart failure that occurs beyond 550 mg/m<sup>2</sup><sup>13,15-18</sup>. Multiple mechanisms appear to be involved in DOX-induced cardiotoxicity, including its reduction to toxic doxorubicinol (DOXol) by cytosolic NADPH-dependent aldo-keto reductases (AKR1C3, AKR1A1, CBR1, CBR3)<sup>19-21</sup>, interruption of calcium and iron

homeostasis, and generation of reactive oxygen and nitrogen species (RONS)<sup>22,23</sup>.

In order to improve the therapeutic profile of DOX, we analyzed synthetically modified DOX derivatives, GPX-150 and GPX-160 (Figure 1). These novel analogs were designed to reduce DOX-mediated cardiotoxicity by removing functional groups that promote formation of the toxic DOXol metabolite and reactive oxygen and nitrogen species (RONS), while retaining cytotoxicity against tumor cells. In the GPX-150 analog, the C-13 carbonyl group was removed to prevent reduction to cardiotoxic DOXol. In addition, a carbonyl oxygen in the quinone ring was replaced with a nitrogen to create an iminoquinone with reduced capacity to stimulate formation of RONS<sup>24</sup>. The GPX-160 analog was further derived from GPX-150 by replacing the primary amine at the 3' position in the sugar moiety with a pyrrolino- group. This alteration in other analogs has been shown to enhance the binding to the DNA-drug ternary complex<sup>25,26</sup> and to reduce the susceptibility to P-glycoprotein (P-gp) mediated drug efflux that is a common mechanism of drug resistance in tumor cells<sup>27</sup>.



**Figure 2.1. The structures of DOX, GPX-150, and GPX-160.**

In this report, we evaluate the *in vitro* inhibitory activity of the DOX analogs against topoisomerase II  $\alpha$  (Top2 $\alpha$ ), since this is a primary target of anthracycline action. The *in vitro* cytotoxicity of the compounds against a panel of STS, carcinoma, and normal cells were also determined to investigate how alterations to chemical structure influence their

anticancer profile. Finally, we report the comparative activity of DOX, GPX-150, and GPX-160 analogs in an *in vivo* murine xenograft model of human fibrosarcoma. The result demonstrates the efficacy of these analogs at reducing tumor growth and suggest their usefulness as novel anticancer agents.

## 2. Results/Discussion

### 2.1 Inhibition of Topoisomerase II $\alpha$

DOX is a DNA intercalating agent that stabilizes the topoisomerase II $\alpha$  (Top2 $\alpha$ )-DNA ternary cleavage complex to stall Top2 $\alpha$  enzyme activity and interrupt DNA replication<sup>28</sup>. The ability of the DOX analogs to inhibit Top2 $\alpha$  activity was investigated to gauge the effect of analog structural changes on this primary mechanism of drug action. Enzyme activity was studied using gel electrophoresis to examine Top2 $\alpha$  decatenation of tangled kinetoplast DNA (kDNA) into its monomeric circular and linear forms. As seen in Figure 2A, incubation with increasing concentrations of GPX-160 inhibited the appearance of decatenated circular kDNA. Based on densitometry of the electrophoretically separated reaction

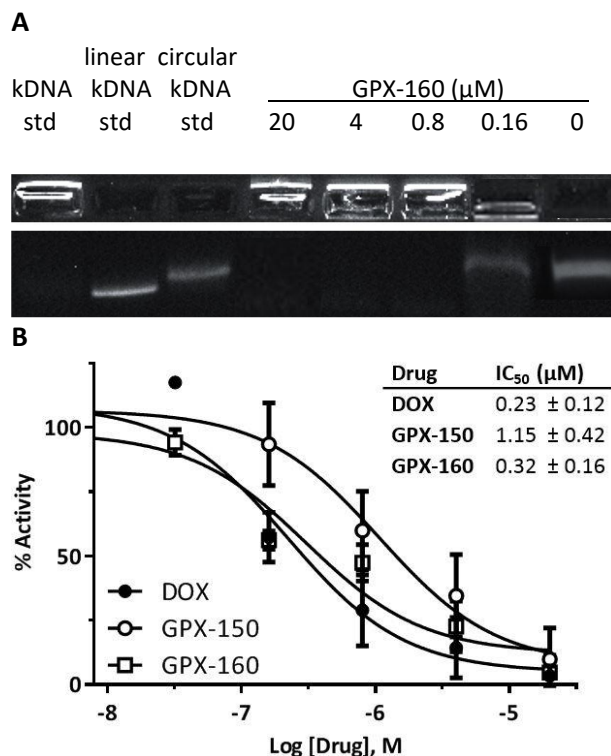


**Figure 2.2 Topoisomerase inhibitory activity.** [A] Representative agarose gel of Top2 $\alpha$ -kDNA decatenation reaction products. High molecular weight catenated kDNA, low molecular weight linear kDNA and decatenated circular kDNA standards are seen in the first three lanes. The remaining lanes show Top2 $\alpha$  reactions containing 0–20  $\mu$ M of GPX-160. [B] Graph of Top2 $\alpha$  activity based on densitometry of low molecular weight decatenated and linear kDNA bands. The graph shows the relative percent enzyme activity in DOX or GPX-containing reactions compared to uninhibited reactions. The IC<sub>50</sub> results (inset) are the average of 4 experiments  $\pm$  standard error of the mean ( $\pm$  SEM).

products, the concentration of DOX and GPX compounds required to inhibit 50% ( $IC_{50}$ ) of Top2 $\alpha$  activity was estimated (Figure 2B). The  $IC_{50}$  of GPX-150 (1.15  $\mu$ M) was approximately 3-4 fold higher than the  $IC_{50}$  for GPX-160 (0.32  $\mu$ M) and DOX (0.23  $\mu$ M). This finding may help explain the generally less potent *in vitro* cytotoxicity profile exhibited by GPX-150 as ascribed below. The findings also suggest that the alterations to DOX structure that reduce the GPX-150 inhibition of Top2 $\alpha$  (loss of C-13 carbonyl, iminiquinone ring) are largely overcome by changing the 3' amine group on the sugar moiety to the bulkier pyrrolino-group found in GPX-160, which appears to promote the formation of the ternary complex of drug-DNA-Top2 $\alpha$  important for topoisomerase inhibition<sup>25</sup>. Our study shows the effect of 3' substituents on the ability to stimulate Top2-mediated DNA cleavage and is consistent with earlier studies<sup>29</sup>.

## 2.2 Cytotoxicity studies

The antiproliferative activities of DOX, GPX-150, and GPX-160 against a panel of seven STS, two breast carcinoma cell lines, and two normal cell lines were measured using a resazurin reduction assay<sup>30</sup>. Representative graphs of cytotoxicity profiles against DOX-sensitive and DOX-resistant human uterine sarcoma lines are shown in Figure 3. DOX showed an  $IC_{50}$  of 0.56  $\mu$ M for the drug sensitive MES-SA cell line, while the  $IC_{50}$  increased about 25-fold to 13.3  $\mu$ M for the drug-resistant MES-SA/MX2 line. This result is consistent with literature reports that attribute DOX resistance to the upregulation of P-glycoprotein (P-gp) efflux protein expression<sup>27</sup>. In contrast, GPX-160 showed similar  $IC_{50}$  values (0.76  $\mu$ M and 0.73 $\mu$ M) against both the DOX sensitive and resistant MES-SA lines (Table 1).

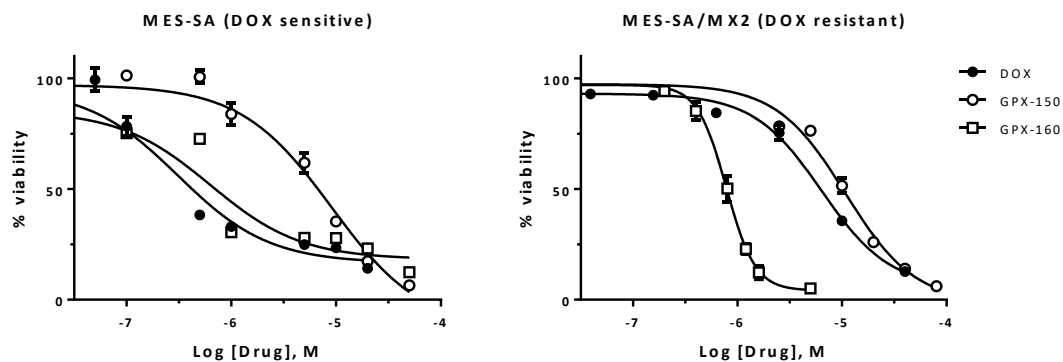


**Figure 2.3.** *In vitro* drug sensitivity profiles for human uterine sarcoma cell lines, MES-SA (DOX sensitive, left) and MES-SA/MX2 (DOX resistant, right). The graphs represent the average of 3-5 independent experiments  $\pm$ SEM.

Our results suggest that replacement of the 3' amino group of the sugar with a 3' pyrrolino- group reduces the drug susceptibility to P-gp activity. Supporting this observation, Frezard et al. (2001) reported that modification of anthracyclines with the electrophilic pyrrolino group decreased P-gp-mediated efflux kinetics and improved intracellular retention time<sup>31</sup>. Other investigators have also proposed that the C-3' position in the sugar moiety is important not only as a substrate for P-gp mediated efflux, but also for impacting the sequence specificity and binding affinity of the drug in the minor groove of DNA<sup>25-27</sup>.

The results of anticancer drug sensitivity studies are summarized in Table 1. GPX-150 was the least potent analog, with IC<sub>50</sub> values in the low micromolar range against sarcoma and carcinoma cells. These concentrations were generally an order of magnitude (or greater) than those found for DOX, which fairly consistently yielded sub-micromolar IC<sub>50</sub> values. Our *in vitro* antiproliferative efficacy of DOX showed similar results to previously reported studies against several STS<sup>32</sup> and carcinoma cell lines<sup>33</sup>. With the exception of the

**Table 2.1. Summary of drug activity against human sarcoma and carcinoma cell lines.**

Cell Line	Tumor Type	IC <sub>50</sub> (μM)*		
		DOX	GPX-150	GPX-160
HT1080	Fibrosarcoma	0.48 ± 0.21	47.6 ± 15.5	3.87 ± 0.50
HT1080-luc2	Fibrosarcoma	0.73 ± 0.26	3.32 ± 0.59	3.51 ± 1.79
RDCCL136	Rhabdomyosarcoma	0.43 ± 0.05	11.9 ± 3.99	0.44 ± 0.13
SW-982	Synovial sarcoma	4.28 ± 1.46	0.80 ± 0.68	0.45 ± 0.14
SW-872	Liposarcoma	0.35 ± 0.89	7.38 ± 0.45	0.57 ± 0.23
MES-SA (DOX <sup>S</sup> )	Uterine sarcoma	0.56 ± 0.08	10.6 ± 1.00	0.76 ± 0.16
MES-SA/MX2 (DOX <sup>R</sup> )	Uterine sarcoma	13.3 ± 1.68	17.8 ± 0.52	0.73 ± 0.04
MCF-7	Breast carcinoma	0.34 ± 0.04	43.9 ± 9.13	0.44 ± 0.21
MDA-MB-231	Breast carcinoma	0.20 ± 0.01	7.14 ± 1.92	0.17 ± 0.01

\*Expressed values are the mean (±SEM) of 3-5 independent experimental determinations.

HT1080 fibrosarcoma cell line, GPX-160 showed sub-micromolar IC<sub>50</sub> values against cancer cells. Overall, the GPX-160 cytotoxicity profile was more similar to DOX than to GPX-150.

The cytotoxicity of DOX, GPX-150, and GPX-160 against two normal human cell lines, human adult dermal fibroblasts (HADF) and human umbilical vein endothelial cells (HUVEC-2) were also examined and are summarized in Table 2. Our IC<sub>50</sub> values of DOX against fibroblast and endothelial cells correlate to previously reported studies<sup>34</sup>. Non-proliferative HADF cells were insensitive to the compounds, with IC<sub>50</sub> values of approximately 300 μM for all three drugs. Non-proliferative HUVEC-2 cells were also

**Table 2.2 Summary of drug activity against normal human cell lines.**

Cell Type	Cell Status	IC <sub>50</sub> (μM)*			
		DOX	GPX-150	GPX-160	
HADF	Dermal fibroblast	Proliferative	57.5 ± 14.8	19.2 ± 1.1	5.6 ± 1.2
		Non-proliferative	342 ± 123	322 ± 72.4	299 ± 68.0
HUVEC-2	Umbilical endothelium	Proliferative	5.4 ± 2.1	34.1 ± 10.4	14.0 ± 2.0
		Non-proliferative	41.9 ± 8.1	110 ± 22.6	33.9 ± 4.8

\*Expressed values are the mean (±SEM) of 3-5 independent experimental determinations.

resistant to compounds, although the IC<sub>50</sub> values were at least 3-fold or lower than those seen for HADF cells. As expected, both normal cell lines showed increased sensitivity to all three drugs when they were in a proliferative state, with the IC<sub>50</sub> values reduced to the 5-50 μM range. These IC<sub>50</sub> values were still generally 10- to 100-fold higher than those found for cancer cells. The results suggest that GPX-150 and GPX-160 will show selectivity for cancer cells that is similar to that seen with DOX.

### 2.3 Inhibition of human sarcoma xenografts

The efficacy of GPX-150 and GPX-160 treatment on tumor growth was studied using luciferase-expressing human fibrosarcoma xenografts established in female (Foxn1nu) nude mice. Tumor growth was monitored using bioluminescent imaging (BLI) and caliper measurements in PBS, DOX, GPX-150, and GPX-160 treated mice (Figure 4). On day 20 post-tumor engraftment, mice were imaged for the final time, and the tumor volume and weights were measured following euthanasia. PBS-treated (control) mice showed the largest tumors, averaging approximately 4100 mm<sup>3</sup> or 3.1 g in weight (Figure 4, panel B and C). Reflective of their similar *in vitro* activities against the HT1080-luc2 cells (Table 1), GPX-150 and GPX-160 treatment (2.4 mg/kg) resulted in similar decreases in tumor volume and weight. On average, treatment with the GPX compounds significantly decreased tumor volume by 71-76% and tumor weight by 60-67% relative to the PBS treatment ( $p < 0.0001$ ). In contrast, mice treated with DOX (2.4 mg/kg) showed the most dramatic inhibition of tumor growth, with a 99% reduction in volume and 96% decrease in weight. Although this was a highly effective response to DOX treatment, the mice in this group exhibited the strongest signs of drug toxicity, based on poor activity, hunched appearance, and a 10% decrease in body weight relative to control animals (data not

shown). This result is consistent with other reports that have attributed these observations to the well-known cardiotoxic side effects of DOX<sup>35-37</sup>.

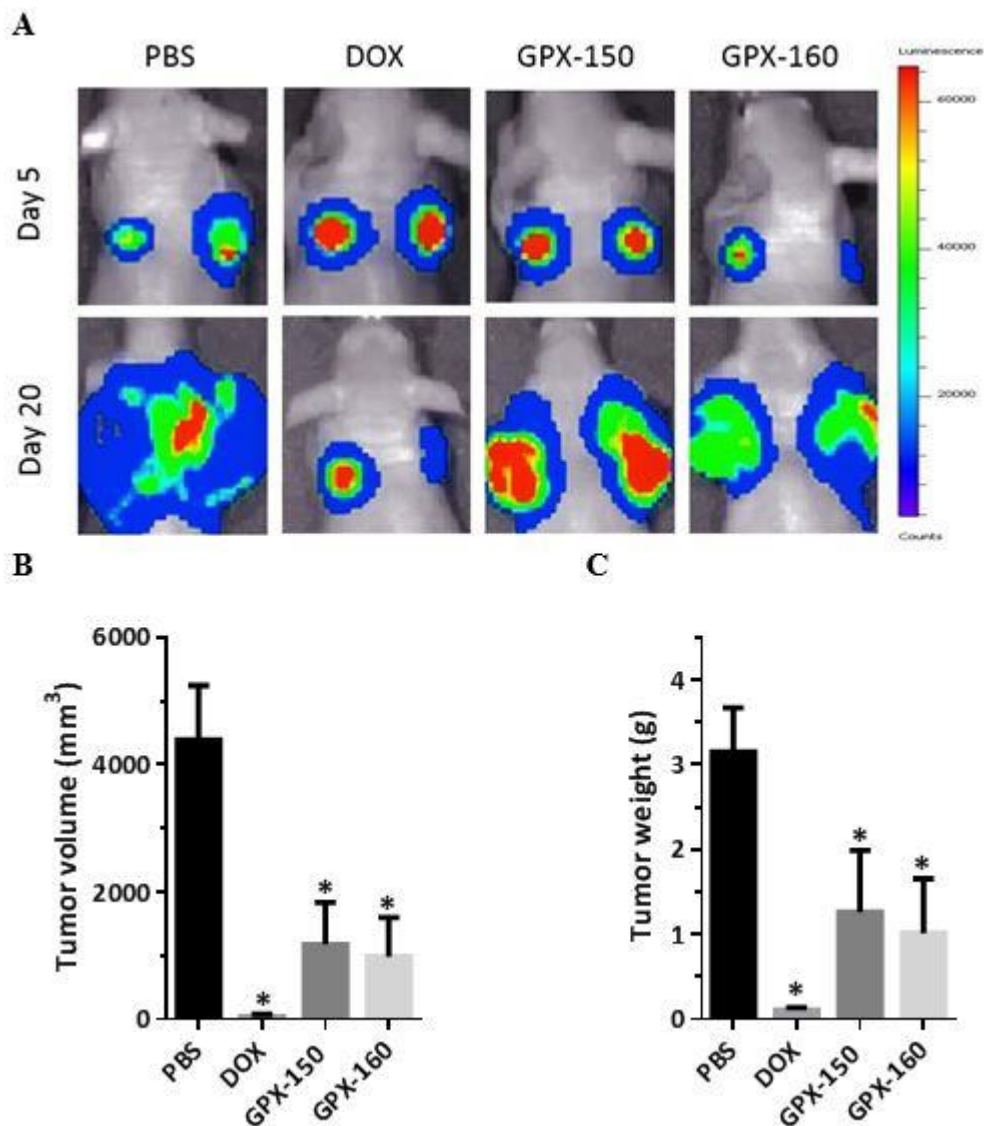


**Figure 2.4.** Effects of DOX, GPX-150, and GPX-160 treatment (2.4 mg/kg) on human HT1080-luc2 fibrosarcoma xenograft tumor growth in female athymic nude mice (Foxn1nu). [A] Representative BLI of xenografts at the start (day 5) and end of treatment (day 20). [B] Average tumor volumes ( $\pm$  SEM) at sacrifice (day 20). [C] Average tumor weights ( $\pm$  SEM) at sacrifice (day 20). Graphs show the average of data collected from groups of 4 (PBS) or 5 (DOX, GPX-150, GPX-160) mice, each bearing 2 tumors. \*  $p < 0.0001$  when compared to PBS control treated mice.

### 3. Conclusion

The biological activities of DOX and two novel DOX analogs, GPX-150 and GPX-160, were characterized and compared. The analogs were designed to decrease potential cardiotoxic side effects of DOX by eliminating the C-13 carbonyl group and altering the quinone ring structure to an iminoquinone that produces less RONS formation. In addition, in the GPX-160 analog the 3' amino group on the sugar in the GPX-160 analog was replaced with a pyrroline to improve intracellular retention. Both GPX-150 and GPX-160 were potent inhibitors of human Top2 $\alpha$ , although the IC<sub>50</sub> value for GPX-150 (1.15  $\mu$ M) was 3- to 5-fold higher than seen with either DOX or GPX-160. In *in vitro* antiproliferation assays against a panel of sarcoma and carcinoma cells, the IC<sub>50</sub> values obtained for GPX-160 were generally in the sub-micromolar range and resembled those found for DOX. GPX-160 was also consistently superior to GPX-150 in antiproliferative activity, probably due to decreased activity as a substrate for P-gp mediated drug efflux. Support for this assertion can be seen in the results from the MES-SA (DOX<sup>S</sup>) and MES-SA/MX2 (DOX<sup>R</sup>) cell studies. MES-SA/MX2 cells overexpress P-gp and showed a 20-fold increased resistance to DOX, but remained susceptible to GPX-160. This suggests that the incorporation of the bulkier pyrroline in place of the amino group of the sugar was successful in reducing efflux of the drug through P-gp. Finally, a pilot study using a human fibrosarcoma xenograft model in nude mice indicates that GPX-150 and GPX-160 are promising anticancer drugs with the ability to significantly reduce both tumor volume and weight. This finding is supported by the results of an initial clinical trial for GPX-150 treatment of advanced sarcoma patients that was recently reported by Holstein et al.<sup>24</sup>. In this study, sarcoma patients treated with GPX-150 showed clinically significant

improvements in disease progression and no demonstrable drug-induced cardiotoxicity, although the required dose of GPX-150 was four-fold higher than what would be used for DOX. Future studies will include a more extensive examination of drug efficacy and delivery schedules in the HT1080-luc2 fibrosarcoma xenograft model. Considering the overall better antiproliferative profiles seen for GPX-160 in drug-resistant cells, future work will also include studies of efficacy using *in vivo* models of drug resistant tumors in mice.

## **4. Materials and Methods**

### **4.1 Materials and Reagents**

GPX-150 and GPX-160 were supplied by Gem Pharmaceuticals, LLC (Birmingham, AL). DOX-HCl was purchased from Advanced ChemBlocks, Inc. (Burlingame, CA). All compounds were dissolved in 100% anhydrous dimethyl sulfoxide (DMSO) obtained from Sigma-Aldrich (St. Louis, MO) to 30 mM and stored frozen at -80 °C. Unless otherwise noted, all media and media constituents were purchased from Thermo Fisher Scientific (Pittsburgh, PA).

### **4.2 Topoisomerase II $\alpha$ Assay**

Top2 $\alpha$  activities against antitumor agents were evaluated by observing the decatenation of kinetoplast DNA (kDNA), which consists of highly catenated networks of minicircular (2.5 kb) and maxicircular DNA (8 kb), using a Topoisomerase II assay kit (TopoGEN Inc., Buena Vista, CO). The measurement of decatenation activity is ATP-dependent and results in individual minicircles of DNA. The assay was performed in a reaction mixture (20  $\mu$ l) containing 232 ng of kDNA, 2 units of human Top2 $\alpha$ , varying concentrations of test compounds, and assay buffer consisting of 50 mM Tris-HCl (pH 8), 155 mM NaCl, 10 mM

MgCl<sub>2</sub>, 0.5 mM dithiothreitol (DTT), 30 µg/ml bovine serum albumin (BSA), and 2 mM ATP. DOX and DOX analogs were pre-incubated with kDNA for 6 hours at 37 °C prior to initiating the reaction by addition of enzyme. After 60 min incubation at 37 °C, the reaction was terminated with stop buffer to achieve a final concentration of 1% Sarkosyl, 0.025% bromophenol blue, and 5% glycerol. The reaction products were separated by electrophoresis on a 1% agarose gel submerged in 1x TAE buffer at 12V/cm, followed by ethidium bromide staining (0.5 µg/ml in 1x TAE). Gels were visualized and imaged using ultraviolet illumination on a FluorChem E gel imager (ProteinSimple, San Jose, CA).

#### 4.3 Cell Lines and Cell Culture

Six human soft tissue sarcoma (STS) cell lines (HT1080, RDCCL, SW-982, SW-872, MES-SA, MES-SA/MX2) were purchased from American Type Culture Collection (ATCC, Manassas, VA). The bioluminescent HT1080-luc2 fibrosarcoma line was purchased from Perkin Elmer (Waltham, MA). Normal human umbilical vein endothelial cells (HUVEC-2) and human adult dermal fibroblast (HADF) were purchased from Thermo Fisher Scientific. MCF-7 and MDA-MB-231 breast carcinoma were the kind gift of Dr. Cheryl Jorcyk (Boise State University). All cells were cultured at 37 °C with 5% CO<sub>2</sub> in a humidified atmosphere. RDCCL136, SW-982, SW-872, MES-SA, MES-SA/MX2, MDA-MB-231 and MCF-7 cells were cultured in Dulbecco's Modified Eagle Medium (DMEM) supplemented with 10% (v/v) fetal bovine serum (FBS), 1% (v/v) penicillin/streptomycin (pen/strep). The drug-resistance phenotype of MES-SA/MX2 was maintained by culturing in the presence of 1 µM DOX until the assay treatment of DOX and DOX analogs. Huvec-2 and HADF were grown in complete endothelial growth medium and fibroblast medium, respectively (ScienCell Research Laboratories, Carlsbad,

CA). HT1080 and HT1080-luc2 were grown in Minimum Essential Medium (MEM), containing 10% FBS and 1% pen/strep.

#### 4.4 Antiproliferative Assays

*In vitro* antiproliferative studies were performed using a resazurin reduction assay as previously described<sup>33</sup>. Briefly, cells were washed three times with sterile PBS (Thermo Fisher Scientific, Waltham, MA) and suspended in trypsin-EDTA (Lonza, Walkersville, MD) for less than 5 min at 37°C. Cells were centrifuged at 200 x *g* for 5 min and resuspended in the appropriate media to yield 250,000 – 400,000 cells/mL. Cells were seeded into sterile 96-well plates (5,000 – 8,000 cells/well) and then incubated overnight at 37°C in a 5% CO<sub>2</sub> humidified atmosphere. The media was then replaced with 200 µl of fresh media with the appropriate concentration of drug. For cytotoxicity test against MES-SA/MX2, 1 µM of DOX pressure was applied during cell culture prior to the drug treatment. Cells were incubated with drug for 48 h followed by addition of 20 µL of 0.1% (w/v) resazurin to each well. Fluorescence scans (excitation/emission: 530/590 nm) were obtained after 4-24 hours using a BioTek Synergy HT Multi-detection microplate reader (Winooski, VT). Fluorescence data was graphed as the % viability (Equation 1) versus drug concentration using GraphPad Prism software (La Jolla, CA).

$$\% \text{ viability} = \frac{\text{drug treated fluorescence} - \text{blank fluorescence}}{\text{Drug-free fluorescence}} \times 100 \quad \text{Equation (1)}$$

The IC<sub>50</sub> values of DOX and DOX analogs were determined using a non-linear fit of the % viability vs. log [drug].

#### 4.5 *In vivo* Fibrosarcoma Xenograft Model

The *in vivo* protocol was modified from Wang et al. (2010). All animal manipulations and protocols were conducted and approved by the Boise State University Institutional

Animal Care and Usage Committee #007-AC17-012 (IACUC). Four to five-week-old female immunodeficient mice (Hsd:ATHymic Nude-*Foxn1*<sup>tmu</sup>) were purchased from Envigo (Hayward, CA) and housed in the Boise State University vivarium. Animals were acclimated to the facility for two weeks prior to the beginning of the experiment. To create the fibrosarcoma xenografts, HT1080-luc2 cells were cultured and harvested as described as above, resuspended in sterile MEM ( $1 \times 10^7$  cells/mL) and placed on ice until injection. Mice were injected subcutaneously over both left and right shoulders with 0.1 mL tumor cells ( $1 \times 10^6$  cells per site). Mice were observed daily for tumor growth and overall health, and body weights collected three times per week. On day 5 following HT1080-luc2 cell injection, engrafted tumors were visualized by BLI. For BLI, mice were injected intraperitoneally (IP) with 0.2 mL sterile D-luciferin solution (15mg/mL in PBS), and the luciferin allowed to absorb for 10-15 min. The mice were then imaged using a Xenogen Spectrum IVIS instrument (PerkinElmer, Waltham, MA). Mice were randomly assigned to treatment groups (4-5 mice/group) consisting of drug (DOX, GPX-150, GPX160) or vehicle control (PBS). The mice received 100  $\mu$ L of freshly prepared test compound (2.4 mg/kg) three times per week by intraperitoneal (IP) injection for a total of six treatments (days 5, 7, 10, 12, 14, 17). Tumor size was measured three times a week with a Vernier caliper and the tumor volume calculated using the formula for an ellipsoid (Equation 2)<sup>38</sup>.

$$Tumor\ volume = \frac{4}{3}\pi \cdot \left(\frac{L}{2}\right) \cdot \left(\frac{W}{2}\right) \cdot \left(\frac{H}{2}\right) \quad Equation\ (2)$$

To image the luciferase labeled tumors, d-Luciferin potassium salt (PerkinElmer, Waltham, MA) was dissolved in sterile PBS at 10 mg/mL, and injected intraperitoneally 10 min prior to image acquisition. BLI images were collected twice per week until day 21 (sacrifice). Mice were sacrificed 21-days after tumor cell engraftment due to the excessive

enlargement of the tumor ( $> 1.5 \text{ cm}^3$ ). Lungs and primary tumors were excised to determine metastasis and to measure the volumes and weights, respectively. The excised tumors and organs were preserved in the 10% formalin tissue fixatives (Sigma-Aldrich, St. Louis, MO) for further analysis. Prior to tumor injections, euthanasia, and BLI measurements, all the animals were anesthetized under isoflurane inhalation.

## **5. Acknowledgment**

The project presented was funded by an Institutional Development Award (IDeA) from the National Institute of General Medical Sciences of the National Institutes of Health (NIH/NIGMS) under Grants #R15CA113464, #P20GM103408 and #P20GM109095. Additional funding was provided by Gem Pharmaceuticals LLC. The project also received support from The Biomolecular Research Center (BRC) at Boise State University with funding from National Science Foundation (NSF) grants #0619793 and #0923535; the MJ Murdock Charitable Trust; the Idaho State Board of Education; and Idaho Global Entrepreneurial Mission (IGEM). The contents of this article are entirely the responsibility of the authors and do not share the official perspectives of the NIH or the State of Idaho.

## REFERENCES

- (1) Cassier PA, Labidi-Galy SI, Heudel P, Dutour A, Méeus P, Chelghoum M, Alberti L, Ray-Coquard I, Blay J-Y. *Expert Opin. Pharmacother.* **2011**, *12* (16), 2479. [PubMed: 21313865]
- (2) Clark M A, Fisher C, Judson I, Thomas JM. *N. Engl. J. Med.* **2005**, *353* (7), 701. [PubMed: 16107623]
- (3) Coindre J M, Terrier P, Guillou L, Doussal VL, Collin F, Ranchre D, Sastre X, Vilain MO, Bonichon F, Bui BNG. *Cancer* **2001**, *91* (10), 1914. [PubMed: 11346874]
- (4) Weiss SW. *Springer Berlin Heidelberg.* **1994**. pp 7–14.
- (5) Baroudi MR, Ferguson PC, Wunder JS, Isler MH, Mottard S, Werier JA, Turcotte RE. *J. Surg. Oncol.* **2014**, *110* (6), 676. [PubMed: 24910319]
- (6) Di Marco A, Cassinelli G, Arcamone F. *Cancer Treat. Rep.* **1981**, *65* (4), 3. [PubMed: 7049379]
- (7) Arcamone F, Cassinelli G, Fantini G, Al E. *Biotechnol. Bioeng.* **1969**, *11* (6), 1101.
- (8) Cortes-Funes H, Coronado C. *Cardiovascular Toxicology.* **2007**, *7* (2), 56. [PubMed: 17652804]
- (9) McCredie KB, Bodey GP, Freireich EJ, Hester JP, Rodriguez V, Keating MJ. *Cancer.* **1981**, *47* (6), 1256. [PubMed: 6939477]
- (10) Hortobdgyi G. *Drugs.* **1997**. *54* (4). 1. [PubMed: 9361955]
- (11) Lahoti TS, Patel D, Thekkemadom V, Beckett R, Ray SD. *Curr. Neurovasc. Res.* **2012**, *9* (4), 282. [PubMed: 22873725]
- (12) Steinberg JS, Cohen AJ, Wasserman AG, Cohen P, Ross AM. *Cancer* **1987**, *60* (6), 1213. [PubMed: 3621107]

- (13) Lenaz L, Page J. A. *Cancer Treat. Rev.* **1976**, 3 (3), 111. [PubMed: 822941]
- (14) Steinherz LJ, Steinherz PG, Charlotte TC, Heller G, Murphy L. *JAMA* **1991**, 266 (12), 1672. [PubMed: 1886191]
- (15) Lefrak EA, Pitha J, Rosenheim S, Gottlieb J. A. *Cancer* **1973**, 32 (2), 302. [PubMed: 4353012]
- (16) Pai VB, Nahata MC. *Drug Saf.* **2000**, 22 (4), 263. [PubMed: 10789823]
- (17) Kushner JP, Hansen VL, Hammar SP. *Cancer* **1975**, 36 (5), 1577. [PubMed: 172214]
- (18) Volkova M, Russell R. *Curr. Cardiol. Rev.* **2011**, 7 (4), 214. [PubMed: 22758622]
- (19) Thorn C, Oshiro C, Marsh S, Hernandez-Boussard T, McLeod H, Klein T, Altman R. *Pharmacogenet Genomics* **2012**, 21 (7), 440. [PubMed: 21048526]
- (20) Forrest GL, Akman S, Doroshov J, Rivera H, Kaplan WD. *Mol. Pharmacol* **1991**, 40, 502. [PubMed: 1921984]
- (21) Minotti G, Recalcati S, Mordente A, Liberi G, Calafiore AM, Mancuso C, Preziosi P, Cairo G. *FASEB J.* **1998**, 12 (7), 541. [PubMed: 9576481]
- (22) Solem LE, Henry TR, Wallace KB. *Toxicol. Appl. Pharmacol.* **1994**, 129 (2), 214. [PubMed: 7527602]
- (23) Weinstein D, Mihm M, Bauer J. *J. Pharmacol. Exp. Ther.* **2000**. 294 (1), 396. [PubMed: 10871338]
- (24) Holstein SA, Bigelow JC, Olson RD, Vestal RE, Walsh GM, Hohl RJ. *Invest. New Drugs.* **2015**, 33 (3), 594. [PubMed: 2568442]
- (25) Capranico G, Supino R, Binaschi M, Capolongo L, Grandi M, Suarato A, Zunino F. *Mol. Pharmacol.* **1994**, 45 (5), 908. [PubMed: 8190107]
- (26) Cashman D, Kellogg G. *J. Med. Chem.* **2004**, 47 (6), 1360. [PubMed: 14998326]
- (27) Gosland M, Lum B, Sikic B. *Cancer Res.* **1989**, 49 (24), 6901. [PubMed: 2582432]

- (28) Capranico G, Binaschi M, Borgnetto ME, Zunino F, Palumbo M. *Trends. Pharmacol. Sci.* **1997**, 18 (9), 323. [PubMed: 9345851]
- (29) Stepankova J, Studenovsky M, Malina J, Kasparkova J, Liskova B, Novakova O, Ulbrich K, Brabec V. *Biochem. Pharmacol.* **2011**, 82 (3), 227. [PubMed: 21570955]
- (30) Mallory CM, Carfi RP, Moon S, Cornell KA, Warner DL. *Bioorganic Med. Chem.* **2015**, 23 (23), 7378. [PubMed: 26541587]
- (31) Frézard F, Pereira-Maia E, Quidu P, Priebe W, Garnier-Suillerot A. *Eur. J. Biochem.* **2001**, 268 (6), 1561. [PubMed: 11248673]
- (32) Samuels BL, Murray JL, Cohen MB, Safa AR, Sinha BK, Townsend AJ, Beckett MA, Weichselbaum RR. *Cancer Res.* **1991**, 51, 521. [PubMed: 1845955]
- (33) Sikic BI, Ehsan MN, Harker WG, Friend NF, Brown BW, Newman RA, Hacker MP, Acton EM. *Science* **1985**, 228 (4707), 1544. [PubMed: 4012308]
- (34) El-Awady RA, Semreen MH, Saber MM, Cyprian F, Menon V, Al-Tel TH. *DNA Repair (Amst)*. **2016**, 37, 1. [PubMed: 26590797]
- (35) Ferrero ME, Ferrero E, Gaja G, Bernelli-Zazzera A. *Biochem. Pharmacol.* **1976**, 25 (2), 125. [PubMed: 177021]
- (36) Quintieri, L.; Rosato, A.; Amboldi, N.; Vizler, C.; Ballinari, D.; Zanovello, P.; Collavo, D. *Br. J. Cancer* **1999**, 79 (7–8), 1067. [PubMed: 10098738]
- (37) Wang S, Ren W, Liu J, Lahat G, Torres K, Lopez G, Lazar AJ, Hayes-Jordan A, Liu K, Bankson J, Hazle JD, Lev D. *Clin. Cancer Res.* **2010**, 16 (9), 2591. [PubMed: 20406839]
- (38) Schmidt KF, Ziu M, Schmidt NO, Vaghasiz P, Cargioli TG, Doshi S, Albert MS, Black PM, Carroll RS, Sun Y. *J. Neurooncol.* **2004**, 68 (3), 207. [PubMed: 15332323]

CHAPTER THREE: ANALYSIS OF NOVEL IMINOQUINONE ANALOGS  
REVEALS DISTINCT *IN VITRO* PHARMACOKINETIC PROFILES

**Abstract**

Two iminoquinone analogs, GPX-150 and GPX-160, have been explored as anthracycline replacements to overcome cardiotoxic side effects and drug resistance profiles commonly encountered with doxorubicin (DOX) therapy. *In vitro* pharmacokinetic characteristics were determined to better understand how GPX-150 and GPX-160 compare to drug parameters displayed by DOX. Drug stability studies in serum containing media show that both analogs have 3-8 fold longer half-lives than DOX. The apparent permeability coefficients ( $P_{app}$ ) across human epithelial colorectal adenocarcinoma (Caco-2) cell monolayers demonstrate that both analogs show increased transepithelial transport rates in both apical (AP) to basolateral (BL) and BL to AP directions compared DOX. The results also show that the transepithelial efflux-to-uptake ratio of both GPX-150 and GPX-160 are lower than DOX in the BL to AP direction. This suggest the analogs will be less sensitive to drug efflux and loss into the intestinal lumen. Human liver microsome cytochrome P450 (CYP450) metabolism of the analogs was examined with and without CYP450 selective inhibitors. The results showed that CYP2C8 and CYP3A4 were the most prevalent enzymes involved in modification of GPX-150 and GPX-160. Importantly, both analogs were insensitive to aldo-keto reductase (AKR) activity responsible for the conversion of DOX to cardiotoxic doxorubicinol. Mass spectrometry analysis of the liver microsomal drug products demonstrated metabolism of GPX-150 and GPX-160 occurred

through dealkylation, demethylation, and deglycosylation routes. Ultimately, the *in vitro* pharmacokinetics characterization of GPX-150 and GPX-160 will be useful in promoting their use as DOX replacements in cancer chemotherapeutic regimens.

## 1. Introduction

Doxorubicin (DOX, Adriamycin<sup>®</sup>) is a chemotherapeutic agent used for various forms of cancer such as breast and ovarian carcinoma, lung and pediatric cancers, lymphoma, leukemia, multiple myeloma, and soft tissue sarcomas<sup>1</sup>. The anticancer effects of DOX are known to be mediated through a number of mechanisms, but primarily by acting as a DNA intercalating agent that stabilizes the DOX-DNA-topoisomerase II ternary complex<sup>2</sup>. Despite the therapeutic successes of DOX, its clinical application is limited due to dose-dependent acute and chronic cardiotoxicity that can lead to congestive heart failure (CHF)<sup>3,4</sup>. In addition, innate or acquired DOX resistance by cancer cells is a commonly encountered cause of treatment failure and necessitates the development of new chemotherapeutics<sup>5,6</sup>.

Numerous mechanisms of DOX cardiotoxicity have been studied and proposed<sup>7</sup>. One of the major mechanisms responsible for DOX cardiotoxicity is the aldo-keto reductase (AKR) mediated reduction of the C-13 carbonyl group to the corresponding alcohol metabolite, doxorubicinol (DOXol)<sup>8,9</sup>. DOXol accumulates in the cardiomyocyte and is up to ten-fold more potent than DOX in stimulating cardiotoxicity<sup>10</sup>. DOXol inhibits the Na<sup>+</sup>-K<sup>+</sup> pump of the cardiomyocyte sarcolemma, interrupting ion signaling involved in cardiac contraction and leading to CHF<sup>11</sup>.

To prevent the formation of DOXol and overcome the undesirable side effects of DOX, the iminoquinone analogs GPX-150 and GPX-160 were developed (Figure 1)<sup>12</sup>. GPX-150

contains two structural changes from DOX: the elimination of the C-13 carbonyl group to prevent formation of DOXol, and the replacement of a carbonyl in the quinone ring to

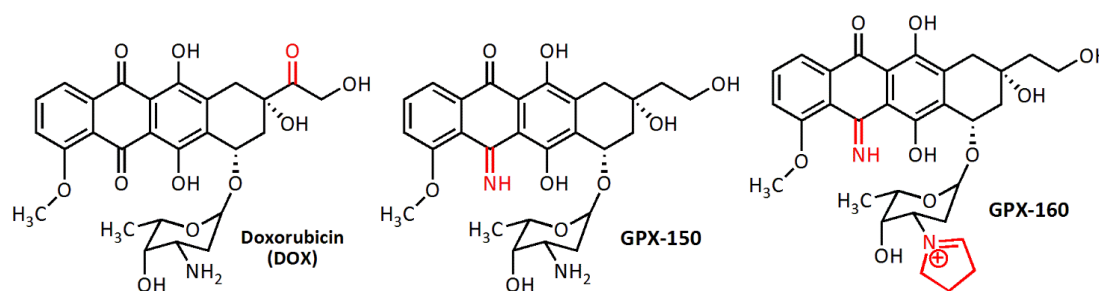


**Figure 3.1. The structures of doxorubicin, GPX-150, and GPX-160.**

create an iminoquinone with reduced capacity to generate reactive oxygen and nitrogen species (RONS)<sup>11–15</sup>. GPX-160 retains the basic structure of GPX-150, but replaces the primary amine on the sugar with a pyrrolino group that is proposed to reduce its susceptibility to P-glycoprotein (P-gp) mediated efflux [PMID: 21075206]. GPX-150 and GPX-160 display *in vitro* cytotoxicity and efficacy profiles that are comparable to DOX (see chapter 2).

The purpose of this study is to better understand *in vitro* pharmacokinetics of GPX-150 and GPX-160 relative to the parent DOX compound. The analogs were evaluated for drug stability, fluorescence profiles, *in vitro* intestinal permeability, and identification of the CYP450 isozymes involved in their metabolism. Using liquid chromatography tandem mass spectrometry, metabolic breakdown products of DOX and its analogs were identified and compared. Ultimately, these studies illuminate aspects of basic drug characteristics that demonstrate several superior features for the analogs over DOX, and serve as useful background information for future drug development and predicting the behavior of these compounds in clinical trials. ADD Mitchell's Intro Sentence HERE.

## 2. Materials and methods

### 2.1 Drug stability studies

The stability of DOX, GPX-150, and GPX-160 in a biological environment was examined by diluting samples of drug stock solutions (10 mM in DMSO) to a final concentration of 250  $\mu$ M in Dulbecco's Minimal Essential Medium (DMEM) containing 10% fetal bovine serum (FBS) (v/v) and 1% pen/strep (100 U/ml penicillin and 100  $\mu$ g/ml streptomycin). Samples were vortexed briefly to mix, filtered through 0.22  $\mu$ m PTFE syringe filters, and analyzed by high-performance liquid chromatography (HPLC). Analysis was performed on a 50 mm x 4.6 mm Hypersil GOLD phenyl column (5  $\mu$ m pore size) using an Agilent 1100 series HPLC equipped with a diode array detector. Mobile phases A and B consisted of 52 mM Tris base (pH 7.2) and 99.9% HPLC-grade acetonitrile, respectively. Gradients were conducted with a flow rate of 1.0 ml/min for 15 min with the following linear program: t = 0 min (70%; A, 30%; B), t = 10 min (30%; A, 70%; B), t=12min (30%; A, 70%; B), t=12.1min (70%; A, 30%; B), and t = 15 min (70%; A, 30%; B). Samples (20  $\mu$ L) were injected every 15 min until near complete decomposition was observed. The retention times for DOX, GPX-150, and GPX-160 were 4.3, 3.8, and 4.9 minutes, respectively. Drug decomposition was observed as decreases in integrated peak areas. Drug half-lives were calculated from plots of integrated peak area vs. time, and fit using one-phase decay based on first-order kinetics.

### 2.2 Drug transport studies

To develop epithelial cell monolayers,  $1.5 \times 10^5$  Caco-2 cells (ATCC, Manassas, VA) were seeded in 24-well plates containing Transwell<sup>®</sup> permeable polycarbonate inserts (6.5 mm diameter; Corning, Tewksbury, MA) and cultured in  $\alpha$ -MEM (Thermo Fisher

Scientific, Waltham, MA) supplemented with 10% FBS and 1% pen/strep. The media was replenished every 2 day. The plates were incubated at 37 °C in a 5% CO<sub>2</sub> humidified atmosphere for 21 days until the cell monolayers were fully developed. In the polarized cell monolayers, the apical and basolateral sides face the upper and lower transwell chamber, respectively. The integrity of the polarized monolayers was evaluated by transepithelial electrical resistance (TEER) measurements using an EVOM<sup>2</sup> epithelial voltohmmeter (World Precision Instruments Inc., Sarasota, FL). Transport studies were initiated when the TEER values of each well surpassed 300 Ω•cm<sup>2</sup>. TEER values of 555 ± 32 Ω•cm<sup>2</sup> at 37 °C, and low Lucifer yellow (LY) permeability rates (<0.5×10<sup>-5</sup> cm/s) indicate good integrity of the Caco-2 monolayer.

For transport experiments, both upper and lower Transwell<sup>®</sup> chambers were washed three times with pre-warmed 1x Hank's balanced salt solution (HBSS, HyClone Laboratories, Inc., Logan, UT). After washing, the plates were incubated in fresh HBSS for 30 min at 37 °C. For the apical to basolateral (AP-BL) uptake experiment, 450 µl of test solutions (25 µM drug) was added to the AP side, and 1600 µl of pre-warmed HBSS was added to the BL well chamber. LY (25 µM) served as a control for non-specific paracellular transport. At intervals of 30, 60, 90, 120, 150 min later by removing 200 µl from the BL chamber. This volume was replaced with an equivalent volume of fresh HBSS. The plates were incubated in an orbital shaker at 37 °C at 50 rpm between the time intervals.

To evaluate the BL-AP drug efflux of the test compounds, 1600 µl of the test solutions (containing 50 µM drug in HBSS) was added to the BL chamber, while 450 µl of HBSS without test compound was added to AP side. A 150-µl aliquot was collected from the AP side at time intervals of 30, 60, 90, 120, and 150 min, and was replaced with an equivalent volume of HBSS. Sample concentrations were assessed using a BioTek fluorescence

microplate reader with the following settings: DOX (ex. 490/em. 590 nm); GPX-150 (ex. 560nm/ em. 630nm); and GPX-160 (ex. 560 nm/ em. 630 nm). The amount of transported drug was determined from standard curves of drug concentration versus fluorescence. The apparent permeability coefficients ( $P_{app}$ , cm/s) for the test compounds were determined according to the following equation<sup>18</sup>:

$$P_{app} = (dC_r/dt) \times V_r / (A \times C_o) \quad \text{Equation (1)}$$

where  $dC_r/dt$  is the change of concentration of test compounds in the receiver chamber ( $\mu\text{g/s}$ ),  $V_r$  is the volume of receiver chamber,  $A$  is the area of the inserts ( $0.33 \text{ cm}^2$ ), and  $C_o$  is the initial concentration of drugs ( $50 \mu\text{M}$ ). The efflux ratio was determined as:

$$\text{Efflux ratio (ER)} = P_{app}(\text{BL-AP}) / P_{app}(\text{AP-BL}) \quad \text{Equation (2)}$$

### 2.3 Microsomal metabolism of DOX and DOX analogs

The initial rates of DOX and DOX analog metabolism by human liver microsomes (HLMs) were determined based on the method of Quintieri et al.<sup>19</sup> that follows the change in fluorescence of the reaction as NADPH is oxidized to  $\text{NADP}^+$ . The 2-ml reaction mixture consisted of 0.1 M potassium phosphate (pH 7.4), 0.15 mM NADPH, and  $50 \mu\text{M}$  DOX or DOX analog. The reaction was preincubated for 3-minute at  $37^\circ\text{C}$ , and initiated with the addition of 0.1 mg/ml HLMs (50 donor pool, Sekisui XenoTech LLC, Kansas City, KS) containing approximately 50 nmol CYP450 protein. Controls consisted of reactions conducted without microsomes, without NADPH, or without test drug. All reactions were tested in triplicate using a Cary Eclipse spectrofluorometer (Varian, Palo Alto, CA) and scanned (ex. 340 nm/em. 460 nm) for 1 hour at  $37^\circ\text{C}$ .

To begin to identify the microsomal enzymes responsible for GPX-150 and GPX-160 metabolism, fluorometric HLM assays (above) were conducted in the presence and absence

of aldo-keto reductase (AKR), alcohol dehydrogenase (ADH), or CYP450 isozyme specific enzyme inhibitors selected based on literature reports<sup>11,15-17</sup>. All inhibitors were obtained from Sigma-Aldrich (St. Louis, MO). ADH- and AKR-specific inhibition was measured using 50  $\mu$ M 4-methylpyrazole (ADH) or 50  $\mu$ M quercitrin (AKR), or. For CYP specific inhibition, the following selective inhibitors were used: 10  $\mu$ M xanthotoxin (CYP2A6), 60  $\mu$ M quercetin (CYP2C8), 30  $\mu$ M sulfaphenazole (CYP2C9), 10  $\mu$ M quinidine (CYP2D6), 5  $\mu$ M ketoconazole (CYP3A4).

#### 2.4 Identification of DOX and DOX analog metabolic products by mass spectrometry

HLM metabolites of DOX, GPX-150, and GPX-160 were identified using HPLC and mass spectrometry (HPLC-MS). HLMs assays were performed as described above, but modified to contain 50  $\mu$ M test drug and scaled to a final volume of 400  $\mu$ l. Controls consisted of reactions with denatured microsomes (45 °C / 30 min), reactions without NADPH, or reactions without test drug. Reactions were terminated after 60 minutes at 37 °C with the addition of 400  $\mu$ l ice-cold acetonitrile. Precipitates were removed by centrifugation at 10,000 x g for 30 min. Sample aliquots (20  $\mu$ l) were injected onto a Hypersil GOLD phenyl analytical column (50 mm x 4.6 mm) using an Agilent 1100 HPLC coupled to a HCTultra ETDII electrospray ionization mass spectrometer (Bruker Daltonik GmbH, Bremen, Germany). Chromatographic separations were achieved using a 1 mL/min flow rate of 79 mM ammonium formate (Solvent A, pH 4.2) and 100% acetonitrile (solvent B) as mobile phases. A gradient elution program: t = 0 min (70% A, 30% B), t = 10 min (30% A, 70% B), and t = 12.1 min (70% A, 30% B) was used. Doxorubicin elution was detected at 495 nm. GPX-150 and GPX-160 elution were detected at 560 nm. The retention times of DOX, GPX-150, and GPX-160 were 4.1, 4.1, and 5.2 minutes, respectively.

The mass spectrometer was operated in positive ion mode using a 6 kV of source voltage. Data were collected under full scan mode from 100 – 800  $m/z$  and analyzed using an Esquire 6000 software program. Nine  $m/z$  values (544.2, 529.2, 581.2, 382, 364, 346, 321, 200, and 147  $m/z$ ) were used to conduct an enhanced quadratic calibration within the expected mass range of fragments of the compounds.

### 3. Results

#### 3.1 Drug stability of DOX, GPX-150, and GPX-160

Drug decomposition rates in media containing serum were determined to compare the stability of the analogs to DOX. As seen in Figure 2, the average half-life of DOX was at 6.8 hours. Compared to DOX, GPX-150 was approximately 8-fold more stable ( $t_{1/2} = 55.9$  h) and GPX-160 was 3-fold more stable ( $t_{1/2} = 20.7$  h). The stability of the drugs in nanopure water was substantially longer (data not shown), suggesting that serum constituents play a role in the drug breakdown.

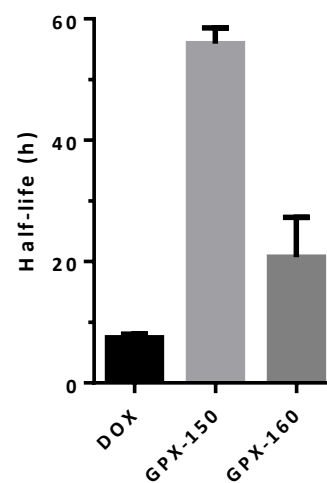


**Figure 3.2. Drug degradation of DOX, GPX-150, and GPX-160. Drug half-lives were determined based on one phase decay analysis of integrated peak areas from HPLC.**

#### 3.2 Transport studies of DOX analogs across intestinal epithelia

The *in vitro* transport rates of DOX, GPX-150, and GPX-160 were evaluated using mature, polarized Caco-2 cell monolayers to simulate the human intestinal environment. In the assay, monolayer integrity was indicated by examining the transport of hydrophilic Lucifer yellow (LY) dye, which is poorly transported across the intact epithelial cell membrane bilayer<sup>20</sup>. The apparent permeability coefficients ( $P_{app}$ ) for DOX, GPX-150, and

GPX-160 were evaluated as a preliminary investigation into transport capability across the intestinal epithelia. As seen in Figure 3 and summarized in Table 1, measurements of basal to apical (BL-AP) permeability coefficients indicate that GPX-150 and GPX-160 have significantly greater efflux ( $p \leq 0.05$ ) across the monolayer relative to DOX. Similarly, apical to basal (AP-BL) permeability coefficients that were significantly higher in GPX-150 and GPX-160 ( $p \leq 0.05$  and  $p \leq 0.01$ ) compared to DOX. The results show that GPX-150 and GPX-160 are much more permeable across the monolayer in either direction than DOX. When the ratio of efflux-to-uptake is considered, DOX exhibits a strong preference for BL-AP efflux with a  $P_{app}$  ratio of 2.5 (Figure 3). In contrast, GPX-150 and GPX-160 exhibited ratios near 1, which indicates no strong preference for direction of transport.

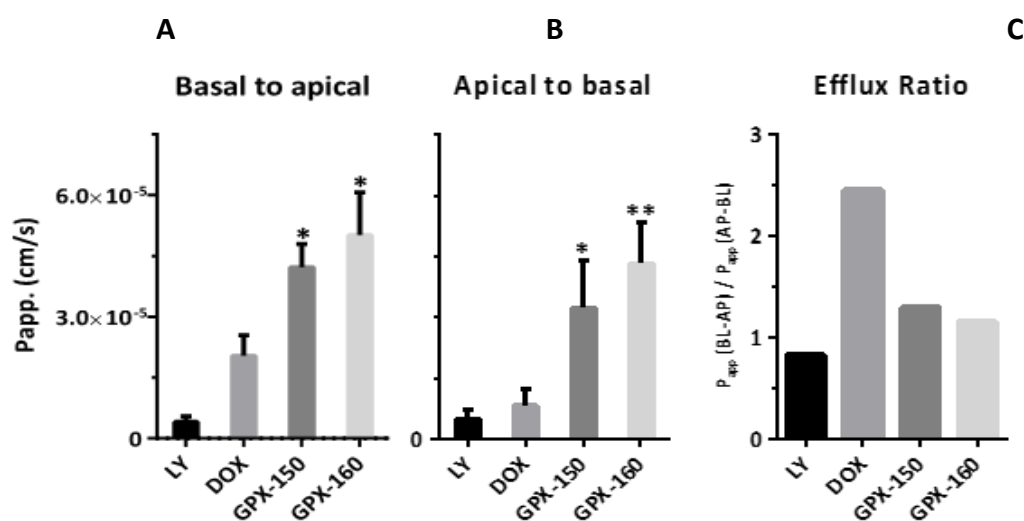


**Figure 3.3.** Apparent permeability rates ( $P_{app}$ , cm/s) of DOX, GPX-150, and GPX-160 transport in basal to apical (A) and apical to basal (B) directions. The figures show the average of three independent experiments ( $\pm$  SEM). \* and \*\* represent  $p \leq 0.05$  and  $p \leq 0.01$ , respectively. The efflux ratio (C) explains the ratio of average permeability rates of efflux (BL-AP) to uptake (AP-BL) across the epithelial monolayer.

**Table 3.1. Summary of apparent permeability rates (P<sub>app</sub>) of bidirectional drug transport.**

	Ave. P <sub>app</sub> (x10 <sup>-6</sup> cm/s)*			
	<b>LY**</b>	<b>DOX</b>	<b>GPX-150</b>	<b>GPX-160</b>
<b>BL to AP</b>	4.0 ± 1.4	20.0 ± 5.0	42.0 ± 5.8	50.1 ± 10.5
<b>AP to BL</b>	4.8 ± 2.4	8.3 ± 4.0	32.4 ± 12.8	43.3 ± 10.0
<b>Efflux ratio</b>	0.83	2.46	1.30	1.16

### 3.3 Microsomal metabolism of DOX and DOX analogs

The preliminary data on the microsomal metabolism of DOX, GPX-150, and GPX-160 was determined by examining the loss in fluorescence (ex. 340 nm / em. 460 nm) of a reaction that accompanies the corresponding oxidation of NADPH to NADP<sup>+</sup>. As seen in Figure 4 (upper left panel), the microsomal oxidation rate of NADPH when GPX-150 or GPX-160 were substrates was approximately half that seen for DOX.

The application of selective inhibitors to the HLM assays provided initial information on the enzyme activities important for DOX, GPX-150, and GPX-160 metabolism. The results of the analysis show that DOX metabolism was inhibited by 40-85% when inhibitors of five CYP450 isoforms (2A6, 2C8, 2C9, 2D6, 3A4), alcohol dehydrogenase (ADH) or aldo-keto reductase (AKR) were incorporated into the reactions (Figure 4). Of these results, quercetin (CYP2C8-selective, 85% inhibition), ketoconazole (CYP3A4-selective, 70% inhibition) and quercitrin (AKR-selective, 81% inhibition) showed the greatest effects, indicating that CYP2C8, CYP3A4, and AKR were most important enzymes in DOX microsomal metabolism.

In contrast to DOX, GPX-150 and GPX-160 metabolism was relatively insensitive ( $\leq$  20% inhibition) to xanthotoxin (CYP2A6-selective), sulphenazole (CYP2C9-selective), quinidine (CYP2D6-selective), 4-methylpyrazole (ALDH-selective), or quercitrin (AKR-

selective). The most striking inhibition of GPX-150 and GPX-160 metabolism occurred only when reactions contained quercetin (CYP2C8-selective, ~ 60% inhibition) and ketoconazole (CYP3A4-selective inhibitor, ~ 50-70% inhibition.). As expected based on the loss of the C-13 carbonyl group and poor quercitrin inhibition (AKR-selective), aldo-keto reductase activity was not an important factor in GPX-150 or GPX-160 metabolism.

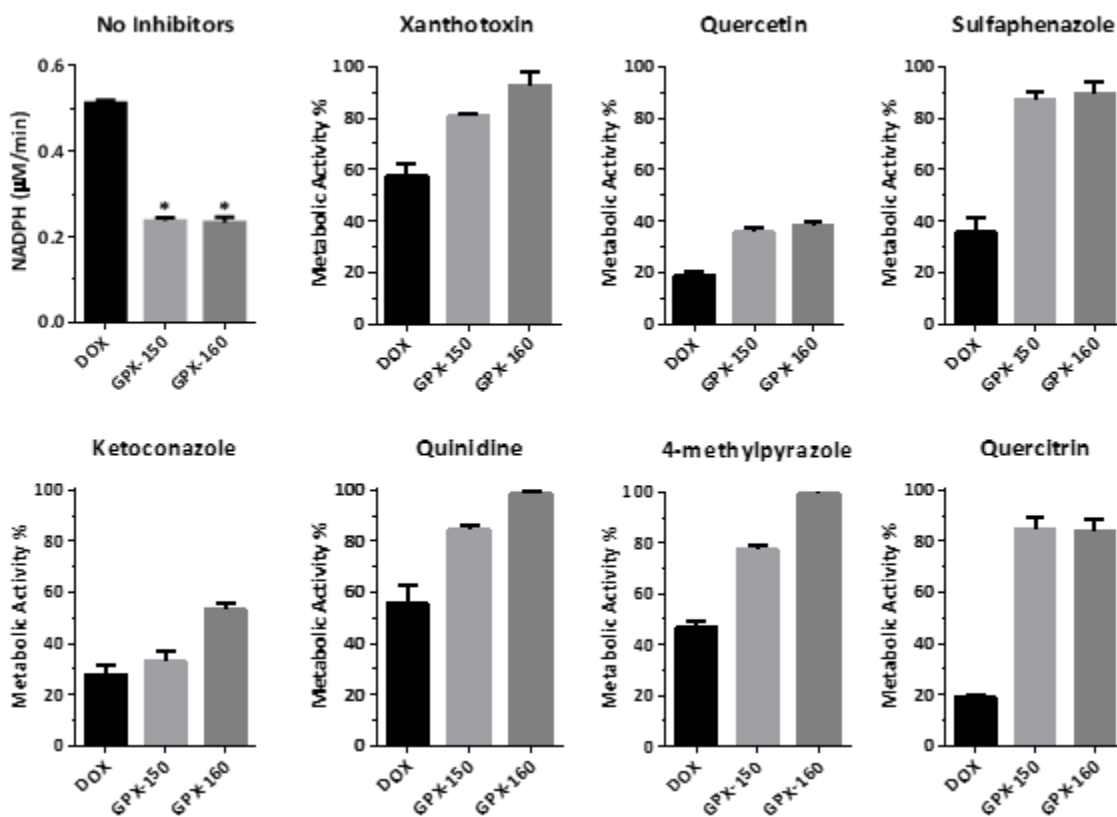


**Figure 3.4** HLM metabolism of DOX, GPX-150, and GPX-160. NADPH oxidation rates were > 2-fold higher for DOX than for the DOX analogs (upper left panel). The remaining panels show percent metabolic activity (compared to uninhibited reactions) when selective cytochrome P450, ADH, or AKR inhibitors were incorporated into the reactions. The selective inhibitors were xanthotoxin (CYP2A6), quercetin (CYP2C8), sulfaphenazole (CYP2C9), ketoconazole (CYP3A4), quinidine (CYP2D6), 4-methylpyrazole (ADH), and quercitrin (AKR). \*represents  $p \leq 0.0001$  in comparison to DOX.

### 3.4 Identification of DOX and DOX analog metabolic products

The products of HLM metabolism of DOX, GPX-150, and GPX-160 were analyzed by reverse phase HPLC-tandem mass spectrometry (Figure 5). The primary DOX peak eluted at 4.1 minutes. NADPH in the reactions eluted at 1.9 minutes (data not shown) without overlapping other compounds (i.e. CYP450 inhibitors and the anticancer compounds). DOX metabolites (DOXol, etc) were primarily detected at a retention time of 2.4-2.6 minutes and identified by mass spectrometry. Mass spectra and a schematic for the metabolic decomposition of DOX can be found in Appendix B.

GPX-150 showed a retention time of 4.1 minutes on the HPLC chromatogram, and the majority of its metabolites eluted at 2.8 minutes (Figure 5B). The mass spectra and a schematic for the metabolic decomposition of GPX-150 can be found in Appendix B.

GPX-160 and its metabolites (M) showed retention times of 5.2 and 4.7 minutes, respectively (Figure 5C). The

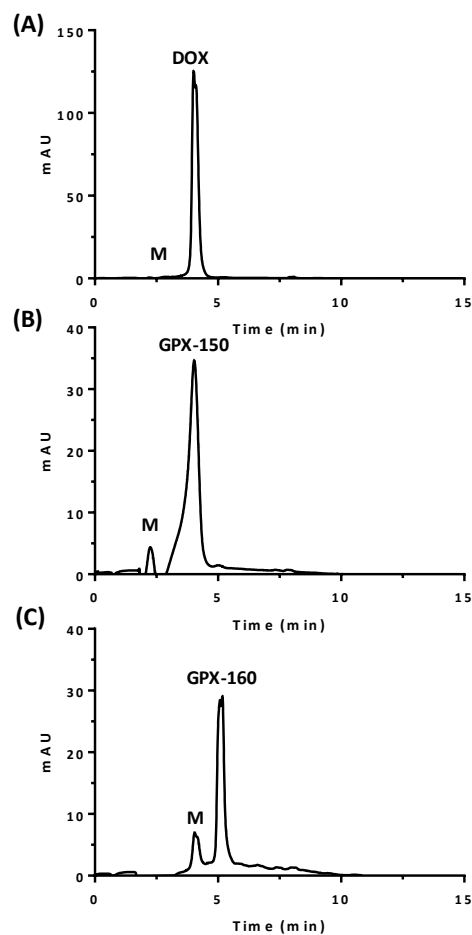


**Figure 3.5.** HPLC elution profiles for HLM reactions containing (A) DOX, (B) GPX-150, and (C) GPX-160. The spectra were collected at the  $\lambda_{\max}$  for the respective compounds: DOX (495 nm), GPX-150 and GPX-160 (560 nm). The retention times for DOX, GPX-150, and GPX-160 were 4.1, 4.1, and 5.2 minutes, respectively. Metabolites (M) were eluted at 2.5, 2.8, and 4.7 minutes.

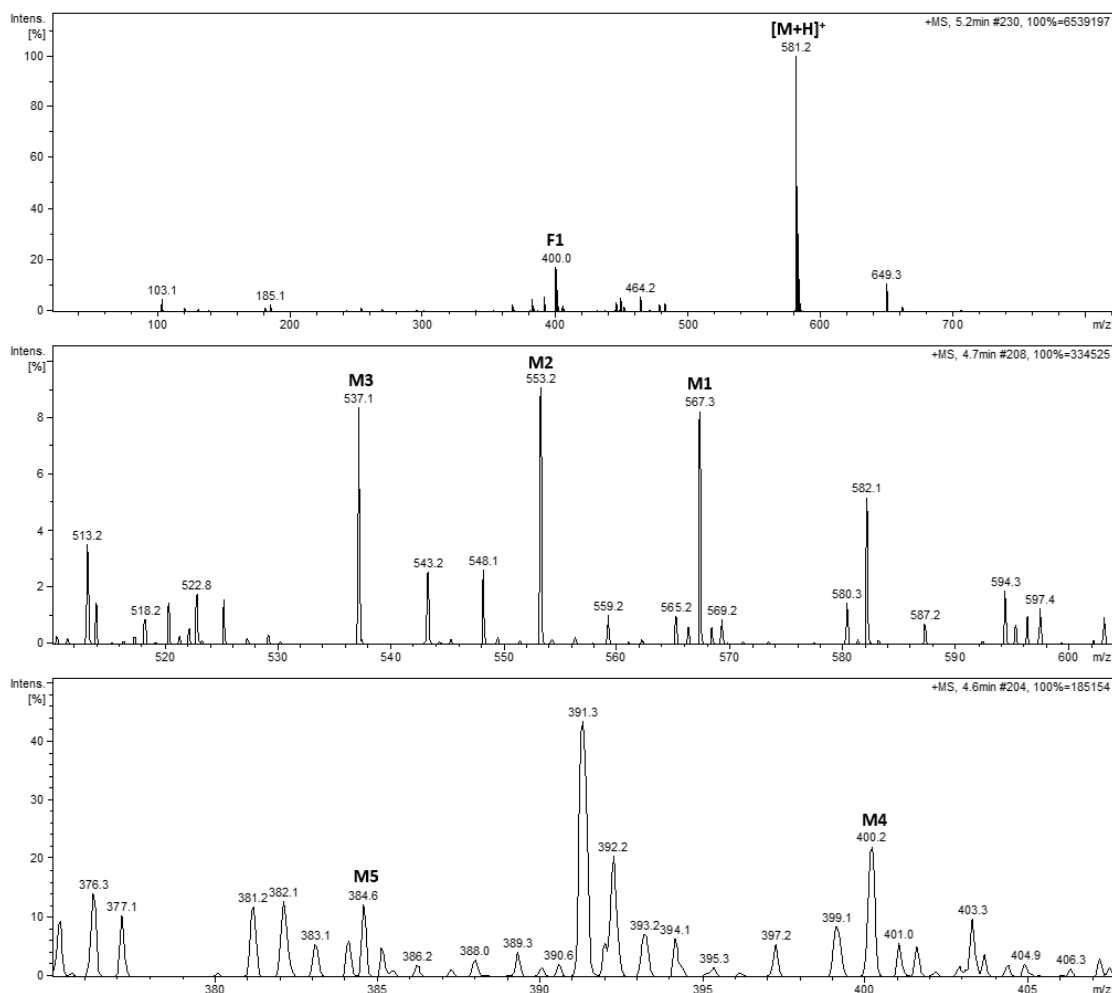


**Figure 3.6.** Mass spectra of GPX-160 [M+H]<sup>+</sup> and its HLM metabolites. F1 denotes a GPX-160 fragment with a characteristic loss of the sugar moiety. The major metabolites (M1-M5) of GPX-160 eluted at 4.6 - 4.7 minutes from the HPLC and correspond to the predicted 4-*O*-demethylation (M1), 5'-demethylation (M2), dealkylation (M3), hydroxyaglycone (M4) and 7-deoxyaglycone (M5) products.

mass spectra for GPX-160 and its metabolites can be seen in Figure 6. The identity of the metabolic breakdown products of GPX-160 was assigned using the mass spectra fragmentation pattern (Figure 6), and predictions of how the compound would be expected to be metabolized based on literature reports of the mass spectra of CYP450 decompositions of DOX<sup>19</sup>.

A summary of the compounds identified in the mass spectra of HLM metabolized DOX, GPX-150 and GPX-160 is found in Table 2. DOX has an observed characteristic

$[M+H]^+$  peak at 544.17 m/z and a minor peak at 397.1 (F1) that agrees with the predicted mass of a deglycosylated fragment (Appendix B). Cardiotoxic DOXol, the AKR metabolite of DOX, appears in the spectra as a peak at 546.75 m/z, close to its predicted 546.19 m/z peak. Fragments corresponding to demethylation, dealkylation, and deglycosidation

**Table 3.2. Identities of the m/z peaks in the mass spectra of HLM metabolized (A) DOX, (B) GPX-150, and (C) GPX-160.**

(A) Peaks	Compounds /reaction	Measured m/z	Theoretical m/z	Error (ppm)	Retention time (min)
1	Doxorubicinol	546.7500	546.1897	1025.8	2.5
2	Doxorubicin	544.1644	544.1741	17.8	4.1
3	Dealkylation	486.2882	486.1686	246.0	2.4
4	Doxorubicinone	415.1250	415.0951	72.0	2.6
5	7-deoxydoxorubicinol	401.1587	401.1158	107.0	2.5
6	7-deoxydoxorubicinone	399.1886	399.1002	221.5	2.5
7	F1	397.0806	397.0923	29.5	4.1
8	Demethylation	387.0625	387.1002	97.4	2.5
9	F2	379.1376	379.1182	51.2	2.4
10	F3	321.0823	321.0763	18.7	4.1

(B) Peaks	Compounds /reaction	Measured m/z	Theoretical m/z	Error (ppm)	Retention time (min)
1	GPX-150	529.1987	529.2108	22.9	4.1
2	4-O-demethylation	515.2496	515.1951	105.8	2.8
3	Dealkylation	485.2241	485.1846	81.4	2.8
4	F1	400.1268	400.1318	12.5	4.1
5	Hydroxyglycone	400.125	400.3900	661.9	2.8
6	7-deoxyglycone	384.0625	384.1369	193.7	2.8
7	F2 (loss of water)	382.1305	382.1576	70.9	4.1

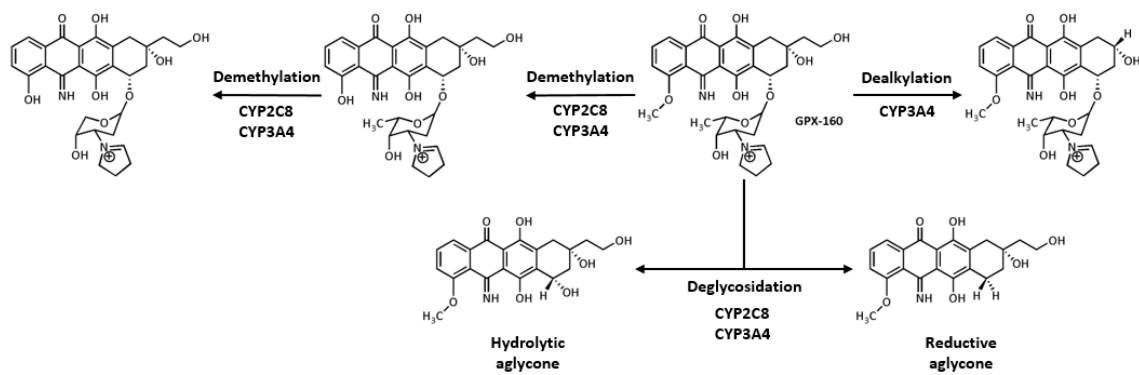
  

(C) Peaks	Compounds /reaction	Measured m/z	Theoretical m/z	Error (ppm)	Retention time (min)
1	GPX-160	581.2654	581.2499	26.7	5.2
2	4-O-demethylation	567.2658	567.2343	55.5	4.7
3	5'-demethylation	553.2239	553.2186	9.6	4.7
4	Dealkylation	537.1425	537.2237	151.1	4.7
5	Hydroxyglycone	400.2021	400.3900	469.3	4.6
6	F1	400.1167	400.1318	37.7	5.2
7	7-deoxyglycone	384.1250	384.1369	31.0	4.6

reactions of DOX, particularly those catalyzed by CYP2C8 and CP3A4 were observed (Table 2A).

The  $[M+H]^+$  fragment of GPX-150 was found at 529.2 m/z and its expected CYP2C8 and CP3A4 induced metabolites were observed as a series of 384 – 515 m/z peaks. A GPX-

160 m/z value was found at 581.26, as well as its proposed demethylated (M1, M2), dealkylated (M3) and deglycosylated (M4, M5) products between 384 - 567 m/z. A schematic of the proposed metabolic routes of GPX-160 is presented in Figure 7.



**Figure 3.7. Schematic of proposed GPX-160 metabolites by CYP2C8 and CYP3A4.**

#### 4. Discussion

This pharmacokinetic study was conducted to describe the *in vitro* stability, transport and metabolism of novel iminoquinone analogs of DOX in order to forecast *in vivo* drug characteristics of the compounds when they are used as anticancer agents.

Good drug stability can facilitate improved drug retention and distribution of potential candidates for cancer treatment<sup>21,22</sup>. To evaluate the drug degradation rates, we tested morphologically modified DOX derivatives that replaced the quinone structure with an iminoquinone to decrease the potential to produce reactive oxygen species associated with acute cardiotoxicity. The iminoquinone GPX-150 clearly shows an 8-fold increase in drug stability relative to DOX.

The removal of the C-13 carbonyl from GPX-150 and GPX-160 could increase the hydrophobicity of the compounds, which could result in increased lipophilicity longer blood circulation time and higher accumulation in tumors<sup>23</sup>. GPX-160 showed a 3-fold

increase in stability relative to DOX, but was less stable than GPX-150. Increased stability in our assay is potentially due to the less reactive nature of the iminoquinone found in GPX-150 and GPX-160. Compared to GPX-150, the reduced stability of GPX-160 may be due to the positively charged 2-pyrrolino moiety, which is a stronger electrophile than the primary amine of GPX-150. Potentially, this could lead to GPX-160 non-specifically reacting with proteins and other biological constituents in the media.

This study also evaluated the bidirectional transcellular transport pathway of DOX, GPX-150, and GPX-160. The lack of a C-13 carbonyl makes both GPX-150 and GPX-160 more hydrophobic than DOX. This potentially explains the increased transport rate of these compounds in both the AP to BL and BL to AP directions. Numerous studies have defined the permeability coefficient less than  $1 \times 10^{-6}$  cm/s exhibits poor (0-20%), between  $1 \times 10^{-6}$  cm/s and  $10 \times 10^{-6}$  cm/s shows moderate (20-70%), and greater than  $10 \times 10^{-6}$  cm/s displays substantial absorption (100%)<sup>24</sup>. Since GPX-150 and GPX-160 show transport rates of  $30-50 \times 10^{-6}$  cm/s, these compounds would be classified as substantially absorbed. In contrast, DOX represents a moderately observed compound. Increased transport rates suggest that GPX-150 and GPX-160 could potentially be delivered orally to treat cancer. However, further investigation of oral bioavailability such as *in vivo* studies are necessary to fully estimate the potential for these compounds to be useful by oral administration.

Furthermore, ratio of efflux to absorption of the anticancer drugs were determined from ratio between the  $P_{app}$  of BL to AP and AP to BL (Figure 3). DOX shows almost 2.5-fold higher in BL to AP than AP to BL pathway indicating a high ER (Table 2), which yields lower cellular uptake of DOX in the intestinal environment as a safety mechanism to protect the body from xenotoxins<sup>25</sup>. In contrast, GPX-150 and GPX-160 show ER that are

evenly balanced between BL to AP and AP to BL (ER near 1).

The metabolism of DOX, GPX-150, and GPX-160 was initially established using a NADPH-mediated reaction with HLMs. Further, the CYP450 isozymes responsible for the drug metabolism was explored using selective CYP inhibitors identified from reported studies of DOX metabolism<sup>60-62</sup>. The faster oxidation rate of NADPH to NADP<sup>+</sup> in DOX metabolism is due to the presence of the C-13 carbonyl group that is the substrates for carbonyl reductase (CR), which is a member of the aldo-keto reductase (AKR) family, is a major AKR enzyme that reduces DOX to DOXol in the cardiomyocyte<sup>26</sup>. DOXol is very potent in inducing chronic progressive cardiotoxicity and eventually causes CHF<sup>27</sup>. Without the presence of C-13 carbonyl in side chain, the oxidation of NADPH in reactions containing GPX-150 and GPX-160 diminishes as the main active site of CR disappears. The importance of CR interaction with quinone ring of DOX has also been explained by enzymatic and computational studies<sup>28</sup>.

CYP3A4 participates in approximately 50% of CYP450 of the drugs oxidative metabolism examined up to date<sup>30</sup>. In adults, 29% of the liver CYP450 enzyme expression is CYP3A4<sup>31</sup>, while this value rises to 50% in the small intestine<sup>32</sup>. It is the most abundant of all of the human CYP isoforms, and is localized in the GI tract, kidney, and liver where it is particularly relevant to drug elimination<sup>33</sup>. The results of our studies show that CYP2C8 and CYP3A4 are the most significant CYP450 isozymes responsible for the biotransformation of DOX, GPX-150, and GPX-160. The CYP3A4 metabolism of these compounds is consistent with the reported literature<sup>39-41</sup>. Interestingly, CYP3A4-mediated metabolism is also required to transform the pro-drug MMDX (PNU-152243) into the

active DOX derivative, a compound which was explored in phase I and II clinical trials as an anticancer agent<sup>29</sup>.

Our results also showed that CYP2C8 is involved in DOX, GPX-150, and GPX-160 metabolism which is consistent with a literature<sup>34</sup>. Other studies have shown that CYP2C8 is responsible for the metabolism of numerous drugs including tetracyclic compounds<sup>35,36</sup>. CYP2C8 is regulated by the expression of the pregnane X receptor (PXR), which stimulates expression of P-gp that increase drug resistance of human lung carcinoma<sup>37</sup>.

Defining the pharmacologic and toxicologic profiles of xenobiotics is an important prelude to clinical trials. HPLC-MS-MS analysis was used to separate and identify the parent compounds and their biotransformation products. Based on the major roles of CYP2C8 and CYP3A4 in GPX-160 metabolism, a proposed schematic of metabolites is shown in Figure 9. The m/z value of the GPX-160 parent ion was 581.26. CYP2C8<sup>40</sup> and CYP3A4<sup>41</sup> deglycosidation products of GPX-150 and GPX-160 by hydrolytic or reductive cleavage of the sugar moiety generated the same aglycones with peaks at 400.39 and 384.14 m/z, respectively. Furthermore, CYP3A4-specific dealkylation of GPX-160 would be predicted to yield a fragment with an m/z value of 537.1<sup>43</sup>, which is supported by the mass spectra (Figure 6). The remaining demethylation or deglycosidation products seen in mass spectra could be formed by the action of either CYP2C8 or CYP3A4.

Similar to GPX-160, the aglycone metabolites of GPX-150 were assumed to be produced by both CYP2C8 and CYP3A4 due to their roles in deglycosidation reactions. In GPX-150, this corresponds to metabolites peaks with m/z values at 400.39 and 384.14, respectively (Appendix B). These represent aglycones formed by hydrolytic or reductive mechanisms. Furthermore, the peaks at m/z of 515.52 and 485.18 suggest demethylation<sup>44</sup>

and dealkylation reactions by CYP3A4<sup>43</sup>. The peak at 382.1 m/z is in agreement with the cleavage of the sugar residue from GPX-150 with subsequent loss of a water molecule.

In the mass spectra of DOX (Appendix B), the main peak occurs with a m/z of 544.16. Notable peaks with m/z values of 397.1 and 379.1 can be explained by the protonation of DOX at C-7, loss of the sugar residue, and subsequent collision induced loss of water<sup>38,39</sup>. The peak at 321 m/z is consistent with the loss of both the sugar moiety and the alkyl side chain at C-9<sup>19</sup>. The peaks at m/z 415.2 and 399.2 represent glycosidic cleavages yielding hydrolytic (doxorubicinone) and reductive (7-deoxydoxorubicinone) aglycones. These are predominantly formed by CYP2C8<sup>40</sup> and CYP3A4<sup>41</sup>. Further reduction of the C-13 carbonyl by carbonyl reductase result in 7-deoxydoxorubicinone that corresponds to the peak at 401.12 m/z. Doxorubicinone can also be reduced by carbonyl reductase to yield doxorubicinolone<sup>42</sup>. The peaks at 486.7 and 387.1 m/z correspond to CYP3A4-mediated dealkylation of the side chain and demethylation of 7-deoxydoxorubicinone, respectively<sup>43</sup>.

As with DOX, metabolites of GPX-150 and GPX-160 may show unique toxicities. However, these are not yet identified. Potentially co-administration of potent inhibitors of CYP2C8, such as quercetin or glitazones<sup>45</sup> and/or inhibitors of CYP3A4, such as azole antifungals (e.g., ketoconazole and itraconazole)<sup>35</sup> and macrolide antibiotics (e.g., erythromycin and troleandomycin)<sup>46</sup>, could preserve the chemotherapeutic efficacy of GPX-150 and GPX-160. This may be useful when using these analogs to treat certain human carcinomas including hepatocellular carcinomas that show increased CYP3A4 expression<sup>44</sup>.

## 5. Conclusion

In conclusion, our studies show that GPX-150 and GPX-160 have increased biological stability and transport rates relative to DOX across Caco-2 monolayers. This suggests they may have potential for oral delivery. The results of our *in vitro* studies using CYP450 selective inhibitors demonstrated that the two analogs were predominantly metabolized by CYP2C8 and CYP3A4. Importantly, the absence of a C-13 carbonyl group abrogated CR-mediated formation of toxic alcohol metabolites and significantly decreased microsomal drug metabolism. This suggests that these analogs could persist longer *in vivo* than DOX. Mass spectrometry analysis of the microsomal drug metabolites was consistent with predictions of CYP2C8- and CYP3A4-mediated metabolism based on known degradation pathways of DOX. Future animal studies will expand our understanding of the absorption, distribution, metabolism, and excretion (ADME) of these novel DOX analogs.

## REFERENCES

1. Cortés-Funes H, Coronado C. *Cardiovasc. Toxicol.* **2007**, 7 (2), 56-60. [PubMed: 17652804]
2. Binaschi M, Bigioni M, Cipollone A, Rossi C, Goso C, Maggi C, Capranico G, Animati F. *Curr. Med. Chem. Anticancer. Agents* **2001**, 1 (2), 113-30. [PubMed: 12678762]
3. Minotti G, Cairo G, Monti E. *FASEB J.* **1999**, 13 (2), 199-212 [PubMed: 9973309].
4. Swain, S. M., Whaley, F. S. & Ewer, M. S. Congestive heart failure in patients treated with doxorubicin: A retrospective analysis of three trials. *Cancer* **97**, 2869–2879 (2003). [PubMed: 12767102]
5. Pai VB, Nahata MC. *Drug Saf.* **2000**, 22 (4), 263-302. [PubMed: 10789823]
6. El-Awady RA, Semreen MH, Saber MM, Cyprian F, Menon V, Al-Tel TH. *DNA Repair (Amst)*. **2016**, 37, 1-11. [PubMed: 26590797]
7. Monneret C. *Eur. J. Med. Chem.* **2001**, 36, 483-93. [PubMed: 11525839]
8. Minotti, G. *et al.* The secondary alcohol metabolite of doxorubicin irreversibly inactivates aconitase/iron regulatory protein-1 in cytosolic fractions from human myocardium. *FASEB J.* **12**, 541–52 (1998). [PubMed: 9576481]
9. Minotti G, Cavaliere AF, Mordente A, Rossi M, Schiavello R, Zamparelli R, Possati G. *J. Clin. Invest.* **1995**, 95 (4), 1595-605. [PubMed: 7706466]
10. Piska K, Koczurkiewicz P, Bucki A, Wojcik-Pszczola K, Kolaczkowski M, Pekala E. *Invest. New Drugs.* **2017**, 35 (3), 375-385. [PubMed: 28283780]
11. Boucek RJ, Olson RD, Brenner DE, Ogunbunmi EM, Inui M, Fleischer S. *J. Biol. Chem.* **1987**, 262 (33), 15851-6. [PubMed: 2890636]

12. Frank NE, Cusack BJ, Talley TT, Walsh GM, Olson RD. *Invest. New Drugs*. **2016**, *34* (6) 693–700. [PubMed: 27581956]
13. Tokarska-Schlattner M, Zaugg M, Zuppinger C, Wallimann T, Schlattner U. *J. Mol. Cell. Cardiol.* **2006**, *41* (3), 389-405. [PubMed: 16879835]
14. Minotti G, Ronchi R, Salvatorelli E, Menna P, Cairo G. *Cancer Res.* **2001**, *61* (23), 8422-8. [PubMed: 11731422]
15. Wang, G. W.; Klein, J. B.; Kang, Y. J. *J. Pharmacol. Exp. Ther.* **2001**, *298* (2), 461-8. [PubMed: 11454906]
16. Fogli S, Nieri P, Breschi MC. *FASEB J.* **2004**, *18* (6), 664-75. [PubMed: 15054088]
17. Berthiaume JM, Wallace KB. *Cell Biol. Toxicol.* **2007**, *23* (1), 15-25. [PubMed: 17009097]
18. Zhang L, Zheng Y, Chow MSS, Zuo Z. *Int. J. Pharm.* **2004**, *287* (1-2) , 1–12. [PubMed: 15541906]
19. Quintieri L, Geroni C, Fantin M, Battaglia R, Rosato A, Speed W, Zanovello P, Floreani M. **2005**, *11* (222), 1608. [PubMed: 15746066]
20. Wingler K, Müller C, Schmehl K, Florian S, Brigelius-Flohé, R. *Gastroenterology* **2000**, *119* (2), 420-30. [PubMed: 10930377]
21. Duncan R. *Nat. Rev. Drug Discov.* **2003**, *2* (5), 347-60. [PubMed: 12750738]
22. Moghimi SM, Hunter AC, Murray JC. *Pharmacol. Rev.* **2001**, *53* (2), 283-318. [PubMed: 11356986]
23. Cho YW, Park SA, Han TH, Son DH, Park JS, Oh SJ, Moon DH, Cho KJ, Ahn CH, Byun Y, Kim IS, Kwon IC, Kim SY. *Biomaterials* **2007**, *28* (6), 1236-47. [PubMed: 17126900]
24. Yee, S. *Pharm. Res.* **1997**, *14* (6), 763-6. [PubMed: 9210194]
25. Batrakova EV, Li S, Miller DW, Kabanov AV. *Pharm. Res.* **1999**, *16* (9), 1366-72. [PubMed: 10496651]

26. Forrest GL, Gonzalez B, Tseng W, Forrest GL, Gonzalez B, Tseng W, Li X, Mann J. *Cancer Res.* **2000**, 5158-64. [PubMed: 11016643]
27. Cortes EP, Gupta M, Chou C, Amin VC, Folkers K. *Cancer Treat. Rep.* **1978**, 62 (6), 887-91. [PubMed: 667863]
28. Slupe A, Williams B, Larson C, Lee LM, Primbs T, Bruesch AJ, Bjorklund C, Warner D, Peloquin J, Shadle SE, Gambliel HA, Cusack BJ, Olson RD, Charlier HA Jr. *Cardiovasc. Toxicol.* **2005**, 5 (4), 365-76. [PubMed: 16382174]
29. Quintieri L, Fantin M, Palatini P, De Martin S, Rosato A, Caruso M, Geroni C, Floreani M. *Biochem. Pharmacol.* **2008**, 76 (6), 784-95. [PubMed: 18671948]
30. Guengerich FP. *Annu. Rev. Pharmacol. Toxicol.* **1999**, 39, 1-17. [PubMed: 10331074]
31. Shimada T, Yamazaki H, Mimura M, Inui Y, Guengerich FP. *J. Pharmacol. Exp. Ther.* **1994**, 270 (1), 414-23. [PubMed: 8035341]
32. Paine MF, Khalighi M, Fisher JM, Shen DD, Kunze KL, Marsh CL, Perkins JD, Thummel KE. *J. Pharmacol. Exp. Ther.* **1997**, 283 (3), 1552-62. [PubMed: 9400033]
33. Thummel KE, Wilkinson GR. *Annu. Rev. Pharmacol. Toxicol.* **1998**, 38, 389-430. [PubMed: 9597161]
34. Skarka A, Škarydová L, Štambergová H, Wsól V. *Chem. Biol. Interact.* **2011**, 191 (1-3), 66-74. [PubMed: 21185270]
35. Walsky, R. L.; Obach, R. S. **2004**, 32 (6), 647-60. [PubMed: 15155557]
36. Li XQ, Björkman A, Andersson TB, Ridderström M, Masimirembwa CM. *J. Pharmacol. Exp. Ther.* **2002**, 300 (2), 399-407. [PubMed: 11805197]
37. Chen, Y.; Huang, W.; Chen, F.; Hu, G.; Li, F.; Li, J.; Xuan, A. *Cancer Med.* **2016**, 5 (12), 3564-3571. [PubMed: 27878971]
38. Katzenmeyer JB, Eddy CV, Arriaga EA. *Anal. Chem.* **2011**, 82 (19), 8113-20. [PubMed: 20825163]

39. Monneret C, Sellier N. *Biomed. Environ. Mass Spectrom.* **1986**, *13* (7), 319-26. [PubMed: 2943345]
40. Lin JH, Lu AY. *Clin. Pharmacokinet.* **1998**, *35* (5), 361-90. [PubMed: 9839089]
41. Lee HJ, Lee MG. *Res. Commun. Mol. Pathol. Pharmacol.* **1999**, *105* (1-2), 87-96. [PubMed: 10850372]
42. Salvatorelli E, Menna P, Gianni L, Minotti G. *J. Pharmacol. Exp. Ther.* **2007**, *320* (2), 790-800. [PubMed: 17135345]
43. Chiba M, Hensleigh M, Nishime JA, Balani SK, Lin JH. *Drug Metab. Dispos.* **1996**, *24* (3), 307-14. [PubMed: 8820421]
44. Relling MV, Nemec J, Schuetz EG, Schuetz JD, Gonzalez FJ, Korzekwa KR. *Mol. Pharmacol.* **1994**, *45* (2), 352-8. [PubMed: 8114683]
45. Brandon EFA, Raap CD, Meijerman I, Beijnen JH, Schellens JHM. *Toxicol. Appl. Pharmacol.* **2003**, *189* (3), 233-46. [PubMed: 12791308]
46. Wrighton SA, Schuetz EG, Thummel KE, Shen DD, Korzekwa KR, Watkins PB. *Drug Metab. Rev.* **2000**, *32* (3-4), 339-61. [PubMed: 11139133]

## CHAPTER FOUR: CONCLUSION

DOX is among the most prominent and versatile antitumor agents used to treat a variety of cancer patients. The antineoplastic mechanism of DOX primarily involves intercalating DNA between base pairs, creating DNA adducts, and inhibiting topoisomerase enzyme activity during DNA replication. Although effective as an antitumor agent, DOX also causes a cumulative dose-dependent cardiotoxicity. In an attempt to address this adverse effect while maintaining efficacy, several synthetic modifications have been made to the original structure of DOX. GPX-150 and GPX-160, two novel synthetic DOX analogs, showed inhibitory effects against Top2 $\alpha$ , indicating the analogs participate in forming the Drug-DNA-Top2 $\alpha$  ternary complex similar to DOX. In *in vitro* antiproliferation assays, both analogs exhibited very promising anticancer activity against an array of cancer cell lines. In particular, GPX-160 showed similar IC<sub>50</sub> values to DOX against human STS while lacking the structural properties associated with cardiotoxicity. Importantly, GPX-160 appears to overcome DOX resistance due to P-gp mediated drug efflux. Moreover, the novel analogs both showed promising activity against human fibrosarcoma xenografts in immune-deficient mice, causing significant reductions in both tumor volume and tumor weight.

Furthermore, pharmacokinetic studies showed that the analogs had biological stability that was markedly better than DOX, with drug half-lives in serum containing media that were 3-8 fold longer than DOX. Transport studies of GPX-150 and GPX-160 across Caco-2 monolayers indicate the drugs cross the intestinal epithelial layer much more rapidly than

DOX, and suggest the drugs may have improved oral bioavailability. The drug metabolic turnover by HLM CYP450s, ALDH, and AKR show that GPX-150 and GPX-160 are less metabolically active than DOX. In particular, the lack of C-13 carbonyl in the analogs appears to prevent their metabolism by AKR, and the formation of the corresponding cardiotoxic alcohol metabolite, DOXol. CYP2C8 and CYP3A4 were found to be the most prevalent CYP isozymes for biotransformation of analogs. HPLC-MS-MS analysis determined dealkylation, demethylation, and deglycosidation of DOX, GPX-150 and GPX-160 by CYP2C8 and CYP3A4. Further investigation of these metabolites need to be done to assess potential toxicities. The project was designed to discover and comprehend new generation of anthracyclines with improved potency without severe side-effects compared to that of the parent compound. The novel compounds with structural modifications of DOX certainly represents the groundbreaking development of anticancer agents for amplified chemotherapeutic treatment.

## APPENDIX A

### Fluorescence Profiles and Calibration Curves for DOX, GPX-150 and GPX-160

DOX, GPX-150, and GPX-160 spectrofluorometric profiles were determined using a Varian Cary Eclipse fluorometer to identify the maximum excitation and emission wavelengths. These values are important for detection of the compounds in transport studies, and in assessing drug concentration. Fluorometry identified the maximal excitation/emission wavelengths to be: DOX (ex. 495 nm/em. 593 nm), GPX-150 (ex. 560 nm/em. 630 nm) and GPX-160 (ex. 560 nm/em. 630 nm) as shown in Figure A1. The DOX excitation profile was similar to the reported literature (Paine, M. F.; Khalighi, M.; Fisher, J. M.; Shen, D. D.; Kunze, K. L.; Marsh, C. L.; Perkins, J. D.; Thummel, K. E. *J. Pharmacol. Exp. Ther.* **1997**, 283 (3), 1552). The spectroscopic profiles for both GPX-150 and GPX-160 showed identical wavelengths although GPX-160 contains a pyrrolino group at C-3' position in the sugar moiety. This indicates that the absorption and radiation energy of both of the novel compounds share very similar Stokes fluorescence.

Standard calibration curves were constructed using the optimal excitation and emission wavelengths and a series of drug concentrations (Figure A2). These calibration curves were

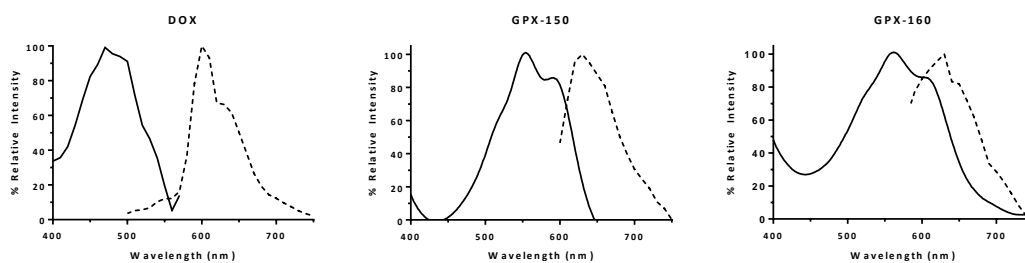


**Figure A1. Spectrofluorometric profiles of DOX, GPX-150, and GPX-160. The compounds were diluted to 2.5  $\mu\text{g/ml}$  in DMEM. Excitation and emission profiles are shown in solid and dashed lines, respectively.**

later used for drug concentration and transport studies. To construct the calibration curves,

8 concentrations of test compounds were diluted in HBSS and the fluorescence measured on a BioTek Synergy MX multiwell plate reader. As can be seen in Figure A2, DOX was approximately 10-20 fold more fluorescent at its optimal excitation/emission conditions than GPX-150 or GPX-160. However, the data was linear for all of the compounds in the 0 – 50  $\mu\text{M}$  concentration range, allowing ready detection of low micromolar concentrations of drug.

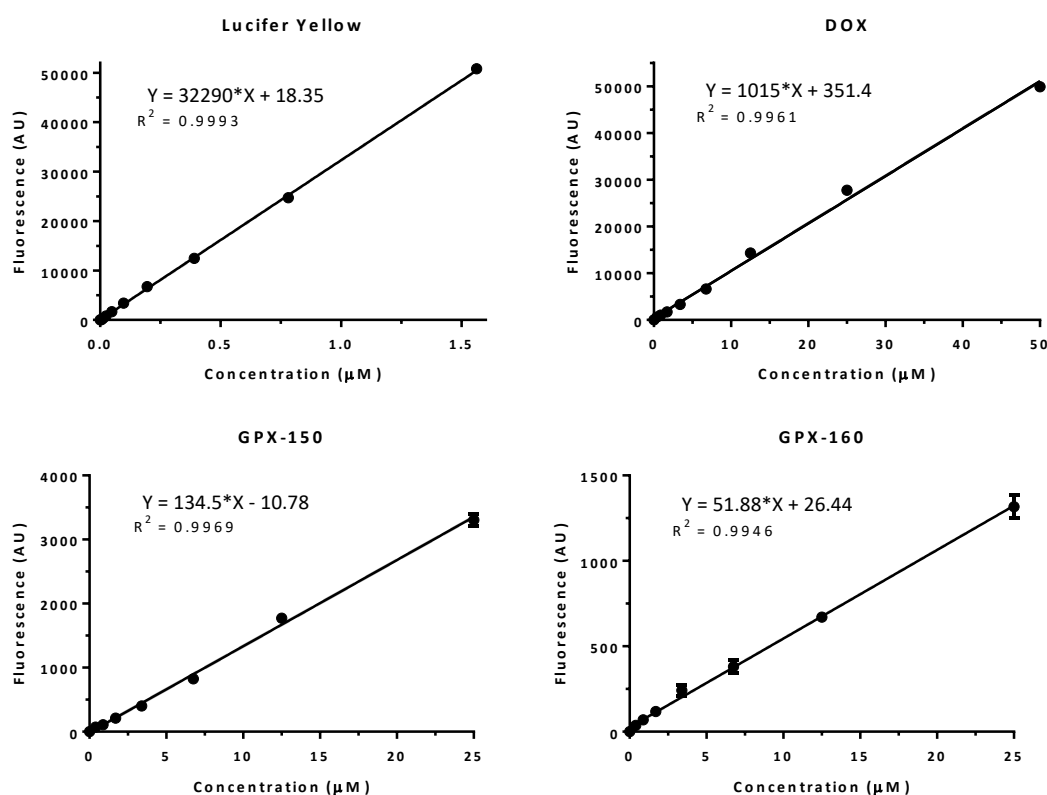


**Figure A2.** Calibration curves of DOX (495/593 nm), GPX-150, GPX-160 (560/630 nm), and Lucifer yellow (428/536 nm). These calibration curves were used to examine drug transport across Caco-2 monolayers.

## APPENDIX B

## B1. Doxorubicin

### B2. GPX-150

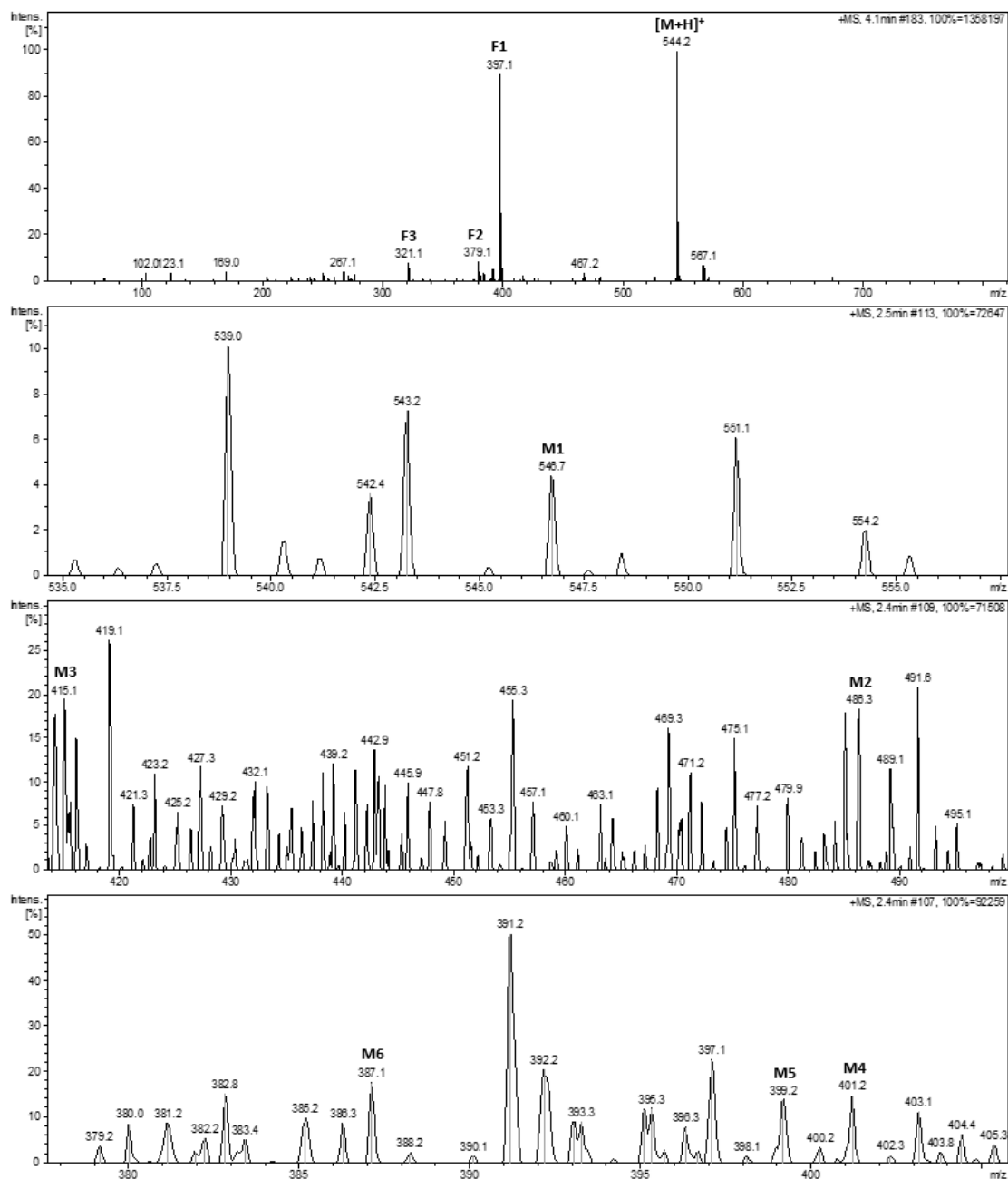


**Figure B1.** HLM metabolites of DOX after 30 min at 37°C. The mass spectra were collected at 4.1 minutes retention time from the HPLC chromatogram for DOX (M+H<sup>+</sup>) and the deglycosylated F1 fragment (top panel). The mass spectra for other metabolites (M1 – M6) was collected at 2.4-2.6 minutes retention time. See Chapter 3, Table 3 for comprehensive list of metabolites.

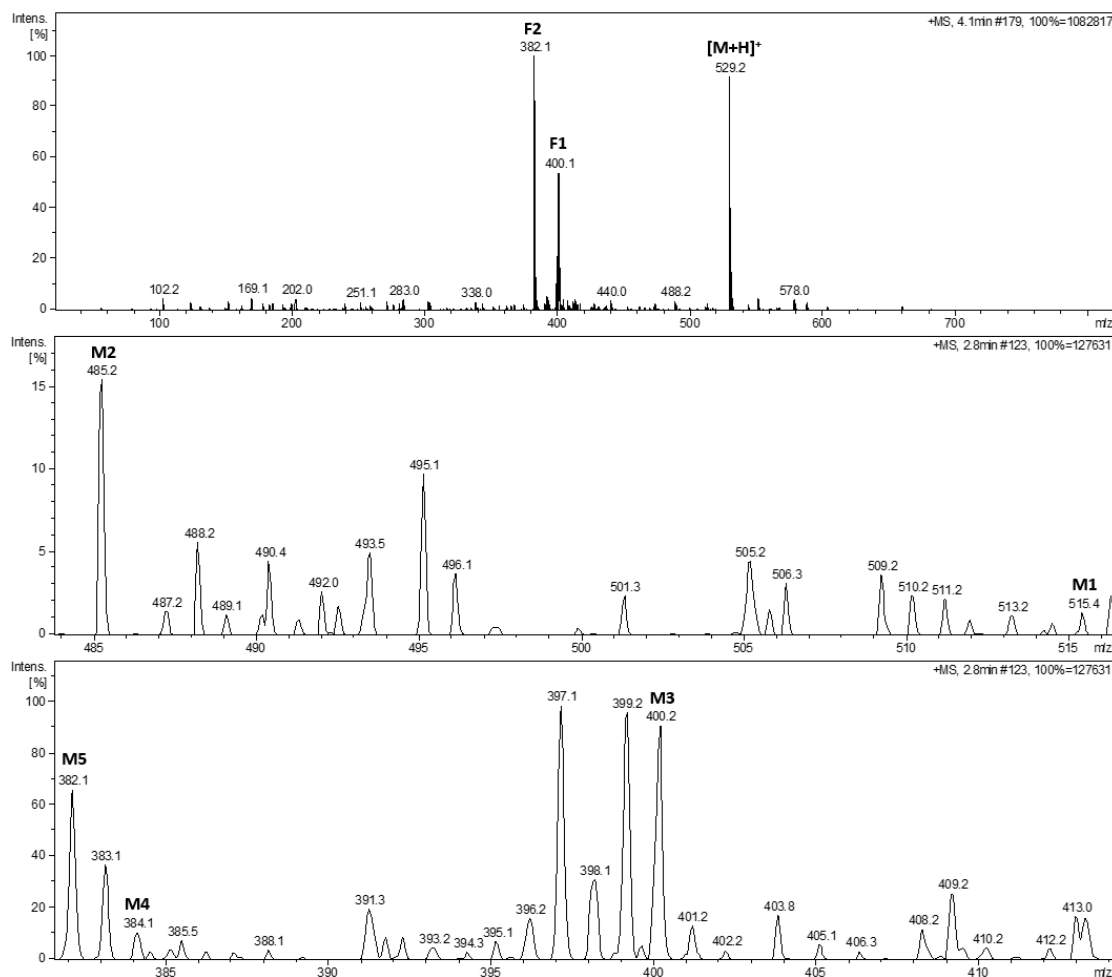


**Figure B2.** HLM metabolites of GPX-150 after 30 min at 37°C. The mass spectra were collected at 2.8 minutes retention time from the HPLC chromatogram to identify GPX-150 ( $M+H^+$ ) and the deglycosylated (F1) and deglycosylated/dehydrated (F2) products. The GPX-150 metabolites (M1-M5) were found at 2.8 minutes retention time. See Chapter 3, Table 3 for comprehensive list of metabolites.

### B3. Schematic of DOX Metabolism

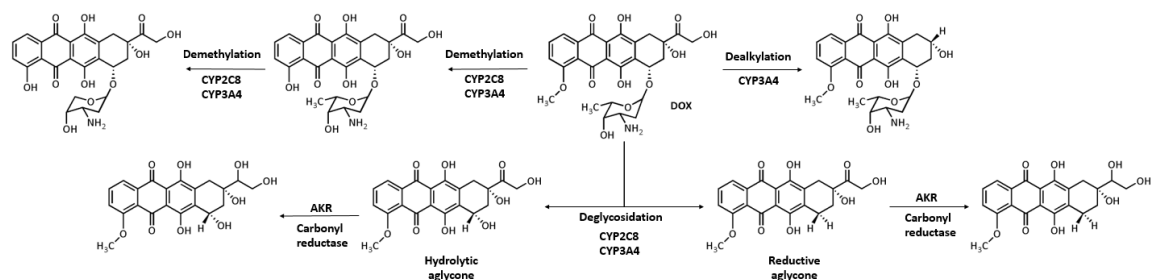


**Figure B3.** Based on LC/MS results, the predicted metabolites of DOX by aldo-keto reductase (AKR) and CYP2C8 and CYP3A4 via human liver microsomes (HLMs).

### B4. Schematic of GPX-150 Metabolism

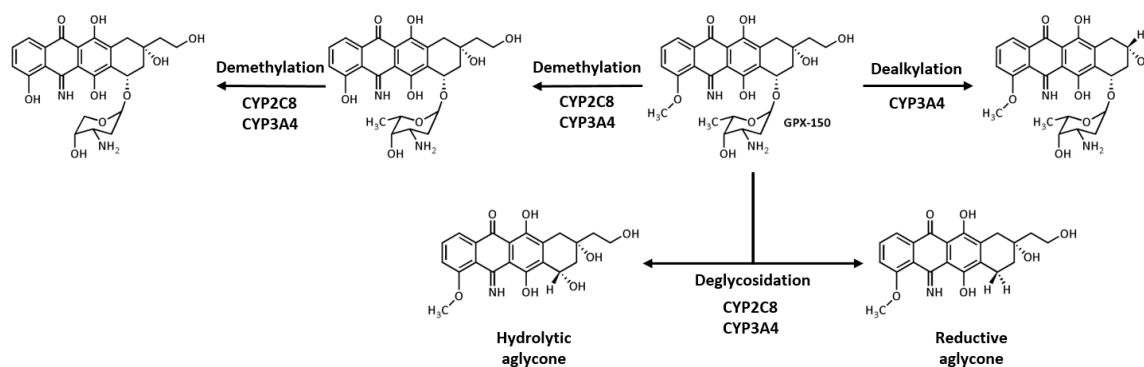


**Figure B4.** Based on LC/MS results, the predicted metabolites of GPX-150 by CYP2C8 and CYP3A4 via human liver microsomes (HLMs).